SBUF

ID: 13136

LUNDS UNIVERSITET

UTVÄRDERING, HANTERING OCH MODELLERING AV TVÅNGSLASTER I BETONGBROAR

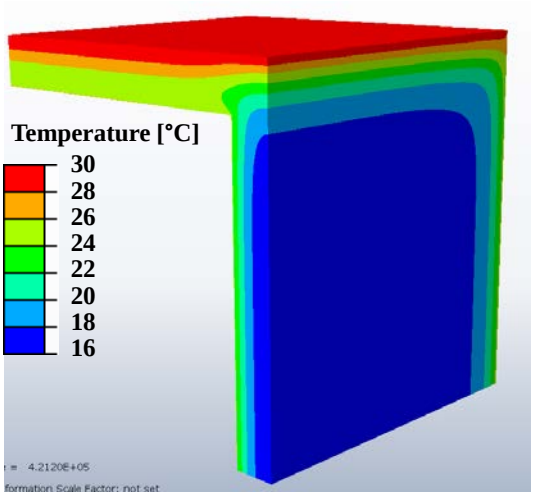

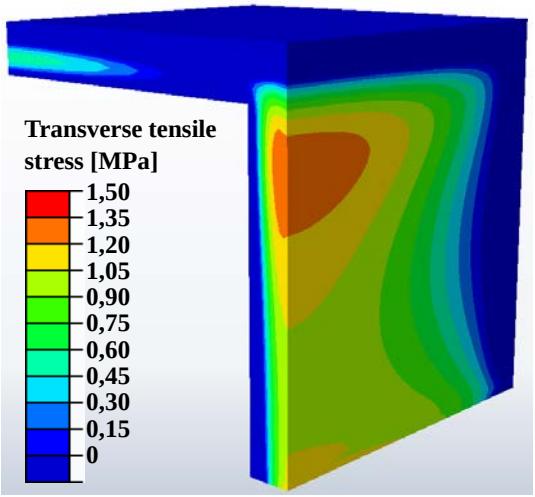

Erik Gottsäter – Lunds tekniska högskola

2018-05-08

FÖRORD

Lunds Universitet önskar att tacka SBUF för medfinansiering av projektet.

Följande personer har varit involverade i projektets utförande:

- Erik Gottsäter, Oskar Larsson Ivanov, Miklós Molnár, Annika Mårtensson och Roberto Crocetti, Lunds tekniska högskola
- Mario Plos, Chalmers tekniska högskola

Följande personer har ingått i projektets referensgrupp:

- Karl Lundstedt, Skanska
- Fredrik Carlsson, WSP
- Johan Kölfors, Scanscot
- Morgan Johansson, Norconsult
- Hans-Ola Öhrström, Trafikverket
- Sven Thelandersson, Lunds tekniska högskola

Lund 2018-05-08

Erik Gottsäter från Lunds tekniska högskola

SAMMANFATTNING

Projektet syftar till att ta fram en metod för dimensionering av broar med hänsyn till tvångseffekter, som förbättrar utnyttjandegraden av armering i broar. Fokus ligger på att utreda temperaturlastens storlek i plattrambroar i Sverige, och på att därefter undersöka tvångskrafternas effekter på sprickvidder i den aktuella brotypen.

SBUF har ingått som delfinansiär i projektet, som utförs som ett doktorandprojekt på Lunds Tekniska Högskola. Resultaten som redovisas i denna rapport visar på att det temperaturlastfall för olika temperatur i olika konstruktionsdelar som finns beskrivet i Eurokod kan ge upphov till stora armeringskrav i närheten av ramhörnen på plattrambroar. Samtidigt visar resultaten att den nuvarande modellen innebär en grov förenkling av verkliga förhållanden, och att en mer realistisk modell för temperaturvariation skulle ge upphov till minskade temperaturlaster i brokonstruktionen. Vidare har projektet validerat användningen av en modell för simulering av temperatur i plattrambroar med hjälp av väderdata, genom att temperatur har uppmätts och simulerats för en och samma bro, vilket gav god överrensstämmelse.

Inom doktorandprojektet pågår nu vidare arbete med att ta fram förslag på temperaturlastvärden för användning som ett nationellt val till det aktuella Eurokod-lastfallet, och med att undersöka den minskning av tvångsspänningar som sker på grund av uppsprickning i bron. Målsättningen är att bestämma den kombinerade effekten av att både ta hänsyn till en mer realistisk temperaturlast vid dimensionering och att kunna justera lastens storlek för att ta hänsyn till den minskning av tvång som sker då sprickor uppkommer i bron.

INNEHÅLL

BILAGOR

BILAGA A:

COMPARISON OF MODELS FOR DESIGN OF PORTAL FRAME BRIDGES WITH REGARD TO RESTRAINT FORCES
KONFERENSBIDRAG, ASCE STRUCTURES CONGRESS, DENVER 2017.

BILAGA B:

SIMULATION OF THERMAL LOAD DISTRIBUTION IN PORTAL FRAME BRIDGES
KONFERENSBIDRAG, IABSE 19:TH CONGRESS, STOCKHOLM 2016

BILAGA C:

SIMULATION OF THERMAL LOAD DISTRIBUTION IN PORTAL FRAME BRIDGES
TIDSKRIFTSARTIKEL, ENGINEERING STRUCTURES, PUBLICERAD 2017

BILAGA D:

MEASUREMENTS AND SIMULATION OF TEMPERATURE IN A PORTAL FRAME BRIDGE
KONFERENSBIDRAG, 40TH IABSE SYMPOSIUM, NANTES 2018, INSKICKAD

BILAGA E:

VALIDATION OF MODEL FOR TEMPERATURE SIMULATION USING MEASUREMENTS IN A PORTAL FRAME BRIDGE
TIDSKRIFTSARTIKEL, UTKAST

1. Projektbakgrund och syfte

Bakgrunden till projektet är att ett av de temperaturlastfall som ska beaktas vid brodimensionering enligt Eurokod, i kombination med nya dimensioneringsmetoder som beaktar brons tvärriktning, ger stora tvångskrafter i vissa brotyper. Det aktuella temperaturlastfallet beskriver att en temperaturskillnad på 15ºC mellan väsentliga konstruktionsdelar ska beaktas vid dimensionering. Eftersom bara ett lastvärde ges, så används det för samtliga brotyper och konstruktionsmaterial, och då det aktuella temperaturlastfallet används för ramben och brobaneplatta i en plattrambro, så kommer stora tvångsspänningar uppstå i brons tvärriktning vid ramhörnet (se bilaga A).

Tidigare dimensionerades brotypen vanligtvis med en 2D-modell, varpå tvärriktningen inte studerades närmare och den aktuella temperaturlasten gav små spänningar i konstruktionen. I dagsläget förväntas emellertid broar dimensioneras med 3D-modeller, varpå effekterna i tvärriktningen uppdagas. Temperaturskillnaden mellan konstruktionsdelarna ger då dragspänningar i tvärled i den kallare konstruktionsdelen, eftersom den varmare delen förhindrar den önskade deformationen. Effekten av temperaturlasten i tvärriktningen noteras därmed inte om en 2D rammodell används, vilket illustreras i figur 1, där tvångsspänningar i tvärriktningen är markerade med pilar.

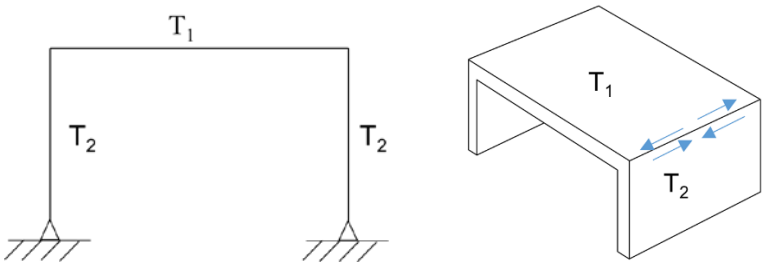

Figur 1. Temperaturlastfall enligt Eurokod för olika temperatur i olika konstruktionsdelar applicerad på en plattrambro.

Den aktuella temperaturlasten är emellertid en grov uppskattning, då den används för samtliga typer av brokonstruktioner. Det är därmed möjligt att det givna lastvärdet är olämpligt att använda vid sprickviddsberäkning för plattrambroar. Dessutom beskriver inte lastfallet hur temperaturen varierar inom respektive konstruktionsdel. Att anta en gradvis övergång mellan temperaturerna i de olika delarna skulle både kunna vara mer realistiskt, och ge upphov till mindre tvångseffekter i dimensioneringsmodellen (se bilaga B).

Tvångslaster uppkommer vid förhindrad töjning, och dess storlek är beroende av hur stor töjning som förhindras, och vilken styvhet konstruktionen har. Ju styvare konstruktionen är, desto större tvångskraft ger en given förhindrad töjning. Eftersom uppsprickning gör att en betongkonstruktion blir mindre styv, så leder uppsprickning till att tvångskrafterna i konstruktionen i sin tur minskar. Om hänsyn tas till detta vid dimensionering av broar utsatta för tvångseffekter kan således den erforderliga armeringsmängden för sprickviddsbegränsning minskas. Broar dimensioneras emellertid normalt med linjärelastiska materialmodeller och utan övrigt hänsynstagande till uppsprickning.

Ett möjligt sätt att ta hänsyn till tvångseffekterna skulle kunna vara att undersöka hur sprickvidderna som fås med olinjära materialmodeller förhåller sig till de som beräknas enligt Eurokod utifrån resultat från spänningsberäkningar gjorda med linjärelastiska materialegenskaper. Därefter skulle en faktor eller ett uttryck som beskriver förhållandet mellan sprickvidderna enligt de olika modellerna kunna tas fram, och på så sätt skulle resultat erhållna utan hänsyn till

uppsprickningens effekter på tvånget kunna justeras, med ex. en justering av ingående tvångslast i linjärelastisk beräkning.

Syftet med detta projekt är att ta fram nya temperaturlastvärden för fallet med olika temperatur i olika konstruktionsdelar i plattrambroar i Sverige. Lastfallet ska inte bara ange ett värde på temperaturskillnaden, utan också beskriva hur temperaturen varierar inom konstruktionen, och vara utformat på ett sätt som är enkelt att hantera för brokonstruktörer. Dessutom syftar projektet till att ta fram en metod som förenklat tar hänsyn till den lastreducerande effekt som uppkommer av uppsprickning, då tvångseffekter är inblandade.

Projektet utförs som ett doktorandprojekt på Lunds Tekniska Högskola. SBUF har bidragit med finansiering till den första delen av projektet, som redovisas i denna rapport. Dessutom ges en beskrivning av återstående moment i doktorandprojektet.

2. Projektmetodik

Följande studier har gjorts inom projektet:

- Undersökning av de nuvarande temperaturlasternas effekt på en brokonstruktion.
- Simuleringar av temperaturfördelningen i plattrambroar med hjälp av väderdata från SMHIs mätstationer. Parameterstudie över geometri och materialparametrar, och undersökning av uppkomna temperaturvariationer inom konstruktionsdelar.
- Framtagande av tänkbar modell för framtida temperaturlast.
- Verifiering av modell för simulering av temperatur genom jämförelse av simulerad och uppmätt temperatur.

3. Resultat

Till denna rapport infogas fem bilagor som går igenom resultaten mer ingående. Sammanfattningsvis har de studier som gjorts hittills visat att:

- Det är det tidigare beskrivna lastfallet, med olika temperatur i olika konstruktionsdelar, som ger de största tvångseffekterna vid dimensionering av plattrambroar (se Bilaga A).
- Simuleringar med väderdata visar att kvasipermanent lastvärde för temperaturskillnad mellan konstruktionsdelar sannolikt är grovt överskattat i Eurokod, då normen används för dimensionering av plattrambroar. Detta innebär att lastvärdet som används vid sprickviddsdimensionering sannolikt kommer att kunna sänkas markant (se Bilaga B, C och E).
- Simuleringar visar att temperaturövergången i ramhörnet sker gradvis längs en sträcka på ca en meter åt vardera håll, vilket i sin tur innebär att tvångseffekterna inte blir lika stora som om en skarp temperaturändring antas (se Bilaga B och C).
- Ett rimligt sätt att beskriva temperaturlastfallet med olika temperatur i olika konstruktionsdelar är att samtidigt ansätta temperaturgradienter över både brobaneplatta och ramben. Detta ger en spänningsfördelning i tvärled i bron som påminner om de spänningar som orsakas av de temperaturfördelningar som fåtts vid simulering (se Bilaga C).
- Den modell som använts för temperatursimulering kan återskapa uppmätta temperaturer i en brokonstruktion, med en noggrannhet på ca 1°C (Bilaga D och E).

4. ÅTERSTÅENDE ARBETE INOM DOKTORANDPROJEKT

Inom ramen för det pågående doktorandprojektet, som planeras att slutföras vid årsskiftet 2019-2020, återstår arbetet med att ta fram temperaturlastvärden för fallet med olika temperatur i olika konstruktionsdelar i plattrambroar. Dessutom ska detta kombineras med effekten av att tvångsspänningar minskas vid uppsprickning. Slutligtvis ska förutom två nya tidskriftsartiklar en manual för branschen skrivas, som ger ett förslag på hur det aktuella lastfallet kan hanteras vid dimensionering. I figur 2 illustreras planen för återstoden av doktorandprojektet:

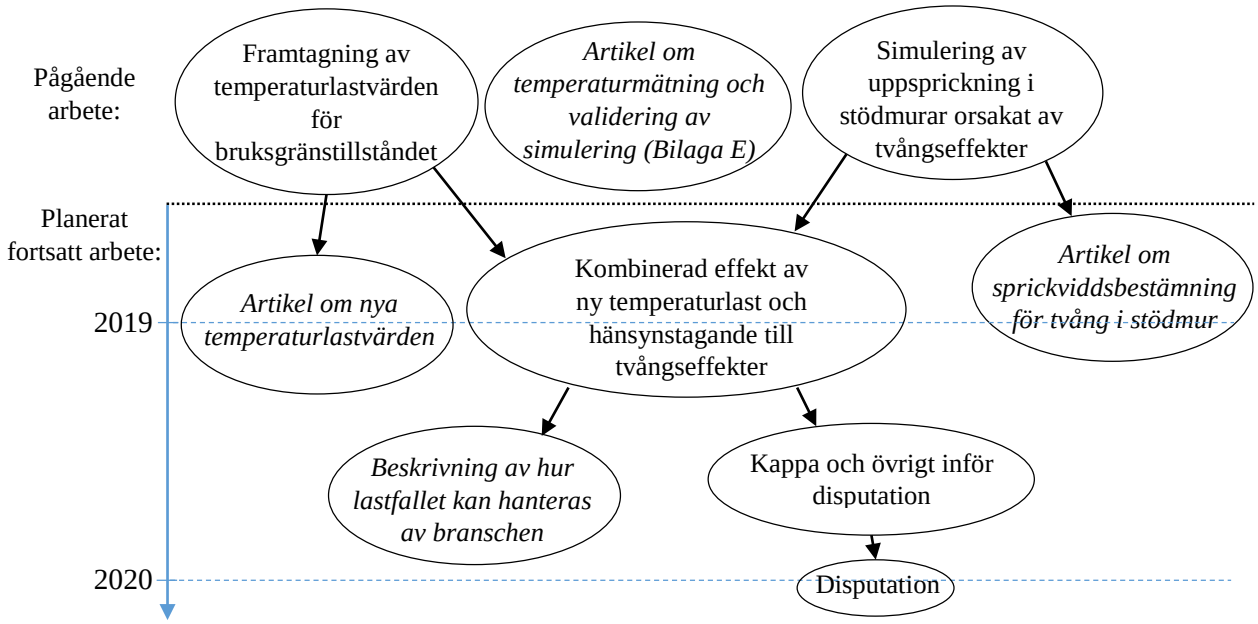

Figur 2. Illustration av pågående och återstående moment inom doktorandprojektet.

BILAGA A:

Comparison of Models for Design of Portal Frame Bridges with regard to Restraint Forces

E. Gottsäter, O. Ivanov, R. Crocetti & M. Molnár
Lund University, Lund, Sweden

M. Plos
Chalmers University of Technology, Gothenburg, Sweden

ABSTRACT
In the design of concrete bridges an important aspect is limiting crack widths, since large cracks can lead to e.g. corrosion and affect the bridge functionality. Restraint forces caused by thermal loads and shrinkage will likely constitute a large part of the total forces acting on the bridge in crack width design. In this paper, restraint stresses in portal frame bridges are calculated according to Eurocode with simple hand calculation models, 2D frame models and linear elastic 3D FE-models. The results are then compared and used in Eurocode crack width design methods. Large tensile restraint stresses were found in the transverse direction close to the frame corners, and the required reinforcement amount significantly exceeded the minimum reinforcement prescribed by codes. The results are however unrealistic since the thermal load distribution is simplified, and the crack width formula does not take the reduction of restraint stresses due to cracking into account. Future studies shall therefore determine a more realistic thermal load distribution and the effects of cracking, in order to create a more accurate linear elastic 3D FE design method.

INTRODUCTION
If the temperature of a concrete structure is changed, the structure will strive to also change its volume. However, the natural volume change is in many cases prevented, leading to the appearance of restraint forces. Restraint forces are therefore fundamentally different from other types of forces in the way that they can be eliminated if the structure is allowed to deform freely. Bridges that normally cannot deform freely are generally affected by restraint forces caused by changes in temperature and shrinkage.

This study compares simple hand calculation methods, 2D frame models and 3D linear elastic models when used in bridge design for calculation of restraint stresses. The stresses are then used in crack width calculations, and the resulting reinforcement amounts are compared. Restraint forces and crack widths are calculated according to Eurocode. The study is focusing on portal frame bridges, in which the abutments are rigidly connected to the bridge deck and connected to the bridge foundation either rigidly or pinned. A simple model of a portal frame bridge is given in figure 1.

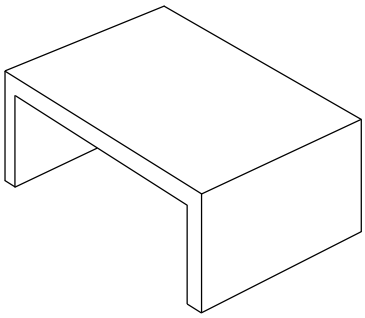

Figure 1. A model of a portal frame bridge investigated in this study.

In Sweden, 2D frame models were previously the numerical model type most commonly used in design of portal frame bridges. However, 3D-models became widely used after the Swedish Transport Administration changed their design regulations, by stating that three-dimensional models must be used unless the structure has an obvious two-dimensional way of working regarding geometry, loads and design conditions (Trafikverket, 2011).

RESTRAINT FORCES

The magnitude of the restraint force caused by a change in temperature ΔT can be calculated as

$$F = R\alpha\Delta TEA \quad (1)$$

where R is the degree of restraint, α is the coefficient of thermal expansion, E is Young's modulus and A is the cross sectional area. Since cracking reduces the structural stiffness, restraint forces are also reduced when cracks appear. This causes the load-deformation relationship to be very different from the case of non-restraint loading. The difference is obvious when figure 2a and figure 2b are compared. Figure 2a portrays the load-deformation relationship for a reinforced concrete bar loaded with a continuously increasing axial tensile force, while figure 2b shows the corresponding relationship for the case of continuously increased deformation.

When the load is increased, figure 2a, the deformation will increase instantly when a crack is formed in the concrete. Thereafter the load continues to increase until the next crack appears, causing another sudden deformation increase. Assuming the concrete strength is rather uniform, all cracks will appear within a small load range until a stabilized crack pattern is reached. If the testing is deformation controlled as in figure 2b, a profoundly different behavior is observed. When a crack appears in this case, the force is reduced due to the reduced stiffness. When the deformation continues to increase, the load will also increase and eventually pass its former peak value before a new crack appears. The choice of deformation controlled or force controlled testing does not affect the load needed to cause the different cracks, nor does it affect the deformation of the bar at the time of cracking (Elbadry and Ghali, 1995).

Figure 2a implies that in the case of non-restraint loading, it is likely that a uniformly loaded concrete element is either not cracked at all or has reached the state of stabilized cracking, making it reasonable to either assume an uncracked element (state I) or neglect the concrete in tensile zones (state II) when estimating the structural stiffness. But in the case of restrained deformations, there is a large span of possible restrained deformations where cracking has occurred but stabilized cracking is not reached, as shown in figure 2b. That makes it difficult to estimate a suitable stiffness value, which can be many magnitudes larger in state I than in state II. Using the stiffness value for state I or state II when calculating the force created by a restrained deformation can therefore lead to a very inaccurate result, as portrayed in figure 3.

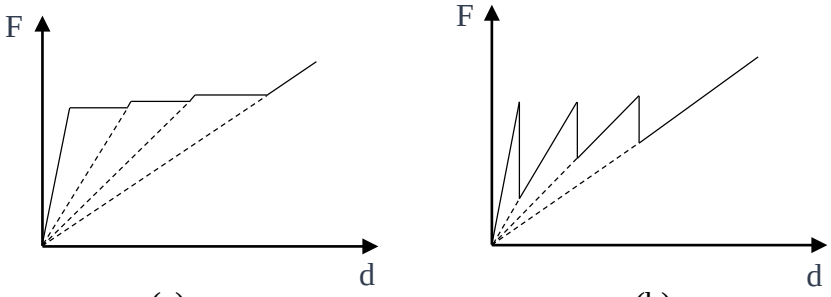

(a) (b)

Figure 2. Illustration of the force – deformation diagram for a force controlled test (a) and for a deformation controlled test (b). When a crack is formed in (a), the stiffness is suddenly reduced, which causes a sudden deformation increase. But when cracking occurs in (b), the stiffness reduction causes a sudden reduction of the force in the test.

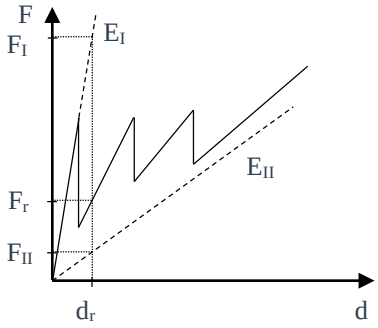

Figure 3. The restrained deformation d_r causes the restraint force F_r. Estimating F_r by using the state I stiffness E_I or by using state II stiffness E_{II} gives the inaccurate results F_I or F_{II} respectively.

It is however not only the stiffness that can be difficult to estimate, but also the value of the degree of restraint, *R*. An expression for the degree of restraint in base restrained walls is found in ACI (1995) and shown in equation 2. The expression can be used in order to calculate the degree of restraint along the restrained edge of the wall.

$$R = c_k / \left(1 + \frac{A_w}{A_r}\frac{E_w}{E_r}\right) \qquad (2)$$

A_w is the cross sectional area of the restrained wall parallel to the retaining surface, A_r is the corresponding area on the restraining structure, E_w is the stiffness of the wall, E_r is the stiffness of the restraining structure and c_k is a factor taking creep into account. The factor is 1 if creep is neglected and can be put to 0.65 if creep is to be considered (Zangeneh Kamali et al., 2013). The value of the restraint degree is valid at the restrained edge of the wall, and is lower at points further away from that edge.

The difficulty of determining the restraint force in a concrete structure, especially after cracking, means that it is also difficult to calculate the width of the appearing cracks, which has an impact on structural durability. Moreover, increasing the reinforcement amount in order to reduce crack widths leads to an increased stiffness, causing the restraint forces to increase as well (Jokela, 1984). Since the restraint force increases, the relationship between reinforcement amount and crack width becomes more complicated, and adding more reinforcement becomes less advantageous. Also, an increased reinforcement amount can be negative for other reasons e.g. increasing the cost of materials and execution.

EUROCODE DESIGN METHODS

Crack width design is performed in SLS with a quasi-permanent load combination, adjusting the loads to their median values over time. In order to do so, characteristic thermal loads are multiplied with 0.5 while traffic loads are multiplied with zero. Shrinkage is considered as a permanent load and is therefore multiplied with 1 (EN 1990, 2002). The large influence of the restraint forces makes the design more complicated regarding estimating the degree of restraint, determining the magnitude of the restraint force after cracking and calculating crack widths.

Thermal loads and shrinkage

The different thermal load cases which shall be included in the design procedure are:

- Uniformly increased or decreased temperature in the entire structure.
- Increased or decreased temperature in the structure, combined with a difference in temperature between structural parts.
- Vertical thermal gradient over the bridge deck cross section, either linear or multi-linear.
- Uniformly increased or decreased temperature in the entire bridge combined with a vertical thermal gradient over the bridge deck (EN 1991-1-5, 2003).

A thermal gradient over the bridge abutment cross sections is also specified for some design cases, this is however not included in this study.

Shrinkage is considered as a tensile strain developing over time in Eurocode and can therefore be treated as a negative thermal load. If a structure is cast in different intervals, shrinkage can cause stresses parallel to the contact surface between the structural parts, due to the difference in shrinkage having occurred in the two parts.

Degree of restraint

Suitable degrees of restraint for slabs with adjacent structures on one, two or three sides are presented in annex L of EN 1992-3, (2006), where the highest degree of restraint is set to 0.5. This value is for example applied at the base of the central zone of a base restrained wall. However, the document EN 1992-3 (2006) specifically treats design of liquid containing structures, which means that it is not supposed to be used in bridge design.

Crack width calculations

Eurocode presents several means of calculating crack widths. One of the methods is given in section 7.3.4 of EN 1992-1-1 (2004), which is intended for concrete structures in general. In the method, the characteristic value of the crack width is calculated as $w_k = s_{r,max}(\varepsilon_{sm} - \varepsilon_{cm})$. $s_{r,max}$ is the maximum distance between cracks at stabilized cracking and $\varepsilon_{sm} - \varepsilon_{cm}$ is the difference between the average strain in steel and concrete along the distance $s_{r,max}$. The method uses the calculated force to estimate the crack widths and is not adapted for restraint forces, meaning it does not take the reduction of the restraint force due to cracking into account. It also assumes that a stabilized crack pattern is developed, which is not certain if restraint forces make up a large part of the total force.

There are however two crack width equations in annex M of EN 1992-3 (2006). These relations are adapted for restraint purposes, one for end restrained and one for edge restrained structural elements. The crack width equations differ only from the previously shown one in their expressions for $\varepsilon_{sm} - \varepsilon_{cm}$. The equation for the end restrained case does not take the restraint force into account. Instead the force which causes cracking, i.e. the tensile stress capacity multiplied by cross sectional area, is used in design. The edge restrained model does not take the restraint force into account either, but instead sets the difference in strain between reinforcement and concrete, $\varepsilon_{sm} - \varepsilon_{cm}$, equal to the restrained strain, $R_{ax}\varepsilon_{free}$ (EN 1992-3, 2006). The correctness of

these two expressions has however been questioned by Bamforth et al. (2010). It is for example noted that in the edge restrained case, the influence of the concrete stress capacity is disregarded. It is also shown in the report that crack spacing is dependent on the wall geometry and degree of restraint, which is also disregarded in the Eurocode expression.

METHODS FOR CALCULATING RESTRAINT STRESSES

In order to exemplify the effects of the different calculation methods, a comparison is made between the results when designing a portal frame bridge with simple hand calculation models, 2D computer models and 3D linear elastic FE-models. The geometry of the bridge is described in table 1, and the material properties used are shown in table 2.

The initial concrete temperature is assumed to be 10ºC and the thermal loads are calculated for Lund in southern Sweden, where the maximum and minimum air temperatures, T_{max} and T_{min}, are +34ºC and –23ºC respectively. Design values for the thermal loads are presented in table 3. Only one thermal load distribution of each type is presented in the table, namely the one causing the largest tensile stresses in the structure. The thermal loads in the table are relative to the initial temperature of 10ºC, which means that if e.g. the concrete is 10ºC, the thermal load is zero.

Casting of the bridge is made in situ in two stages, the foundation and the bridge abutments in the first stage, and the bridge deck in the second stage. The time period between the casting stages is assumed to be ten days. The ambient relative humidity is 80% and the conditions presented give shrinkage values according to table 4. In design with regard to long time effects, a creep coefficient equal to 1.4 is used.

Table1. Geometry parameters used in calculations.

Geometry parameters	Size [m]
Bridge length	8
Bridge width	8
Bridge height	4
Thickness of deck and abutments	0.5

Table2. Material parameters used in calculations.

Material parameters	
f_{ck}	30 MPa
f_{ctm}	2.9 MPa
E_{cm}	33 GPa
Poisson’s ratio	0.2
Thermal expansion factor, α	10^{-5} °C^{-1}
f_{yd}	500 MPa

Table 3. Thermal load design values used in calculations.

Thermal load cases	Bridge deck thermal load [°C]	Bridge abutment thermal load [°C]
Uniform temperature	-13	-13
Temperature difference between structural parts	-13	-5.5
Gradient over bridge deck	+10.5 top side 0 bottom side	0
Gradient and uniformly changed temperature	-9.05 top side -13 bottom side	-13

Table 4. Design values for shrinkage used in calculations.

Shrinkage type	Strain
Autogenous shrinkage, first 10 days	$-2.66 \cdot 10^{-5}$
Autogenous shrinkage, ultimate value	$-5.0 \cdot 10^{-5}$
Drying out shrinkage, ultimate value	$-18.9 \cdot 10^{-5}$

Thermal loads and autogenous shrinkage can develop rather fast and should therefore be considered both with and without the effect of creep. Drying out shrinkage on the other hand develops during a long period of time, therefore it is reasonable to add a creep effect to the load cases in which drying out shrinkage is included. There are therefore two types of quasi-permanent load cases to consider, one with thermal load and a difference in autogenous shrinkage between structural parts, and another with thermal load, difference in autogenous shrinkage, total drying out shrinkage and creep. Other loads such as earth pressure and self-weight are not considered in this study.

Crack width limitation is performed with both the formulas presented in EN 1992-1-1 (2004) and in EN 1992-3 (2006). The crack width limit is 0.3 mm for the structure, which is the recommended value in EN 1992-2 (2005) for bridges without pre-stressed reinforcement.

Simple hand calculations

When calculating thermal loads and shrinkage by hand, separate models are used in order to calculate restraint forces in longitudinal and transversal direction. For calculation in longitudinal direction, a frame model which allows rotations at the bottom end as shown in figure 4a can be used. The bridge deck in the model is first assumed to be able to contract freely when the thermal load and shrinkage is applied. The contraction at each end is equal to $v = \alpha \Delta T L/2$. The effect of shrinkage is expressed as a change in temperature, and is therefore included in ΔT. Then, the abutment bases are assumed to be forced back into their original positions. This makes the frame deform according to figure 4b.

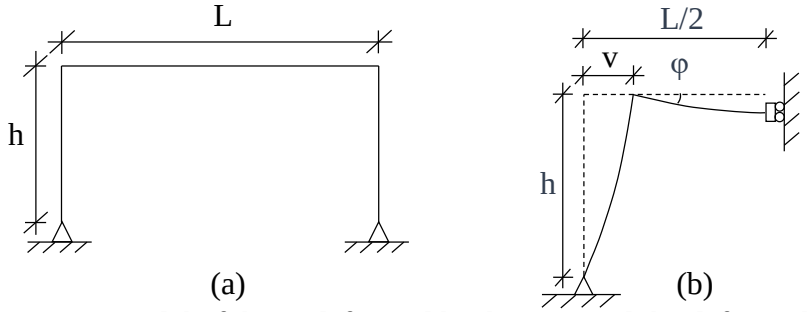

Figure 4. Model of the undeformed bridge (a), and the deformed shape (b) after the bridge deck in (a) has contracted. L is the length of the bridge deck and h is the height of the abutments. In (b), a symmetry condition has been applied at the middle of the bridge span. v is the reduced length of half the bridge deck, and φ is the rotation of the frame corner.

The abutment can in this case be considered as a cantilever which is rigidly connected to the bridge deck and affected by a shear force at its end. The shortening v of the bridge deck can then be derived as $v = Fh3/(3EI)+\varphi h$, assuming that the deformations are small. φ can be derived to $\varphi = FhL/(2EI)$ by regarding half of the bridge deck as a console with a free moment at its end. If the equations are combined, the longitudinal stress in the bridge deck can be expressed as

$$\sigma = \frac{3\alpha\Delta TLEI}{Ah^2(2h+3L)} \qquad (3)$$

where E is the stiffness of the structure, I is the moment of inertia and A is the cross sectional area.

For calculation of restraint stresses in the transversal direction, the restraint force is calculated with equation 1. No outer restraint is assumed to be preventing expansion and contraction of the bridge in the transversal direction. Instead, differences in thermal loads and shrinkage between the structural parts are causing prevented deformations, since the structural

parts are rigidly connected to each other. *R* is calculated with equation 2 which gives *R = 0.5* when creep is neglected and *R = 0.325* if creep is included.

2D Calculations

2D frame models can catch the effects of restraint forces in longitudinal and vertical direction but not the effect in transverse direction. The frame model is the same as the one portrayed in figure 4a, although calculations are also made for abutments rigidly connected to the foundation.

3D Calculations

When linear elastic 3D FE-models are used, the effect of the loads in all three dimensions can be studied. Shell elements are used, making each structural part two-dimensional. The stresses in the longitudinal direction of the bridge deck varies along the transversal direction. Therefore, in order to compare the results with the other methods, mean values of the longitudinal stresses were calculated for each load case.

CALCULATION RESULTS

The calculations generally showed large restraint stresses in transversal direction, and significantly smaller stresses in the longitudinal direction. Including the long time effects of creep and ultimate shrinkage reduced the stresses in most cases.

When calculating by hand, the maximum stress in longitudinal direction was obtained when short time effects were considered. The stress was however a mere 0.0058 MPa. Since the temperature in the bridge deck when uniform thermal load is applied is the same as when different thermal loads are applied to different structural parts, the two load cases give equal results in longitudinal direction assuming the same time period is considered. The maximum stress in transversal direction was on the other hand estimated to 1.6 MPa, when calculating with the load case consisting of different temperature in different structural parts and short term effects. The mean tensile stress capacity of the concrete is however 2.9 MPa, indicating that the quasi-permanent loads are not causing cracking in the structure. All results from hand calculations are displayed in table 6.

Table 6. Hand calculation results. The longitudinal tensile stress values were small but the transversal stress values a lot larger. The long term effects reduced the stresses.

Load case	Time period	Longitudinal direction [MPa]	Transversal direction [MPa]
Evenly lowered temperature	Short	0.0058	0.39
	Long	0.0050	0.11
Bridge deck colder than bridge abutments	Short	0.0058	1.6
	Long	0.0050	0.44

The 2D computer frame model gave similar restraint stresses in longitudinal direction as the hand calculation model. However, the introduction of load cases with thermal gradients over the bridge deck cross section and the adding of fixed supports increased the maximum longitudinal stress value to 0.049 MPa. The worst case thermal distribution consisted of a uniform temperature drop in the entire structure, combined with a gradient heating the top side of the

bridge deck. Since the model does not take the transversal direction into account, no such results were acquired. The entire list of results is shown in table 7.

Table 7. 2D computer frame model calculation results.

Load case	Time period	Longitudinal, pinned [MPa]	Longitudinal, fixed [MPa]
Evenly lowered temperature	Short	0.0058	0.037
	Long	0.0050	0.032
Bridge deck colder than bridge abutments	Short	0.0058	0.037
	Long	0.0050	0.032
Gradient over bridge deck	Short	0.027	0.043
	Long	0.014	0.034
Gradient and evenly lowered temperature	Short	0.015	0.049
	Long	0.0090	0.037

The 3D FE-model results in longitudinal direction are similar to those in 2D computer calculations, and the results in the transversal direction agree well with the hand calculated values. The values are displayed in table 8, where the transversal stresses are maximum values and longitudinal stresses are mean values. Figure 5 shows the transversal stresses in the model for the load case including different thermal loads in bridge deck and bridge abutments.

Table 8. 3D FE-model model calculation results. The values agree well with results from the other calculation methods.

Load case	Time period	Longitudinal, pinned [MPa]	Longitudinal, fixed [MPa]	Transversal [MPa]
Evenly lowered temperature	Short	0.0055	0.037	0.38
	Long	0.0049	0.032	0.16
Bridge deck colder than bridge abutments	Short	0.0042	0.036	1.6
	Long	0.0043	0.031	0.67
	Short	0.031	0.044	0.69

Gradient over bridge deck	Long	0.016	0.036	0.29
Gradient and evenly lowered temperature	Short	0.017	0.051	0.15
	Long	0.0096	0.038	0.070

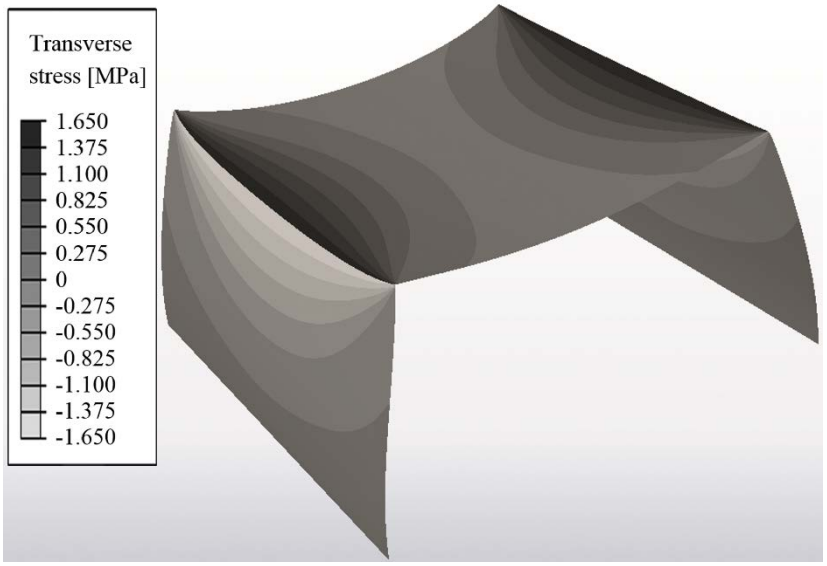

Figure 5. Illustration of the average stress over the cross section in a 3D-model with lower temperature in the bridge deck than in the bridge abutments, and difference in autogenous shrinkage. Large transversal stresses appear close to the frame corners. The stresses are tensile in the bridge deck and compressive in the bridge abutments.

Reinforcement

The reinforcement amounts needed to limit the crack widths when designing in 2D and 3D were calculated with the formulas presented previously. In the longitudinal direction, the EN 1992-1-1 method required Φ20 c-c 640 mm and Φ20 c-c 630 mm for the maximum 2D and 3D-values respectively. These reinforcement amounts are as expected uncontroversial and will be exceeded due to demands for minimum reinforcement, which in this case is $\rho_{s,min} = 0.38\%$, corresponding to Φ20 c-c 160 mm. If the formula for end restrained structures in EN 1992-3 is used, cracking is assumed to have occurred and the required reinforcement is based on the stress capacity rather than the calculated load, making it the same for both calculations. The calculated c-c-distance is in that case only 89 mm.

Using the results from the 3D-calculation in the transverse direction, the required reinforcement is Φ20 c-c 71 mm in the bridge deck if calculated with the method in EN 1992-1-1. The corresponding amount in the bridge abutments becomes Φ20 c-c 90 mm if the positive effect of the autogenous shrinkage on the bridge abutments is neglected. The minimum c-c-distance can be reduced to 85 mm for the bridge deck and 96 mm for the bridge abutments if the force is smoothed out, but the required reinforcement amounts are still significantly higher than the minimum reinforcement amount. The total reinforcement amount needed in transverse

direction, disregarding minimum reinforcement, corresponds to 36 Φ20 reinforcement bars at each frame corner. If instead the method for base restrained walls in EN 1992-3 is used, the result is a total of a mere 1.2 Φ20 bars at each frame corner. The minimum reinforcement will therefore greatly exceed the calculated value in this case.

PARAMETER STUDY

Further 3D calculations were made in order to illustrate the parameter dependency of the transversal restraint force. The investigation was made with the load case causing the highest transversal stress in previous calculations. The parameters investigated were bridge width, height, length, mesh size and thickness of both bridge deck and bridge abutments. Both bridge size and mesh size proved to be insignificant, whereas differences in the height-length ratio (considering either bridge deck or bridge abutment as a base restrained wall) had an expected impact, similar to what has been shown by for example Engström (2007). The thickness ratio between deck and abutments also showed an expected impact on the transversal force. The expected impact was determined by calculating the degree of restraint with equation 2 for different ratios between the cross-sectional areas of the structural parts, and then calculate the transversal force with equation 1.

Another factor investigated was the temperature distribution in the bridge. Instead of applying a uniform temperature in the bridge deck and bridge abutments respectively, a linear temperature variation was applied on the bridge abutments, as is portrayed in figure 6. The temperature on the top of the abutments was the same as the bridge deck temperature, and the temperature at the bottom of the abutments such that the average temperature difference between the parts was equal to the value calculated according to Eurocode.

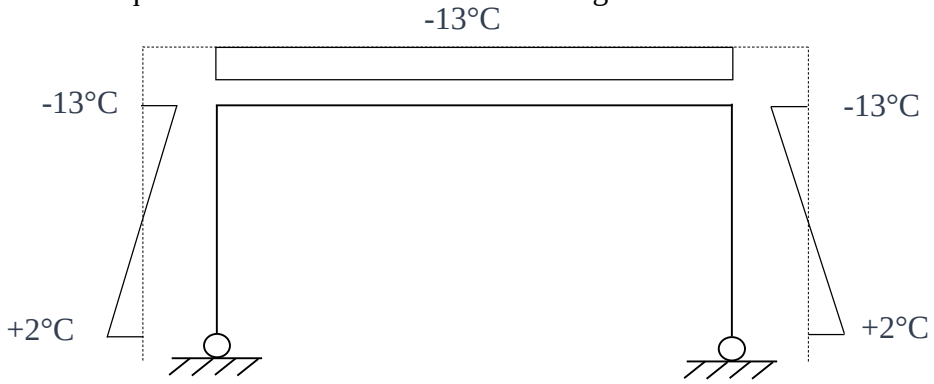

Figure 6. Temperature distribution tested within the parameter study. The difference in average temperature be-tween bridge deck and abutments, 7.5°C, is the same as in previous calculations with temperature differences between structural parts. But in those calculations the temperature was assumed to be uniform also in the bridge abutments.

For this load case, transversal forces appeared in a different pattern than before, with large transversal tensile stresses appearing on both sides of the frame corners and compressive stresses appearing at the bottom of bridge abutments, as shown in figure 7. The maximum value of the transversal stress is still rather large in the figure as it reaches 0.62 MPa at the frame corners, but then the autogenous shrinkage is not considered due to calculation technicalities. Introducing autogenous shrinkage in-creases the tensile stress with 0.38 MPa in the bridge deck beside the frame corners, and reduces the stress in the bridge abutments with the same magnitude.

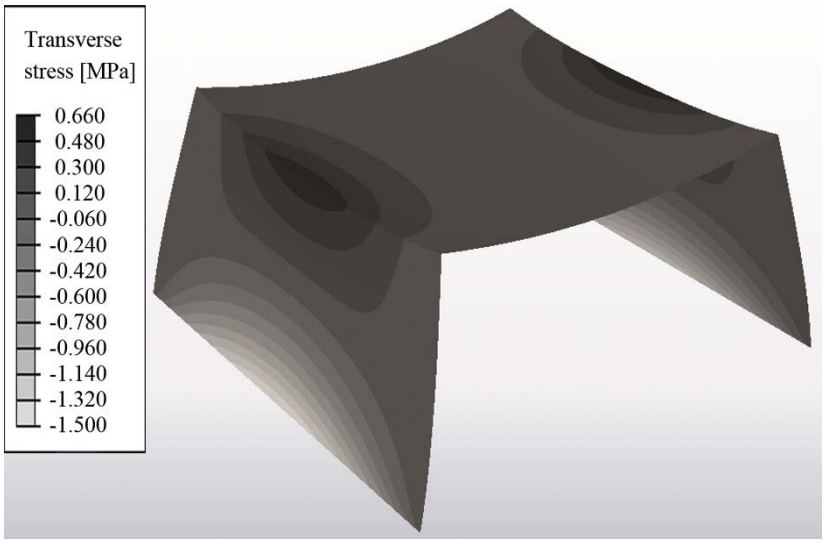

Figure 7. Transverse stresses in the case of a linear thermal distribution in a portal frame bridge, without consideration of autogenous shrinkage.

The stresses at the frame corners are smaller in this case compared to previous calculations. If however the thermal distribution in figure 6 is reversed so that the bridge deck is warmer than the bridge abutments, and the temperature in the bridge abutments increase with the height, the stresses in figure 7 will change sign. This means that reinforcement in the transversal direction is not only needed at the frame corners, but also at the base of the bridge abutments.

CONCLUSIONS AND FURTHER RESEARCH NEEDS

This study has shown that large tensile stresses appear in the transverse direction of portal frame bridges close to the frame corners when designing for restraint forces according to Eurocode. The worst load case includes a lower uniformly distributed thermal load in the bridge deck than in the bridge abutments, combined with a difference in autogenous shrinkage. Including long term effects in the model reduces the transversal stresses.

The thermal load distribution used in the load case is however unrealistic, since in reality the temperature must change over a certain distance. A more smooth thermal distribution could possibly lead to smaller tensile stresses, reducing the required reinforcement amount. The introduction of a linear thermal variation over the height of the bridge did not cause a significant drop in transverse stresses, and it is unclear whether it is a reasonable thermal distribution.

The maximum stress values in transversal direction are similar in hand calculations and linear elastic 3D FE-calculations. The advantage of the FE-model is that it does not only show the maximum value, but also gives an image of the variation of the stress in the bridge. The variation of stresses reveals the variation in degree of restraint, and resembles results for edge restrained walls shown by for example Engström (2007).

The reinforcement amount needed to limit crack widths according to the method presented in EN 1992-1-1 (2004), which covers design of concrete structures in general, is significantly larger than the minimum reinforcement amount. The magnitude of the transversal force is however exaggerated, since the reduction of restraint forces due to cracking is not taken into account in the design procedure. Even though the quasi-permanent load combination only causes stresses which are smaller than the tensile stress capacity of the concrete, the element could crack at a time when the quasi-permanent load is exceeded. Also, the idea of applying reinforcement in order to reduce crack widths calls for the assumption of cracks in the structure.

The cracking and following stiffness reduction would however not affect the reinforcement needed according to EN 1992-3 (2006), the Eurocode document covering design of liquid

containing structures, since the strain difference in the equation only depends on the restrained strain and not on the restrained stress. Several investigations, including Bamforth et al. (2010) and Zangeneh Kamali et al. (2013), have compared crack widths in real experiments or non-linear FE-calculations with values calculated with the edge restrained EN 1992-3-metod, and found them to agree rather well. However, Bamforth et al. (2010) notes that the EN 1992-3-formula does not take several important factors into account, such as concrete stress capacity and wall geometry. Even in the Eurocode document it is stated that there "appears to be little published guidance" for the method (EN 1992-3, 2006). Another issue with using the expression in bridge design is the fact that it is presented in the Eurocode document which regards liquid containing structures, and not bridges. It should therefore not be used in design of a bridge without further investigations being made, including bridge design performed with non-linear FE-calculations.

2D frame models do not capture the effects of transversal restraint forces acting on a portal frame bridge, but they do capture stresses in the longitudinal direction. The stresses in longitudinal direction were found to be a lot smaller than the maximum stress in transversal direction, regardless of the use of calculation method. When calculating reinforcement amounts in longitudinal direction, the required amount according to the method presented in EN 1992-1-1 (2004) was a lot smaller than the minimum reinforcement amount, as could be expected since the load was small. The end restrained model in EN 1992-3 (2006) on the other hand gave reinforcement amounts larger than the minimum reinforcement, since it is based on the assumption that the restraint force equals the concrete tensile load capacity. In this case, that assumption leads to a vast overestimation of the restraint force.

In order to establish a design method which is giving reasonable results and is well adjusted to modern linear elastic 3D FE-models, a more accurate thermal distribution is needed for the load case with different temperatures in different structural parts. The new thermal distribution should be determined by thermal simulations and measurements. The reduction of restraint forces in bridges due to cracking, and the effect of the reduced restraint forces on crack widths should also be investigated. This investigation can be performed with non-linear FE-models.

REFERENCES

ACI Committee 2007 1995. Effect of restraint, volume change and reinforcement on cracking of mass concrete. ACI Materials Journal 87: 271-295.

Bamforth, P., Denton, S. & Shave, J. 2010. The development of a revised unified approach for the design of reinforcement to control cracking in concrete resulting from restrained contraction. ICE Research project 0706.

Elbadry, M. & Ghali, A. 1995. Control of Thermal Cracking of Concrete Structures. ACI Structural Journal 92: 435-450.

Engström, B. 2007. Restraint cracking of reinforced concrete structures. Gothenburg: Chalmers University of Technology.

Jokela, J. 1984. Crack Control of Reinforced Concrete with Continuous Edge Restraint. Nordic Concrete Research 3:100-128.

EN 1990 (2002), Eurocode - Basis of structural design. Brussels: European Committee for Standardization.

EN 1991-1-5 (2003), Eurocode 1: Actions on structures - Part 1-5: General actions - Thermal actions. Brussels: European Committee for Standardization.
EN 1992-1-1 (2004), Eurocode 2: Design of concrete structures – Part 1-1: General rules and rules for buildings. Brussels: European Committee for Standardization.
EN 1992-2 (2005), Eurocode 2: Design of concrete structures - Part 2: Concrete bridges - Design and detailing rules. Brussels: European Committee for Standardization.
SS-EN 1992-3 (2006), Eurocode 2: Design of concrete structures – Part 3: Liquid retaining and containment structures. Brussels: European Committee for Standardization.
Trafikverket 2011. TRVR Bro 11. Trafikverket.
Zangeneh Kamali, A., Svedholm, C. & Johansson, M. 2013. Effects of restrained thermal strains in transversal direction of concrete slab frame bridges. Stockholm: Royal Institute of Technology.

BILAGA B:

Simulation of Thermal Load Distribution in Portal Frame Bridges

Erik Gottsäter, Oskar Larsson, Miklós Molnár, Roberto Crocetti

Lund University, Lund, Sweden

Mario Plos

Chalmers University, Gothenburg, Sweden

Contact: erik.gottsater@kstr.lth.se

Abstract

Uneven exposure to e.g. solar radiation can cause temperature differences between various structural parts of a bridge, which leads to tensile stresses if the parts cannot move freely. In this study, thermal simulations and stress calculations on a model of a portal frame bridge are performed with the aim of evaluating the temperature difference between the bridge parts. It is shown that the temperature difference between parts which is proposed by Eurocode 1 is overestimated, thus the resulting stress distribution being unrealistic. Using the design method proposed by Eurocode 1 is therefore likely to exaggerate the required reinforcement in crack width limit design, which in turn would lead to unnecessary costs and environmental impacts. Further studies are needed in order to determine proper thermal load values and temperature distributions.

Keywords: Thermal load, portal frame bridge, restraint stresses, thermal simulations, Eurocode.

Introduction

Changing weather conditions lead to temperature variations in bridges both over time and space. The temperature variations are caused by e.g. varying air temperature, temperature of adjacent soil, short wave radiation, wind speed, and long wave radiation from the ground and the sky. The air temperature has a large impact on the structural temperature, but impacts the bridge temperature relatively slowly. Increased wind speed makes the structure adjust its temperature faster due to convection. Soil temperature is more constant than the air temperature, and therefore levels out temperature variations in adjacent parts of the structure. Short wave radiation which originates from the sun can heat exposed surfaces significantly, contributing to rapid changes in temperature. Long wave radiation heat transfer to or from the sky can affect temperatures in a similar manner.

Due to these different thermal factors, the temperature in a bridge can at a certain time vary in different ways. One possible way is by temperature gradients over cross sections, investigated by i.e. Larsson [1] and Peiretti et al. [2]. Another type of temperature variation is the temperature differences between structural parts, which might appear e.g. between the flange and the web in a box-section bridge, the beam and the bridge deck in a girder bridge, or between deck and abutment in a portal frame bridge. The temperature variations cause the volume of structural parts to vary, and in structural members prevented from changing their shape, e.g. by expanding, contracting or bending, restraint stresses therefore appear.

Constant temperature loads and linear temperature gradients in cross sections cause restraint stresses if an outer restraint is present, i.e. if an adjacent structure is preventing the desired

expansion or contraction [3]. In cross sections with nonlinear temperature gradients the cross section itself causes stresses to appear, since the strain varies linearly over the cross sectional height. The sum of the stresses over the cross section must be zero if no outer restraint is present [4]. Figure 1 shows an example of a nonlinear temperature distribution over a cross section which is not prevented from bending, and the stresses caused by the temperature. This sort of restraint is called inner restraint, since the restraint is caused by the structural part itself [3] In real structures, both inner and outer restraint situations occur simultaneously although they are generally treated as separate loads in design.

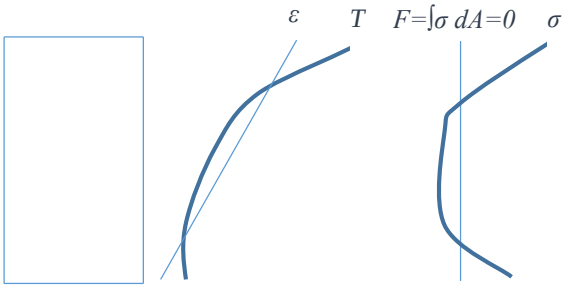

Figure 1. A rectangular cross section (left) is subjected to a non-linear temperature distribution, causing a linear strain (center) which in turn causes varying stresses over the cross section (right). Figure after Jokela [4].

The restraint stresses alone, or in combination with other stresses, may cause cracking of a concrete bridge. Cracking in turn reduces the durability of the structure, and increases the need for maintenance. Therefore, crack widths are limited in bridge design in order to reduce their negative impact on the structure. In Eurocode, quasi-permanent loads, which corresponds to load values that are exceeded 50% of the time, are used when limiting crack widths. The load values are obtained by multiplying the characteristic loads with the ψ_2-coefficient, which equals 0,5 for thermal loads on bridges [5]. The thermal loads themselves are presented in EN 1991-1-5 [6]. Three main types which always shall be included in design are uniform thermal load over the entire structure, linear or bilinear temperature gradient over cross sections, and temperature differences between structural parts. The uniform thermal load shall also be combined with the gradient and temperature difference between structural parts, one at a time. Temperature gradients are however not supposed to be combined with temperature differences between structural parts. Nor are gradients applied in more than one structural part at a time.

The load values of these three different thermal load types are determined based on different factors. For the uniform thermal load, the characteristic load value depends on the bridge type and the location of the bridge. The temperature gradients in bridge decks are determined based on the bridge type, thickness of asphalt layer and cross sectional height. For abutments, a linear temperature difference of 15°C is assigned. In the case of different temperature in different structural parts, a recommended value of 15°C is given. Although not specifically stated in the code, the values for gradients and temperature differences between structural parts are here assumed to be characteristic values. The background document to thermal loads in Eurocode 1, ENV 1991-2-5 [7], does not state the motivation of the choice of 15°C as the temperature difference between structural parts. It is however stated that the previous Spanish code used the value of 5°C for concrete structures, and that the German code also had a value, which according to Římal and Šindler [8] was given in DIN 1072 as 5°C between structural parts of concrete and 15°C for other materials.

In this paper, the temperature difference between structural parts in portal frame bridges is investigated using simulations with climate data from a two-year period in Stockholm. Also, the resulting transversal stresses are calculated and compared with stresses obtained when applying thermal load cases from Eurocode 1. Portal frame bridges were chosen due to their simple geometry and rigid connections between bridge parts that enables restraint effects. Also, the bridge type is very commonly used in Sweden.

Temperature effects on portal frame bridges

In the case of a portal frame bridge as in figure 2, the bridge deck and abutments are rigidly connected. Each structural part can therefore be

considered to be restrained from expanding or contracting in the transverse direction by the adjacent part, since the transverse length of the bridge deck and the abutments must remain the same at the corners. Therefore, restraint stresses will appear in the transverse direction if the structural parts have different temperatures.

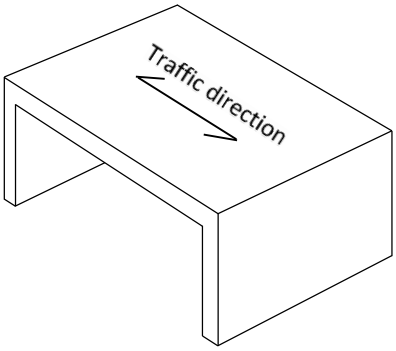

Figure 2. An example of a portal frame bridge. The two abutments are rigidly connected to the bridge deck.

Theoretically, at least three simple reasons for temperature differences between the structural parts can be found for the bridge type shown in figure 2: difference in solar radiation influx, long wave radiation and conduction from soil. The difference in solar radiation is due to the top side of the bridge deck being directly exposed to sunshine, while the abutments are mostly shaded by the bridge deck. The difference in heat influx between the parts is in this case largest when the sun is at its highest position in the sky, indicating that the largest temperature differences due to solar radiation will appear during summer.

A difference in long wave heat radiation appears when there is a large amount of outgoing long wave radiation from the bridge to the sky. This situation is most likely to appear during clear nights, often during winter. A large amount of outgoing radiation will lower the bridge deck temperature more than the abutment temperature, since the abutments are not facing the sky to the same extent.

The soil temperature is affecting the abutments due to their large contact surface. Hillel [9] presents the principal variation of soil temperature during a year, showing that the soil at a depth of at least 1 m is generally colder than the air in summer and warmer than the air in winter. This means that the soil is leveling out the abutment temperature, and will therefore contribute to a larger temperature difference between deck and abutments.

The influence of soil temperature and radiation on the bridge temperature depends on the density, specific heat capacity and thermal conductivity of the asphalt, concrete and soil. The solar absorptivity is also of importance for the asphalt, and the emissivity is of importance for all of the materials, since they are all emitting radiant heat. For the concrete, the density mainly depends on the aggregate type and degree of water saturation, the thermal conductivity mainly depends on the density, degree of water saturation and the thermal conductivity of cement and aggregate. The specific heat capacity of concrete depends mainly on the temperature, moisture content and water cement ratio [10]. For asphalt, the amount of bitumen, which has a lower thermal conductivity than the aggregate, as well as the type of aggregate used, are the main factors influencing the conductivity [11]. The solar absorptivity of asphalt depends on the color of the surface, newer surfaces are generally darker and therefore have larger solar absorptivity values. According to Sundberg [12], the values of the soil parameters depend on the grain size, porosity, water saturation level of the soil and whether the soil is frozen or not. Cohesive soils are generally more conductive due to a larger water saturation degree above ground water level.

Simulation models

The thermal simulations were performed in the commercial FE program Brigade/Plus version 6.1, which uses an Abaqus FEA solver. The model consists of a longitudinal bridge cross section of quadratic elements 50x50 mm^2 and a 4 m wide and 4 m deep (measured from the bottom of the abutments) soil layer, modeled with quadratic elements 250x250 mm^2. Choosing a 4 m wide soil layer beside the bridge is motivated by initial simulations, showing a convergence of results when the width of the model approaches 4 m. Along the bottom of the soil in the model the temperature is set to a constant 5°C, which corresponds to the annual mean temperature of

the location. This choice is based on principal temperature variations over depth in soil given by Hillel [9]. Over the vertical edges of the model, heat transfer is prevented.

The asphalt layer is 0,1 m thick and covers the bridge deck surface and the surface of the adjacent soil. The bridge deck and abutments are both 0,5 m thick, and the system line of the modeled part of the cross section is 4 m long both in vertical and horizontal direction. The abutment is placed on a concrete foundation with a cross section of 2,5x1 m^2, which is not considered as a part of the abutment in calculations but affects the thermal properties of the area. The model is depicted in figure 3.

The material parameters are presented in table 1. Parameters regarding concrete and asphalt are from Larsson [1] whereas soil parameters are derived from Sundberg [12], and are valid for unfrozen sand of porosity 50% above ground water level.

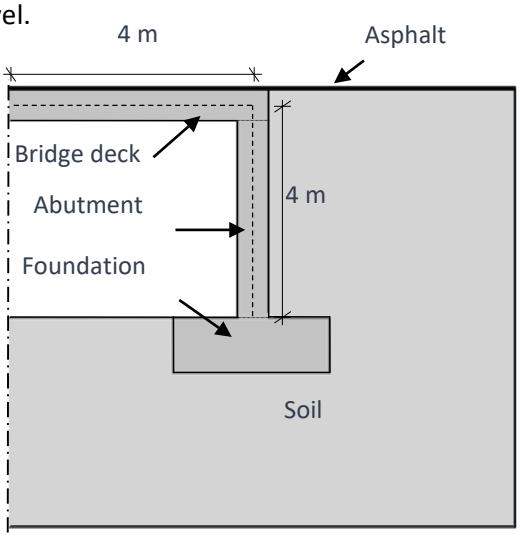

Figure 3. Geometry of the FE-model used in simulations. The model consists of half of a longitudinal bridge cross section and soil.

The method used for the simulation is adopted from Larsson [13] which was verified by temperature measurements at 10 different levels in a 255 mm thick concrete slab. The simulation method has also been validated for a hollow concrete box cross-section in Larsson and Karoumi [14]. Air temperature, solar radiation, long wave heat radiation and convection are used as factors affecting the total heat energy in the model. The climate data used is obtained from two years of measurements in Stockholm, from the 1st of January 1986 to the 31st of December 1987, by the Swedish metrological and hydrological institute (SMHI). Larsson and Thelandersson [15] found the chosen climate data to give the most unfavorable stresses in a concrete structure from a 15 year period of data. Air temperature and wind speed are given for every third hour, and short and long wave radiation for every hour. The convection is assumed to act equally on all surfaces exposed to air, and its coefficient is calculated from measured wind speeds as

$$h_c = 6 + 4V,\ V \leq 5\ \mathrm{m/s} \quad (1)$$

$$h_c = 7{,}4V^{0{,}78},\ V > 5\ \mathrm{m/s} \quad (2)$$

Table 1. Parameters used in simulations.

Material	Density [kg/m3]	Specific heat capacity [J/(kg·°C)]	Thermal conductivity [W/(m·°C)]
Concrete	2400	900	2,5
Asphalt	2200	880	0,7
Soil	1900	660	0,5

Solar radiation is added as heat flux upon the top surface of the bridge deck, which is assumed never to be shaded by any object. No solar radiation is reaching the abutment in the model. These choices cause the largest difference in radiation influx between the structural parts, and are therefore assumed to give a worst case scenario. The solar absorptivity is set to 0,8 and the emissivity to 0,9. Long wave radiation from the sky is treated as a corresponding air temperature, i.e. the sky is treated as a surface with a temperature corresponding to the measured value of long wave radiation. Long wave radiation and convection is thereby added to the model as surface to ambient interactions.

3D stress calculation

The initial simulation was followed by a simulation of a 3D-model of the bridge, in which the bridge is assumed to be 8 m wide, and cubic elements 50x50x50 mm^3 are used. It was only carried out for

a 7-day period of climate data that rendered the largest temperature differences between bridge deck and abutments. The model was used to evaluate the stresses in transverse direction caused by the thermal load, and used the same parameter values as presented above, but soil was excluded from the model, i.e. no heat transfer took place over edges facing soil. The temperature distribution at each time step obtained from the thermal simulation was used in a structural analysis using linear elastic material models and parameter values presented in table 2.

Table 2. Parameters used in stress calculation. No soil was included in the model.

Material	**Young´s modulus [GPa]**	**Poisson´s ratio**	**Coefficient of thermal expansion [°C^{-1}]**
Concrete	33	0,2	10^{-5}
Asphalt	0,003	0,1	10^{-5}

The asphalt layer was assumed to be rigidly connected to the concrete, but in reality it is generally separated from the concrete by a thin film or insulation in order to simplify replacement. Separating the materials causes the asphalt to have a negligible influence on the stiffness of the bridge deck, which was obtained in the model by choosing a relatively low stiffness value. The choice of concrete stiffness and coefficient of thermal expansion is in reality arbitrary, since the resulting stresses vary linearly with both stiffness and thermal expansion. The 3D model utilizes double symmetry, i.e. translations are prevented perpendicular to the symmetry faces, and all vertical translations of the bottom of the abutment are prevented, as well as translations in the longitudinal direction of the bridge. Translations in the transverse direction were however allowed, since the foundation was assumed to expand and contract with temperature in a similar way as the abutment. Since there could be a temperature difference between foundation and abutment as well, there could in reality also be restraint stresses in transverse direction between foundation and abutment. This was however not covered in this study.

The results were compared with simulations of quasi-permanent Eurocode thermal load cases, rendering a 7,5°C temperature difference between the parts, 5,25°C linear temperature difference over the bridge deck cross section and 7,5°C over the abutment. In the simulations with gradients, a heat transfer analysis was performed to determine the temperature of the structure, assigning the temperature along the edges of one of the parts. This rendered a linear temperature variation over one cross section, and a slightly varying temperature in the part not assigned any temperature at its surfaces.

Results

The temperature in the model was shown to vary in an expected way, with regards to the influence of the soil and radiation. Over the entire simulation period, the difference in mean temperature calculated as mean temperature in the bridge deck minus mean temperature in the abutment varies as is shown in figure 4.

The largest positive difference in mean temperature between the parts was 6,8°C, and the largest negative value obtained was -3,7°C. This shows that a quasi-permanent temperature difference of 7,5°C as suggested by Eurocode 1 is likely a significant overestimation of the temperature differences between the structural parts. The positive value was obtained for a day in June and the negative for a day in January. The corresponding temperature in the model for the two occasions is portrayed in figure 5.

In figure 6, the temperature along the system line of the structure is shown for the occasions with the largest positive and negative temperature difference respectively. It is obvious in the figure that a large change in temperature occurs in the corner region, but the change is gradual.

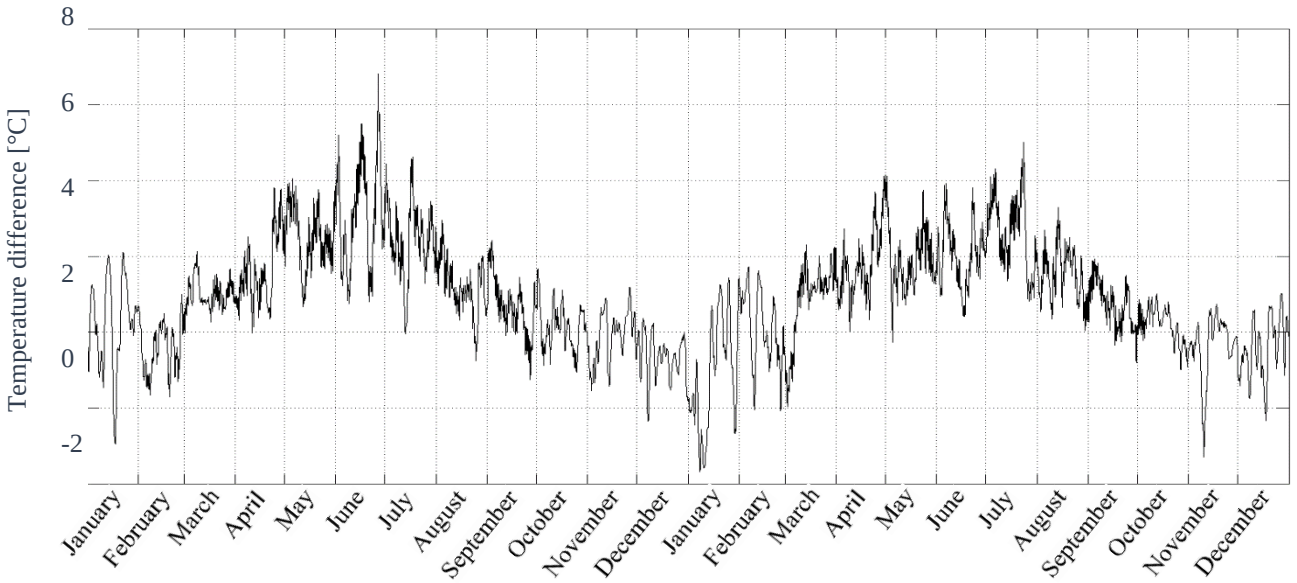

Figure 4. The variation in mean temperature between structural parts, calculated as mean temperature in the bridge deck minus mean temperature in the abutment. It is obvious that there are generally large positive differences during summer, and not quite as large negative differences in winter.

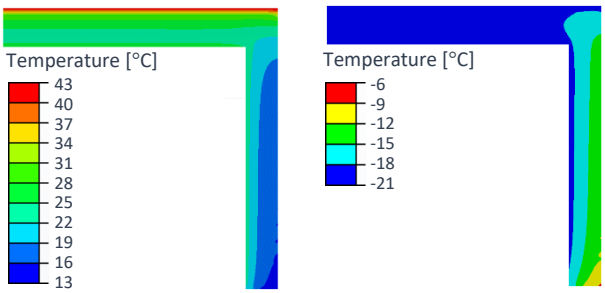

Figure 5. Temperature in the model when the largest positive (left) and negative (right) temperature differences are present between deck and abutment.

Stress calculation in 3D-model

The stress distribution at the time for the largest tensile transverse stresses in the structure is shown in figure 7. The free edges towards the left in the figure are symmetry sections, since double symmetry is used in the model. The maximum stress is in this case about 1,3 MPa and appears on the back side of the abutment. The fact that the stresses are largest at the back of the abutment is not surprising since this is where the bridge is coldest, which was shown in figure 5. The stress is largest close to the top of the abutment, and then decreases further down, due to a lower degree of restraint further away from the restrained edge along the frame corner. Another influencing factor is the curvature of the abutment, which shortens the length of the back side of the abutment.

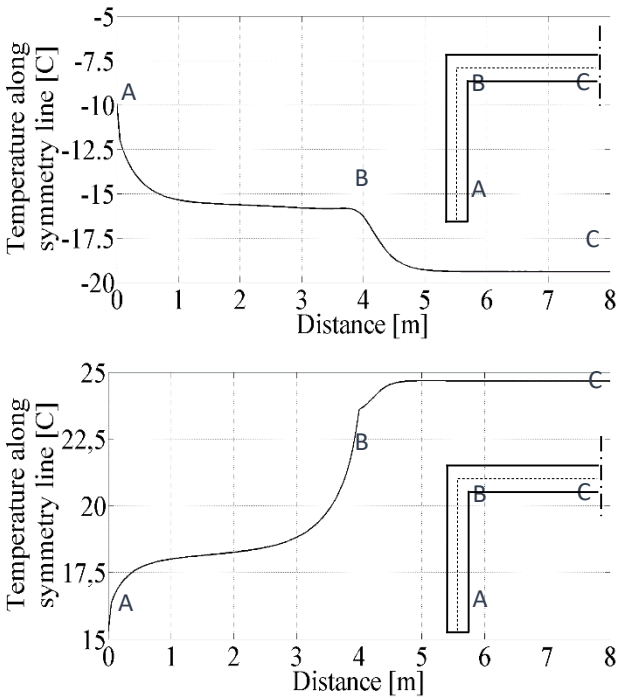

Figure 6. Temperature variation along the system line for the occasions with the largest positive (top) and negative (bottom) temperature difference between structural parts. The distance is measured from the bottom of the abutment, the frame corner is at 4 m and the mid-span at 8 m.

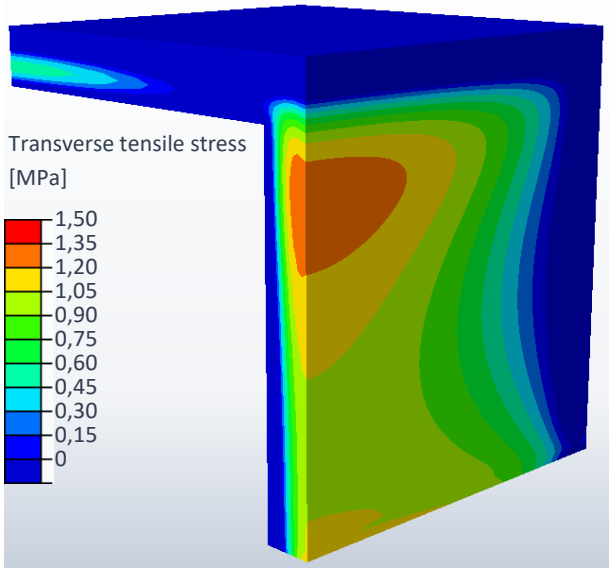

Figure 7. Stress in transversal direction when the largest temperature difference between the structural parts is used in calculations. The visible gables of the bridge are symmetry sections.

Curvature is not only prevented at the top, but also at the bottom edge, by the boundary conditions. This is a likely cause for the stress increase close to the bottom of the abutment.

The design load cases in Eurocode 1 caused stresses according to figure 8, where transversal stresses resulting from different temperature in the two parts as well as gradients in either deck or abutment are shown. It is obvious that the results shown in figure 8 differ from the results obtained with climate data in figure 7, and that some of the stress distributions shown in figure 8 are both unrealistic and unfavourable.

Conclusions

The main conclusions from this paper are:

- Uneven exposure to thermal radiation and conduction causes the mean temperature to vary between the structural parts of a portal frame bridge. The bridge deck is generally warmer than the abutment in summer, and in winter the situation is the opposite.
- The change in temperature along the system line of the structure is most significant close to the frame corner, while gradients can be present in both parts simultaneously.

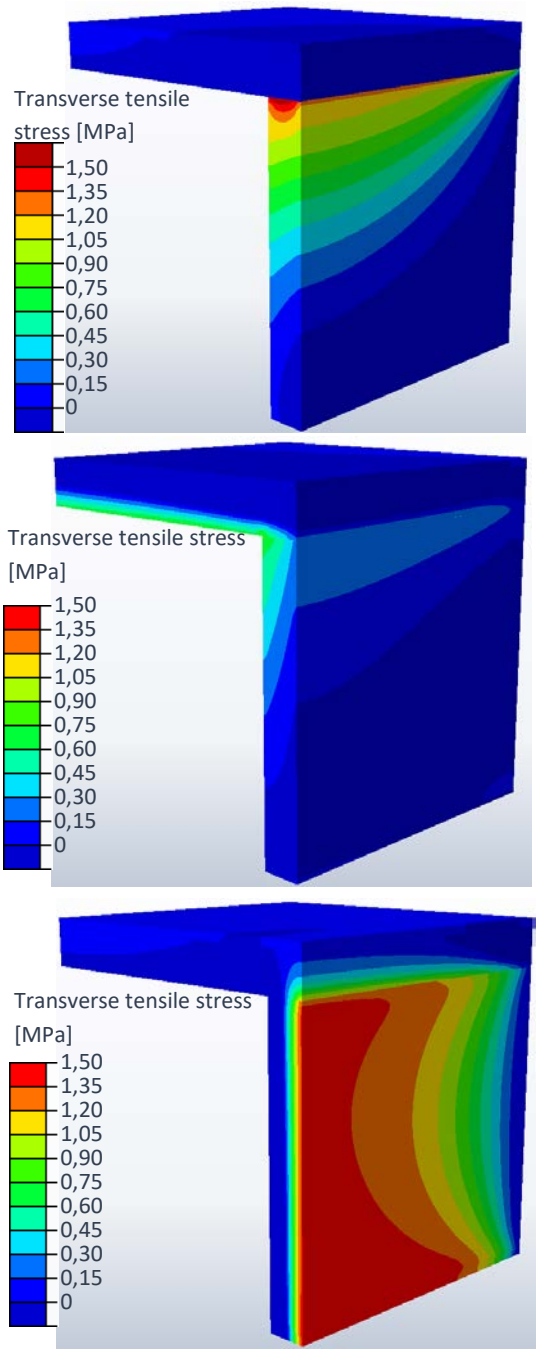

Figure 8. Stress in transversal direction for the following Eurocode load cases: bridge deck being warmer than abutment (top), gradient through bridge deck (middle) and gradient through abutment (bottom). The visible gables of the bridge are symmetry sections.

- The resulting transversal stresses obtained when using temperature distributions acquired from climate simulations are significantly different from the results of Eurocode 1 load cases. Not only the

absolute values of stresses differ, but also the locations of the largest stress values.

- The quasi-permanent value in Eurocode 1 for different temperatures in different structural parts is likely to be exaggerated, since it is significantly larger than the extreme value obtained from the simulation using two years of climate data.

Overestimating thermal loads will lead to the use of exaggerated reinforcement amounts. Therefore, determining a realistic thermal load is likely to reduce the reinforcement needed in portal frame bridges, which in turn makes the bridges cheaper to construct and also reduces the environmental impact of the structure. Further work should aim to determine new load values by using longer time sequences in simulations, and also by using climate data from more locations. Also, a parameter study should be made to investigate the impact of the choice of geometry and the material parameters.

Another aspect that could be accounted for in design is that cracking reduces the restraint stresses. Therefore crack widths will not be as large as expected when using linear elastic models in design, if cracking is caused by thermal stresses. Nonlinear models could be used to estimate the width of cracks caused by restraint effects, which possibly could motivate an even further reduction of reinforcement use.

References

[1] Larsson O. *Climate related thermal actions for reliable design of concrete structures.* PhD Thesis, Lund University, Lund, Sweden: Division of Structural Engineering; 2012.

[2] Peiretti P.H, Parrotta E.J, Oregui B.A, Caldentey P.A, Fernandez A.F. Experimental Study of Thermal Actions on a Solid Slab Concrete Deck Bridge and Comparison with Eurocode 1. *Journal of Bridge Engineering.* 2014; 19(10)

[3] Engström B. *Restraint cracking of reinforced concrete structures.* Chalmers University of Technology, Gothenburg, Sweden: Division of Structural Engineering; 2007.

[4] Jokela J. Behaviour and Design of Concrete Structures under Thermal Gradients. *Nordic Concrete Research.* 1984; (3): 100-128.

[5] EN 1990. *Eurocode - Basis of structural design.* Brussels: European Committee for standardization; 2002.

[6] EN 1991-1-5. *Eurocode 1: Actions on structures - Part 1-5: General actions: Thermal actions.* Brussels: European Committee for standardization; 2003.

[7] ENV 1991-2-5. Eurocode 1: Basis of design and actions on structures - Part 2-5: Actions on structures - Thermal actions ;1996.

[8] Římal J, Šindler D. Comparison of Temperature Loadings of Bridge Girders. *Acta Polytechnica*. 2008; 48(5): 22-28.

[9] Hillel D. *Introduction to environmental soil physics*. San Diego: Academic Press; 2004.

[10] Ljungkrantz C, Möller G, Petersons N. *Betonghandbok - material, 2nd edition*. Solna: Svensk byggtjänst; 1994.

[11] Dickinson E.J. Method for Calculating the Temperature Gradients in Asphaltic Concrete Pavement Structures Based on Climatic Data. *Australian Road Research*. 1978; 8(4): 16-34.

[12] Sundberg J. *Termiska egenskaper i jord och berg.* Linköping: Statens geotekniska institut; 1991.

[13] Larsson O. Modelling of Temperature Profiles in a Concrete Slab under Climatic Exposure. *Structural Concrete*. 2009; 10(4): 193-201.

[14] Larsson O, Karoumi R. Modelling of Climatic Thermal Actions in Hollow Concrete Box-Cross-Sections. *Structural Engineering International*. 2011; 21(1): 74-79.

[15] Larsson O, Thelandersson S. Transverse thermal stresses in concrete box cross-sections due to climatic exposure. *Structural Concrete*. 2012; 13(4): 227-235.

BILAGA C:

Engineering Structures 143 (2017) 219–231

Contents lists available at ScienceDirect

Engineering Structures

journal homepage: www.elsevier.com/locate/engstruct

Simulation of thermal load distribution in portal frame bridges

Erik Gottsäter [a,*], Oskar Larsson Ivanov [a], Miklós Molnár [a], Roberto Crocetti [a], Filip Nilenius [b], Mario Plos [b]

[a] Division of Structural Engineering, Faculty of Engineering, LTH, Lund University, P.O. Box 118, SE-221 00 Lund, Sweden
[b] Department of Civil and Environmental Engineering, Chalmers University, SE-412 96 Gothenburg, Sweden

ARTICLE INFO

Article history:
Received 27 September 2016
Revised 1 March 2017
Accepted 5 April 2017

Keywords:
Thermal simulations
Portal frame bridge
Thermal load
Restraint stresses
Eurocode
Parametric study

ABSTRACT

Uneven exposure to e.g. solar radiation can cause temperature differences between various structural parts of a bridge, which leads to tensile stresses if the parts cannot move freely. In this study, thermal simulations and stress calculations on a model of a portal frame bridge are performed with the aim of evaluating the temperature difference between the bridge parts. Factorial design is used in a parametric study to determine the influence of different factors on the temperature difference and the largest reasonable temperature difference obtainable for the chosen weather data. The study shows that the quasi-permanent temperature difference between parts which is proposed by Eurocode 1 is overestimated, causing tensile stresses in the transverse direction to be exaggerated significantly. Using the design method proposed by Eurocode 1 is therefore likely to overestimate the required reinforcement in crack width limit design, which in turn would lead to unnecessary costs and environmental impacts. The results also indicate that the temperature distribution within the bridge is different from what is given in Eurocode load cases, and consequently, the largest tensile stresses appear in other areas of the bridge. A simplified temperature distribution is therefore investigated and shown to give similar results as the detailed thermal simulations.

1. Introduction

Temperature variations in bridges can occur both over time and space, due to changes in weather conditions such as air temperature, wind speed and solar radiation. The temperature changes due to three modes of heat transfer, namely conduction, convection and radiation. Air temperature affects the temperature of the structure by conduction and convection. Conduction describes heat transfer within a medium or between two media in direct contact with each other. The heat energy is transmitted directly between molecules in either solid, liquid or gas state. Convection on the other hand takes place in either a gas or a liquid, and combines the molecular heat transfer of conduction with a mixing effect, which speeds up the heat transfer. In the case of heat transfer between a gas and a solid, the mixing constantly replaces the gas molecules closest to the surface of the solid, which increases the speed of the conduction at the surface. Thereby, wind speed increases the heat transfer at a bridge surface [1].

Radiation describes heat transfer between objects separated by a transparent medium. The radiant heat can be described as an electro-magnetic wave, and its wavelength depends on the temperature of the emitting body. The higher the temperature of the surface, the shorter the wavelength of the emitted energy [1]. Short wave radiation relates to heat energy emitted by the sun, and long wave radiation relates to heat energy emitted by objects with a temperature similar to that on earth. Long wave radiation reaches the earth from the sky, emitted by various objects and particles in the atmosphere and in space [2].

The temperature in a bridge can at a given time vary in different ways. One possible way is by temperature gradients over cross sections, investigated by i.e. Larsson [3], Peiretti et al. [4]. Another type of temperature variation is temperature differences between structural parts, e.g. between the flange and the web in a box-section bridge [5,6], the box-girder and the bridge deck in a girder bridge [7,8], or between deck and abutment in a portal frame bridge. Temperature variations cause the volume of structural parts to vary, and in structural members prevented from changing their shape, (e.g. by expanding, contracting or bending) restraint stresses therefore appear.

Constant temperature loads and linear temperature gradients in cross sections cause restraint stresses if an outer restraint is present, i.e. if an adjacent structure is preventing the desired expansion or contraction [9]. The cross section itself causes stresses to appear if nonlinear temperature gradients are present, since the strain varies linearly over the cross sectional height. The sum of

* Corresponding author.
E-mail address: erik.gottsater@kstr.lth.se (E. Gottsäter).

http://dx.doi.org/10.1016/j.engstruct.2017.04.012
0141-0296/

the stresses over the cross section must be zero if no outer restraint is present [10]. Fig. 1 shows an example of a nonlinear temperature distribution, and the resulting stresses, over a beam cross section which is not prevented from bending. This type of restraint is called inner restraint, since it is caused by the structural part itself [9]. In real structures, both inner and outer restraint situations occur simultaneously although they are generally treated as separate loads in design.

The restraint stresses alone, or in combination with other stresses, may cause cracking of a concrete bridge. Cracking in turn reduces the durability of the structure, and increases the need for maintenance. Crack widths are limited in bridge design in order to reduce their negative impact on the structure. On the other hand, cracking reduces the stiffness of the structure, which leads to increased deformations. This in turn causes the restraint stresses to decrease. Structures close to collapse are often so deformed that restraint stresses become very small, which is why restraint effects are often only considered in serviceability limit state in design, and not in ultimate limit state. In Eurocode, quasi-permanent loads are used when limiting crack widths. These loads shall correspond to load values that are exceeded 50% of the time. The load values are obtained by multiplying the characteristic loads with the ψ_2-coefficient, which equals 0.5 for thermal loads on bridges [11]. The thermal loads themselves are presented in EN 1991-1-5 [12].

Three main types of thermal loads which always shall be considered in design are uniform thermal load over the entire structure, linear or bilinear temperature gradient over cross sections, and temperature differences between structural parts. The uniform thermal load shall be combined with the gradient and temperature difference between structural parts, one at a time. Temperature gradients are however not supposed to be combined with temperature differences between structural parts. Nor are gradients applied in more than one structural part at a time. The level of these three different thermal load types are determined based on different factors. For the uniform thermal load, the characteristic load value depends on the bridge type and the geographical location of the bridge. The temperature gradients in bridge decks are determined based on the bridge type, thickness of asphalt layer and cross sectional height. For abutments, a linear temperature gradient of 15 °C is assigned. In the case of temperature difference between structural parts, a recommended value of 15 °C is given. Although not specifically stated in the code, the values for gradients and temperature differences between structural parts are here assumed to be characteristic values.

The background document to thermal loads in Eurocode 1, ENV 1991-2-5 [13], does not state the motivation of the choice of 15 °C as temperature difference between structural parts. It is however stated that the previous Spanish code used the value of 5 °C for concrete structures, and that the German code also considered the load case. According to Římal and Šindler [14], the German load value was given in DIN 1072 as 5 °C between structural parts of concrete and 15 °C for other materials.

Applying the Eurocode 1 temperature difference between structural parts causes large stresses in the transversal direction for some bridge types. Especially the crack width limitation design can lead to large reinforcement requirements, if the thermal loads are applied in simplified ways and no consideration is taken to the reduction of restraint stresses due to cracking. Since the large stresses are appearing in the transverse direction, models which do not consider the transverse direction, such as simple 2D frame models, do not show the large stress values. But with the use of 3D-models the effect in transverse direction is captured by the design model. The use of the more advanced 3D-models is thereby in turn requiring more detailed thermal load distributions.

In this paper, the temperature difference between structural parts in portal frame bridges is investigated using thermal simulations with climate data from a two-year period in Stockholm, Sweden. The resulting transversal stresses are calculated and compared with stresses obtained when applying thermal load cases from Eurocode 1. Also, the influence of various material and geometry parameters on the maximum temperature difference between structural parts is analyzed in a parametric study using factorial design. Portal frame bridges were chosen for this study due to their simple geometry and rigid connections between bridge parts, which generates restraint effects. Also, the bridge type is very common in Sweden.

2. Temperature effects on portal frame bridges

In the case of a portal frame bridge as in Fig. 2, the bridge deck and abutments are rigidly connected. Each structural part can therefore be considered to be restrained from expanding or contracting in the transverse direction by the adjacent part, since the transverse length of the bridge deck and the abutments must remain equal at the corners. Therefore, restraint stresses will appear in the transverse direction if the structural parts have different temperatures. In the longitudinal direction, restraint stresses will be smaller, due to a lower degree of restraint. If for example the bridge deck is cooled and strives to contract, the abutments will curve and thus only prevent a relatively small part of the longitudinal contraction.

Theoretically, at least three simple reasons for temperature differences between the structural parts can be found for the bridge type shown in Fig. 2: difference in short wave radiation influx, long wave radiation and heat exchange between abutment and soil. The difference in short wave radiation is due to the top side of the bridge deck being directly exposed to sunshine, while the abutments are mostly shaded by the bridge deck. The difference in heat influx between the parts is in this case largest when the sun is at its highest position in the sky, indicating that the largest temperature differences due to solar radiation will appear during summer.

A difference in long wave heat radiation appears when there is a large amount of outgoing long wave radiation from the bridge to the sky. This situation is most likely to appear during clear nights, often during winter. A large amount of outgoing radiation will lower the bridge deck temperature more than the abutment temperature, since the abutments are not facing the sky to the same extent.

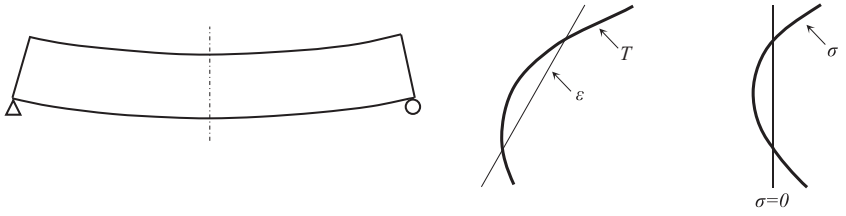

Fig. 1. Stresses and strains caused by a non-linear temperature distribution over the height of a simply supported beam. Figure after Jokela [10].

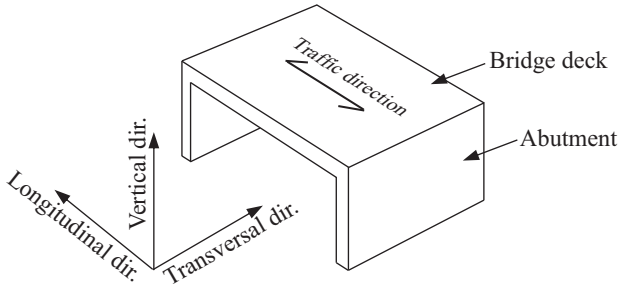

Fig. 2. An example of a portal frame bridge. The two abutments are rigidly connected to the bridge deck.

The soil temperature is affecting the abutments due to their large contact surface. Hillel [15] presents the principal variation of soil temperature during a year, showing that the soil at a depth of at least 1 m is generally colder than the air in summer and warmer than the air in winter. This means that the soil is leveling out the abutment temperature, and will therefore contribute to a larger temperature difference between deck and abutments.

The influence of soil temperature and radiation on the bridge temperature depends on the density, specific heat capacity and thermal conductivity of the asphalt, concrete and soil. The solar absorptivity of the asphalt and the emissivity of all three materials are also of importance. For the concrete, the density mainly depends on the relative volumes of aggregate, cement and porosity, the aggregate type and moisture content. The thermal conductivity mainly depends on the density, moisture content and the thermal conductivity of cement and aggregate. The specific heat capacity of concrete depends mainly on the temperature, moisture content and water cement ratio [16]. For the asphalt, the proportion of bitumen, which has a lower thermal conductivity than the aggregate, as well as the type of aggregate used, are the main factors influencing the conductivity [17]. The solar absorptivity of asphalt depends on the color of the surface, newer surfaces are generally darker and therefore have larger solar absorptivity values [18]. According to Sundberg [19], the values of the soil parameters depend on the grain size, porosity, water saturation level of the soil and whether the soil is frozen or not. Cohesive soils are generally more conductive due to a larger water saturation degree above ground water level.

3. Simulation models

The thermal simulations were conducted with a 2D-model using a two-year period of data, and thereafter with a 3D model using a 7-day period of data shown to cause the largest temperature differences between bridge deck and abutment in the 2D-model. Finally the 2D-model was used again in a parametric study, also using a shorter period of data. The temperature difference between the structural parts was calculated as mean temperature of the nodes in the deck, minus the mean temperature of the nodes in the abutment. In the 3D-model, only nodes in the longitudinal mid-section of the model were used in this calculation. Deck and abutment are defined according to Fig. 3, and the simulations were performed in the commercial FE program Brigade/Plus version 6.1 [20], which uses Abaqus FEA solver [21].

3.1. Initial study

The initial 2D simulation was performed on a model of a longitudinal bridge cross section and adjacent soil. 4-node linear heat transfer quadrilateral elements were used in the model. In the abutment, bridge deck and asphalt layer on top of the bridge, the elements were $50 \times 50\ mm^2$, and in the rest of the model $250 \times 250\ mm^2$. The soil layer beside the abutment is 4 m wide, which was motivated by initial simulations, showing a convergence of results when the width of the model approaches 4 m. Hillel [15] shows principal variations of temperature over depth in soil, motivating the choice of assigning a constant 5 °C to the bottom edge of the model. The value corresponds to the annual mean temperature of the location, and is assigned 4 m below the bottom of the abutment. The vertical edges of the model are isolated, i.e. heat transfer is prevented.

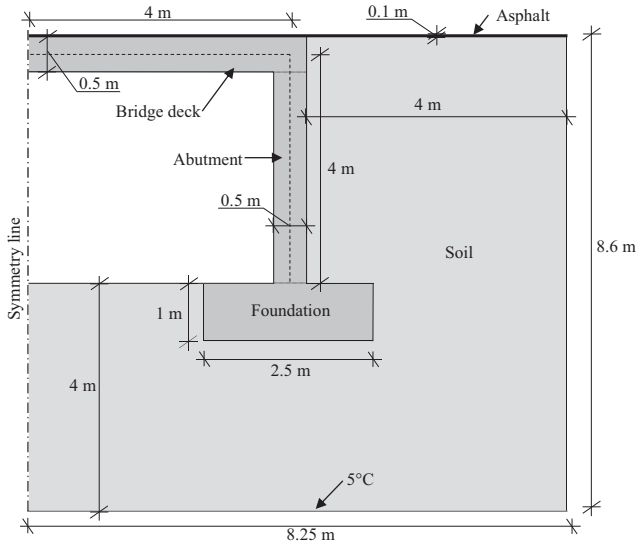

Fig. 3. Geometry of the FE-model used in simulations. The model consists of half of a longitudinal bridge cross section and adjacent soil.

The asphalt layer in the model is 0.1 m thick and covers the bridge deck surface and the surface of the adjacent soil. The bridge deck and abutments are both 0.5 m thick, and the system line of the modeled part of the cross section is 4 m long both in vertical and horizontal direction. The abutment is placed on a concrete foundation with a cross section of $2.5 \times 1\ m^2$, which is not considered as a part of the abutment when calculating the abutment mean temperature, but it affects the thermal properties of the area. The model is depicted in Fig. 3, and the element mesh is shown in Fig. 4.

The material parameters used are presented in Table 1. Parameters regarding concrete and asphalt are from Larsson [3] whereas soil parameters are derived from Sundberg [19], and are valid for unfrozen sand of 25% porosity above ground water level. The method for including thermal effects is adopted from Larsson [22] which was verified by temperature measurements at 10 different levels in a 255 mm thick concrete slab. The simulation method has also been validated for a hollow concrete box cross-section in Larsson and Karoumi [23]. Air temperature, solar radiation, long wave heat radiation and convection are used as factors affecting the total heat energy in the model. The climate data used is obtained from two years of measurements in Stockholm, from the 1st of January 1986 to the 31st of December 1987, by the Swedish Meteorological and Hydrological Institute (SMHI) at the measuring station "Stockholm-Bromma" [24]. Larsson and Thelandersson [25] found the chosen two-year period of climate data to give the most unfavorable thermal stresses in a concrete structure when weather data from 1983 to 1998 was used, and the data was therefore expected to give relatively large temperature differences in this model as well. Air temperature and wind speed are given for every third hour, and short and long wave

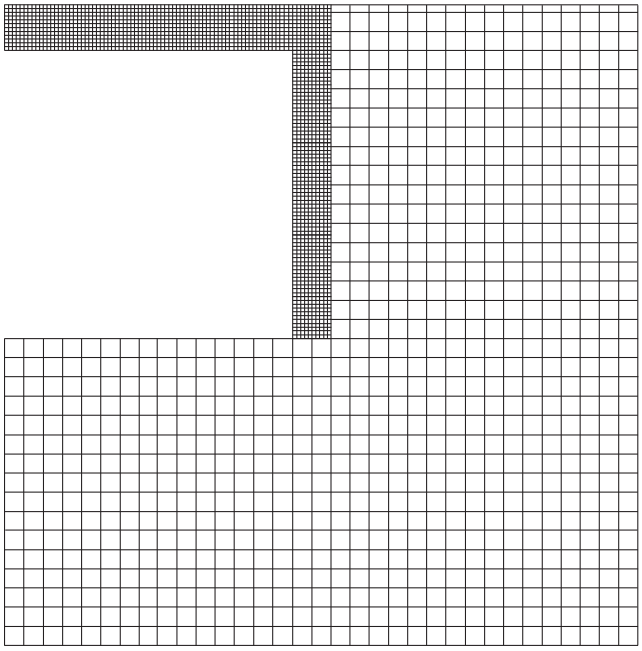

Fig. 4. Image of the element mesh in the model.

radiation for every hour. The convection is assumed to act equally on all surfaces exposed to air, and varies with wind speed according to Eqs. (1) and (2), where V is wind speed in m/s and h_c is the convection coefficient. The equations are given by Nevander and Elmarsson [26].

$$h_c = 6 + 4V,\ V \leqslant 5\ \text{m/s} \tag{1}$$

$$h_c = 7.4V^{0.78},\ V > 5\ \text{m/s} \tag{2}$$

The top surface of the bridge deck is assumed never to be shaded by any object, while no solar radiation is reaching the abutment. These choices cause the largest difference in radiation influx between the structural parts, and are therefore assumed to give a worst case scenario. The solar absorptivity of the asphalt and the emissivity of all three materials are set to 0.9. Long wave radiation from the sky is treated as a surface with a temperature corresponding to the measured value of long wave radiation. On the surfaces not facing the sky, a long wave radiation corresponding to the air temperature is applied. Long wave radiation and convection is thereby added to the model as surface to ambient interactions.

3.2. 3D models

The initial 2D-simulation was followed by a thermal simulation using a 3D-model of the bridge. It was carried out for a 7-day period of climate data that included the day for the largest temperature difference in the initial study, as the aim of the 3D-study was to determine the stresses in the structure at the time for the largest temperature differences between the structural parts. This thermal simulation used the same parameter values as in the initial 2D-simulation, with the exception that soil was excluded from the model to simplify calculations, i.e. no heat transfer took place over edges facing soil. The bridge was assumed to be 8 m wide, and 8 node linear heat transfer brick elements of the size $50 \times 50 \times 50\ \text{mm}^3$ were used in the simulation.

The temperature in the model at each time step was then used in a structural analysis of an identical model, in which the previously used finite elements were replaced with 8 node linear brick elements using reduced integration and hourglass control. Linear elastic material models were assigned to concrete and asphalt, and parameter values of the respective materials are presented in Table 2. The choice of concrete stiffness and coefficient of thermal expansion is in reality arbitrary, since the resulting stresses vary linearly with both stiffness and thermal expansion. The asphalt layer was assumed to be rigidly connected to the concrete, but in reality it is generally separated from the concrete by a thin film or insulation in order to simplify replacement. Separating the materials causes the asphalt to have a negligible influence on the stiffness of the bridge deck, which was obtained in the model by choosing a relatively low stiffness value.

The 3D model utilizes double symmetry, and is shown with its element mesh in Fig. 5. Along the bottom of the abutment, both vertical and longitudinal translations are prevented, while translations in the transverse direction were allowed. Since there could be a temperature difference between foundation and abutment as well, there could in reality also be restraint stresses in transverse direction between foundation and abutment. This was however not covered in this study.

The results were compared with simulations of quasi-permanent Eurocode 1 thermal load cases, rendering a 7.5 °C temperature difference between the parts, 5.25 °C linear temperature difference over the bridge deck cross section and 7.5 °C over the abutment. In the simulations with gradients, a heat transfer analysis was performed to determine the temperature of the structure, assigning the temperature along the edges of one of the parts. This rendered a linear temperature variation over one cross section, and a slightly varying temperature in the part not assigned any temperature at its surfaces.

3.3. Parametric study

A parametric study was performed using a 2^k factorial design, to determine how the maximum temperature difference is influenced by different parameters used in the simulations. Factorial design is a statistical method for designing experiments, see e.g. Box et al. [27], Montgomery [28], and is here applied to FE analyses. The application of factorial design, and Design of Experiments (DoE) in general, to the field of FE analysis has great potential as a means to systematically study the response of complex structural systems, cf. Chen et al. [29], Wiberg et al. [30], Graciano and Mendes [31], Moradi et al. [32] Borges et al. [33], Baroutaji et al. [34], Tran et al. [35]. First, the factors of interest are determined where two, or more, values (or levels) are chosen for each factor. In a full factorial design, all possible combinations of factor values are used in simulations. This gives information on the influence of each factor on the response variable, which is denoted as the "main effect" of the factor. Interaction effects between all possible factor combinations are also captured. The advantage of the method is that the

Table 1
Parameters used in simulations.

Material	Density [kg/m^3]	Specific heat capacity [J/(kg·°C)]	Thermal conductivity [W/(m·°C)]	Reference for parameter values
Concrete	2400	900	2.5	[3]
Asphalt	2200	880	0.7	[3]
Soil	2025	1133	0.5	[19]

Table 2
Parameters used in stress calculation. No soil was included in the model.

Material	Young's modulus [GPa]	Poisson's ratio	Coefficient of thermal expansion [°C^{-1}]
Concrete	33	0.2	10^{-5}
Asphalt	0.003	0.1	10^{-5}

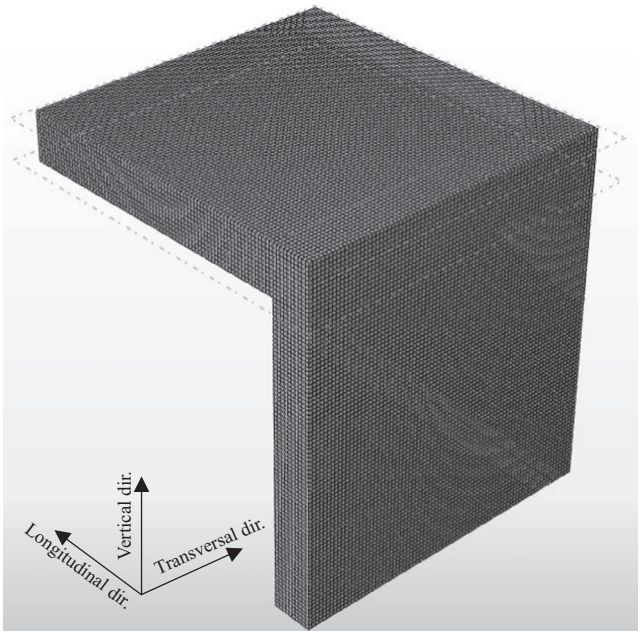

Fig. 5. Element mesh in the 3D-model.

main effect obtained for a specific parameter is valid not just for a specific combination of values for the other parameters, but as long as the other parameter values are within their respective ranges of values chosen for the simulations. Therefore, if each parameter is given an interval that covers its reasonable values, the results can be considered to describe the entire spectrum of possible results.

In a screening process where many factors are investigated, a fractional factorial design can be performed in order to reduce the required number of analyses. In this case, only a few of the total number of possible parameter combinations are used. The results will however confound some interaction effects with main effects and other interaction effects, but the scheme is made in such a way that the lower order interaction effects, i.e. interactions between few parameters, are cancelled out first. This is done since interactions between many factors are assumed to be smaller than interaction effects between a lower number of factors.

The simulations were made for a 30 day period of weather data, of which day 28 caused the record temperature differences in the initial study. The time period before this date mainly serves to adjust the temperature in the model, from the initial rough estimate of the temperature distribution. An initial study determined that including a 28 day period was sufficient for this purpose, as the difference from having a 35 day period was less than 0.1 °C in maximum temperature difference between structural parts.

3.3.1. Fractional factorial design

Initially, a fractional factorial design using 14 factors was performed as a means to screen for important factors that contribute to the thermal response of the bridge. A full factorial design with 14 factors would require $2^{14} = 16{,}384$ runs, but this fractional factorial design is of resolution IV, meaning that two factor interactions are cancelled out, requires only 32 runs. The parametric study aimed to determine which parameters are the most important, but cannot determine their exact influence on the maximum temperature difference between the structural parts. The parameters included in the design, and their respective high and low values, are presented in Table 3. The chosen high and low values, codified as + and −, respectively, in the table represent reasonable high and low values for each parameter. Table 4 shows the choice of factor values in each of the 32 runs of the fractional factorial design, and the maximum temperature difference between the deck and the abutments occurring in the respective runs.

The values for concrete parameters are given in Ljungkrantz et al. [16]. Larsson [3] shows material properties of asphalt used by other authors, of which the highest and lowest values are presented here. The soil values are derived from Sundberg [19], and the values for density and specific heat capacity represent a friction soil above ground water level with porosity of 25% and 50% respectively. Although both density and specific heat capacity are derived from the porosity of the soil, both density and specific heat capacity are kept as two separate parameters to account for possible changes in values due to varying material properties. The upper value for the thermal conductivity represents the kind of soil described above, but the lower value is chosen lower than reasonable in order to capture the effect of disregarding the soil in the model. The used absorptivity range for the asphalt layer is given by Bretz et al. [18], where the higher value corresponds to newly placed asphalt, and the lower to older asphalt. Emissivity values are given by Larsson [3], and are assumed to be equal for all surfaces. The cross sectional thickness of the bridge deck, abutment and asphalt were given values considered to be reasonable by the author.

3.3.2. Full factorial design

After having identified the parameters with the largest influence on the temperature difference with the fractional factorial design, a full factorial design was carried out with the five factors having the largest influence on the result. This was done in order to determine their exact influence on the response variable, and the factor interactions. The worst combination of factors, rendering the highest temperature difference between structural parts of a portal frame bridge practically possible for the investigated weather data, could thereby also be determined. The analyzed parameters were the thickness of the bridge deck, abutment, and asphalt layer, respectively, and the asphalt conductivity and absorptivity. The other parameters were given the respective mean values of the previously used values.

The parametric study was finalized by performing a full 3^5 factorial design, i.e. a full factorial design with three factor values for each factor, with the same five factors as chosen previously. The third value equaled the mean value of the "−" and "+" values shown in Table 3, and the objective of the study was to conclude whether the maximum temperature difference varies linearly or nonlinearly with the five main effects considered most relevant.

4. Results and discussion

4.1. Initial study

The initial simulation using two years of weather data from Stockholm showed that the temperature in the model varied in an expected way, with regards to the influence of the soil and radiation described in Section 2. Over the entire simulation period, the difference in temperature calculated as mean temperature in the bridge deck minus mean temperature in the abutment varied as

Table 3
Parameters and parameter values used in the fractional factorial design. The "–" and "+" columns show the low and high value for each parameter, respectively.

Parameter	Factor	–	+	Unit	Reference for parameter values
Concrete density	X_1	2300	2400	kg/m^3	[16]
Concrete heat conductivity	X_2	1.6	2.5	W/(m·°C)	[16]
Concrete specific heat capacity	X_3	800	1000	J/(kg·°C)	[16]
Asphalt density	X_4	2100	2240	kg/m^3	[3]
Asphalt heat conductivity	X_5	0.7	2.5	W/(m·°C)	[3]
Asphalt specific heat capacity	X_6	840	920	J/(kg·°C)	[3]
Soil density	X_7	1350	2025	kg/m^3	[19]
Soil heat conductivity	X_8	0.05	0.5	W/(m·°C)	[19]
Soil specific heat capacity	X_9	756	1133	J/(kg·°C)	[19]
Emissivity	X_{10}	0.85	0.95		[3]
Absorptivity	X_{11}	0.80	0.95		[18]
Bridge deck thickness	X_{12}	0.35	1	m	
Bridge abutment thickness	X_{13}	0.35	1	m	
Asphalt layer thickness	X_{14}	0.1	0.15	m	

Table 4
Factor values ("–" or "+") used in each analysis, and the resulting maximum temperature difference between the deck and the abutments in the analysis.

Analysis no.	X_1	X_2	X_3	X_4	X_5	X_6	X_7	X_8	X_9	X_{10}	X_{11}	X_{12}	X_{13}	X	Max temp diff. [°C]
1	–	–	–	–	–	–	–	–	–	–	–	–	–	–	8.4
2	–	–	–	–	+	+	+	+	+	+	+	+	–	–	6.8
3	–	–	–	+	–	+	+	+	+	–	–	–	+	+	9.6
4	–	–	–	+	+	–	–	–	–	+	+	+	+	+	7.8
5	–	–	+	–	–	+	+	–	–	+	+	–	+	+	9.1
6	–	–	+	–	+	–	–	+	+	–	–	+	+	+	7.5
7	–	–	+	+	–	–	–	+	+	+	+	–	–	–	9.1
8	–	–	+	+	+	+	+	–	–	–	–	+	–	–	5.0
9	–	+	–	–	–	+	–	+	–	+	–	+	+	–	6.1
10	–	+	–	–	+	–	+	–	+	–	+	–	+	–	15.8
11	–	+	–	+	–	–	+	–	+	+	–	+	–	+	4.3
12	–	+	–	+	+	+	–	+	–	–	+	–	–	+	11.6
13	–	+	+	–	–	–	+	+	–	–	+	+	–	+	5.3
14	–	+	+	–	+	+	–	–	+	+	–	–	–	+	9.2
15	–	+	+	+	–	+	–	–	+	–	+	+	+	–	6.3
16	–	+	+	+	+	–	+	+	–	+	–	–	+	–	13.3
17	+	–	–	–	–	+	–	–	+	–	+	+	–	+	5.1
18	+	–	–	–	+	–	+	+	–	+	–	–	–	+	10.2
19	+	–	–	+	–	–	+	+	–	–	+	+	+	–	7.6
20	+	–	–	+	+	+	–	–	+	+	–	–	+	–	13.3
21	+	–	+	–	–	–	+	–	+	+	–	+	+	–	5.6
22	+	–	+	–	+	+	–	+	–	–	+	–	+	–	15.2
23	+	–	+	+	–	+	–	+	–	+	–	+	–	+	4.9
24	+	–	+	+	+	–	+	–	+	–	+	–	–	+	11.3
25	+	+	–	–	–	–	–	+	+	+	+	–	+	+	9.8
26	+	+	–	–	+	+	+	–	–	–	–	+	+	+	6.9
27	+	+	–	+	–	+	+	–	–	+	+	–	–	–	8.6
28	+	+	–	+	+	–	–	+	+	–	–	+	–	–	5.8
29	+	+	+	–	–	+	+	+	+	–	–	–	–	–	7.8
30	+	+	+	–	+	–	–	–	–	+	+	+	–	–	6.0
31	+	+	+	+	–	–	–	–	–	–	–	–	+	+	7.9
32	+	+	+	+	+	+	+	+	+	+	+	+	+	+	8.1

is shown in Fig. 6. It is obvious that there are generally large positive differences during summer, and not quite as large negative differences in winter. The largest positive difference in mean temperature between the parts was 8.1 °C and appeared during a day in June, while the largest negative value obtained was −4.2 °C, occurring in January.

Although the characteristic load value of 15 °C given in Eurocode 1 is almost twice as high as the maximum temperature difference in the simulation, it cannot be concluded that the characteristic load value in Eurocode 1 is exaggerated. It corresponds to a load with a 50-year return period, meaning that the largest temperature differences in this study, using two years of data, is not comparable with a characteristic value. The study therefore must be continued with longer data series combined with statistical analyses, which includes using newer data to account for possible changes in the climate. Also, if general conclusions are to be drawn for e.g. Sweden or Europe, weather data from more locations are needed. Some locations with e.g. inland climate and larger solar radiation could then be expected to cause larger temperature differences than obtained with the data used in this study. The influence of such climate parameters could therefore also be studied in an extended study.

The median value of the temperature difference was however found to be only 1.3 °C, which indicates that a quasi-permanent temperature difference of 7.5 °C as suggested by Eurocode 1 could be a significant overestimation of the temperature difference between the structural parts for this type of bridge. But also in this case, the two-year period of weather data is too short to determine a new load value, and the study must therefore be continued.

The thermal distribution within the concrete cross section for the occasions with the largest positive and negative temperature difference is portrayed in Fig. 7a and b respectively. In Fig. 8a and b, the temperature along the system line of the structure is shown for the same occasions. It can be seen in the figures

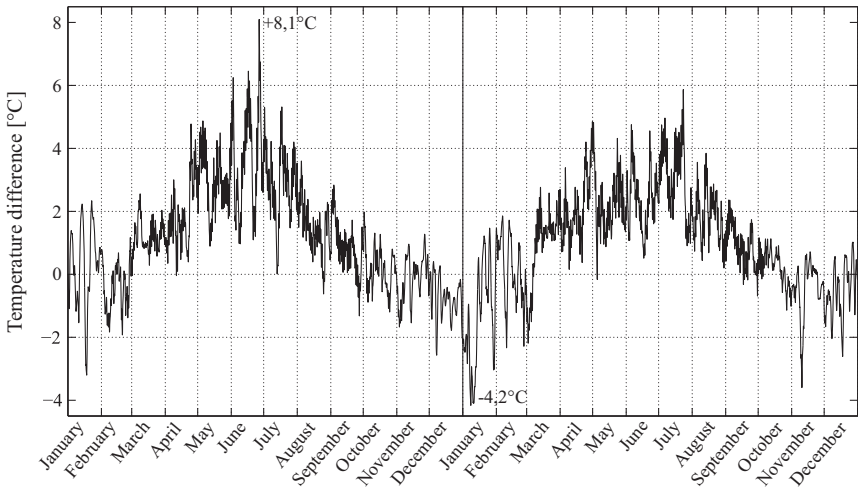

Fig. 6. The variation in mean temperature between structural parts, calculated as mean temperature in the bridge deck minus mean temperature in the abutment.

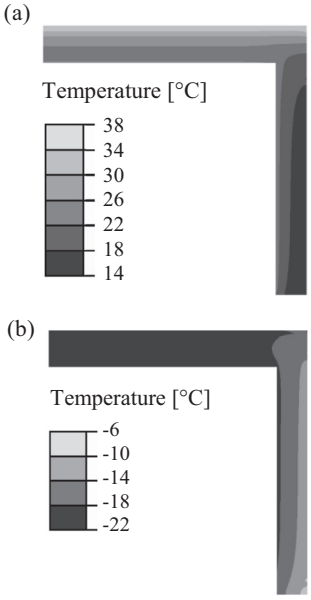

Fig. 7. Temperature in the model when the largest positive (a) and negative (b) temperature differences are present between deck and abutment.

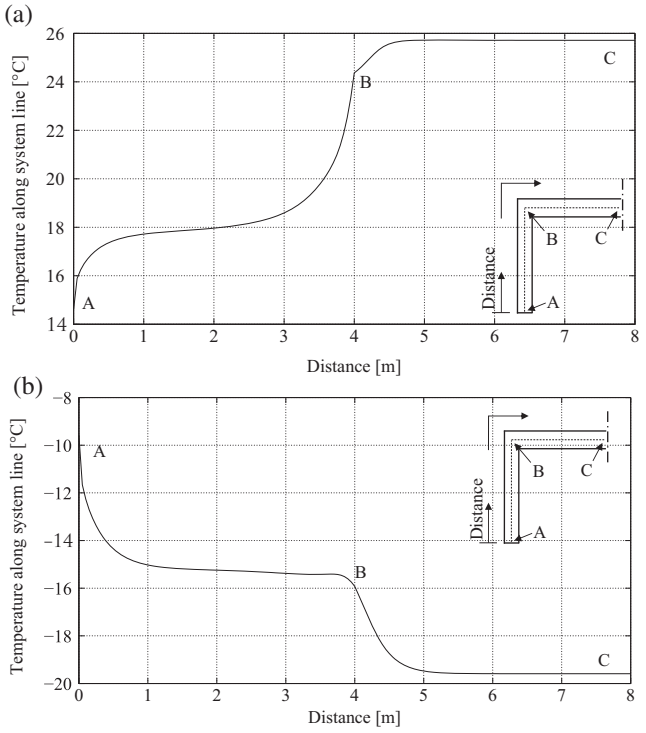

Fig. 8. Temperature variation along the system line for the occasions with the largest positive (a) and negative (b) temperature difference between structural parts.

that a large change in temperature occurred in the corner region, but also that the change is gradual. To apply different thermal loads on the different structural parts of a portal frame bridge is therefore reasonable, but applying uniform temperatures within each part implies a simplification of the thermal load distribution. The consequences of this simplification are shown in Section 4.2.

4.2. Stress calculation in 3D-model

In the 7-day period investigated in the 3D-model, the maximum stress is in this case about 1.3 MPa and appears on the back side of the abutment. The stress distribution in the model at that time, which coincided with the time for maximum temperature difference, is shown in Fig. 9. Double symmetry is used in the model, and the free edges towards the left in the figure are symmetry sections. The fact that the stresses are largest at the back of the abutment is not surprising since this is where the bridge is coldest, which was shown in Fig. 7a. The stress is largest close to the top of the abutment, and then decreases further down, due to a lower degree of restraint further away from the restrained edge along the frame corner. The stresses increase again close to the bottom of the abutment, due to the prevention of movements in the longitudinal direction at the bottom surface. This boundary condition prevents the curvature of the abutment around the vertical axis, which is desired by the abutment since its back side is colder than its front side.

The initial 2D simulation showed that the thermal distribution shown in Fig. 7a is typical for times with large temperature differences, therefore it is expected that the case investigated in 3D is representable for occasions with large positive temperature differences (bridge deck being warmer than abutment) in general. Nevertheless, using longer time periods would increase the certainty of

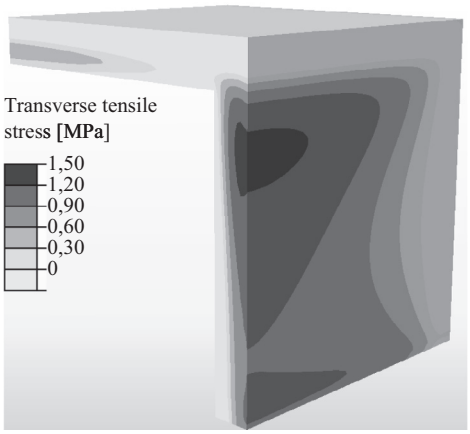

Fig. 9. Stress in transversal direction when the largest temperature difference (8.1 °C) between the structural parts is used in calculations. The visible gables of the bridge are symmetry sections.

the conclusions, needed in order to determine the temperature distribution within a new thermal load case.

The design load cases in Eurocode 1 caused stresses according to Fig. 10a–c, where transversal stresses resulting from different temperature in the two parts as well as gradients in either deck or abutment are shown. It is obvious that the results shown in Fig. 10a–c differ from the result shown in Fig. 9, and that a sudden stress change as shown in Fig. 10a is unrealistic.

It should be noted that the obtained tensile stress levels are lower than the stress capacity of the concrete. This does however not mean that the concrete is uncracked, since quasi-permanent load values are used, and the concrete might have already cracked for a larger short-time load. If the structure is cracked, stresses will however be smaller than the shown values, since the cracking reduces the stiffness of the structure, and thereby allows for some deformation. The loss of stiffness depends on the size and quantity of cracks, and since cracking might have stopped before stabilized cracking is reached, assuming the same crack distance as in cases with non-restraint loading might instead underestimate stresses. In order to find the actual stresses of the structure, an investigation using non-linear material model of concrete and bond-slip interaction between concrete and reinforcement is therefore needed.

4.3. Simplified temperature distribution model

The difference in stress distributions between Fig. 9 and Fig. 10a–c calls for a new simplified model of temperature variation. Based on the thermal distribution in Fig. 7a showing gradients in both structural parts, a thermal load distribution assigning gradients in both structural parts simultaneously is investigated. The gradients correspond to the present Eurocode 1 temperature gradients in both structural parts, i.e. a 5.25 °C linear temperature difference over the bridge deck cross section and 7.5 °C over the abutment. The same temperature was assigned to the surfaces facing the air underneath the bridge on both structural parts, while the back side of the abutment was 7.5 °C colder and the top of the bridge deck was 5.25 °C warmer.

The resulting transverse stress distribution caused by this load case is shown in Fig. 11. Although varying in magnitude from the results obtained with weather data shown in Fig. 9, the pattern of the tensile stresses is similar. An important difference from the case with only a gradient in the abutment (Fig. 10c) is that there in this case are tensile stresses not only on the back side of the abutment, but also along the system line of the abutment.

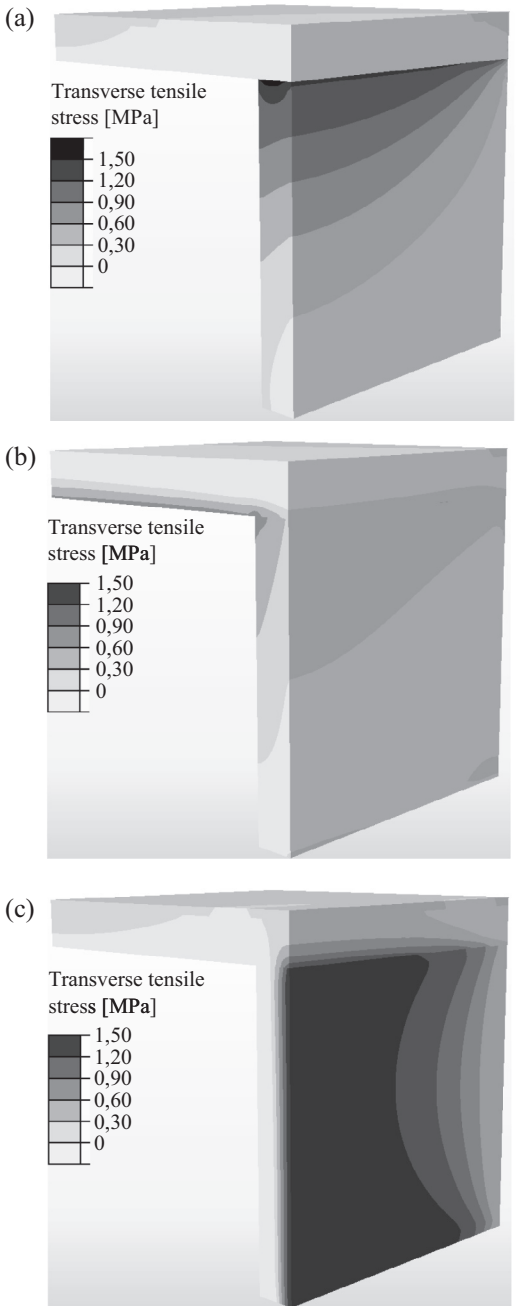

Fig. 10. Stress in transversal direction for the following Eurocode load cases: bridge deck being warmer than abutment (a), gradient through bridge deck (b) and gradient through abutment (c). The visible gables of the bridge are symmetry sections.

In Fig. 12a, the temperature is compared along the system line for the model using temperature from climate data and the model with simultaneous gradients. Fig. 12b shows the corresponding relation for the transverse stress. The change in temperature along the system line is larger in the model using weather data, but the shape of the curves are otherwise similar. But when comparing the transversal stresses, it is obvious that the tensile stress is constantly higher in the model using climate data. At the same time, the stresses at the back of the abutment is larger in the model using simultaneous gradients, which can be seen when comparing Figs. 9 and 11.

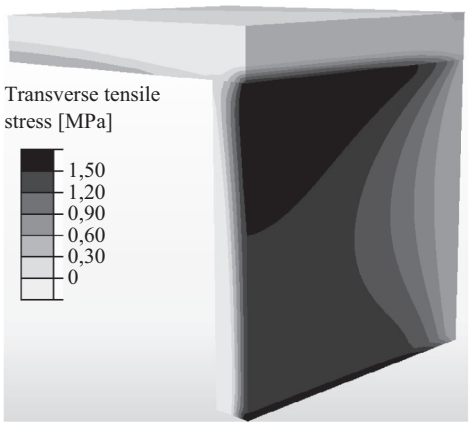

Fig. 11. Transverse tensile stresses in a portal frame bridge subjected to thermal gradients in both bridge deck and abutment simultaneously. The visible gables of the bridge are symmetry sections.

The reason for this can be found when studying the nature of the temperature variation over the cross sections. In the model with simultaneous gradients in the structural parts, the temperature variation over the cross section is linear, as was assigned. But in the model using climate data, the temperature varies nonlinearly. In the abutment, the temperature changes faster close to the surface facing air, than close to the soil. Therefore, the difference in temperature between system line and back side of abutment is smaller in the model using weather data, which leads to a smaller stress difference between the locations. This relation is shown in Fig. 13, where the stress over the abutment thickness is shown for the two different models. It can be seen that the stress varies linearly in the model using simultaneous gradients, and varies nonlinearly in the model using weather data. The two other curves show the principal temperature variation over the cross sections as $\sigma = \Delta T \alpha E$., where ΔT is the change in temperature, α is the coefficient of thermal expansion and E is Young's modulus, indicating that the temperature varies in a similar way as the transverse stress.

These results show that the model with simultaneous gradients will give similar results to the model using weather data, although the linear thermal variation assumed causes the stress to vary over the cross section in a different way. But the results show that a new thermal load case adapted for 3D-simulations of portal frame bridges could be based on a model using simultaneous gradients over the structural parts. More simulations are however needed to confirm that the observed thermal distribution actually corresponds to a realistic worst case scenario to be accounted for in design.

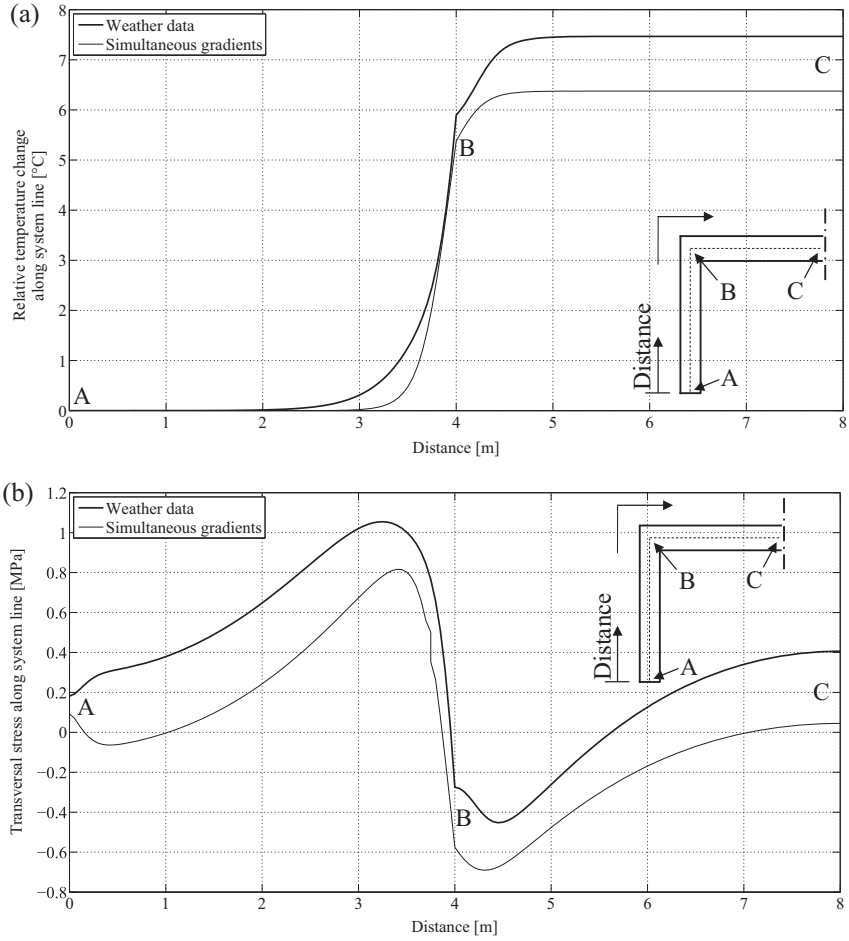

Fig. 12. Temperature (a) and transversal stress (b) along the system line of the structural parts for the model using weather data and simultaneous gradients to simulate temperature.

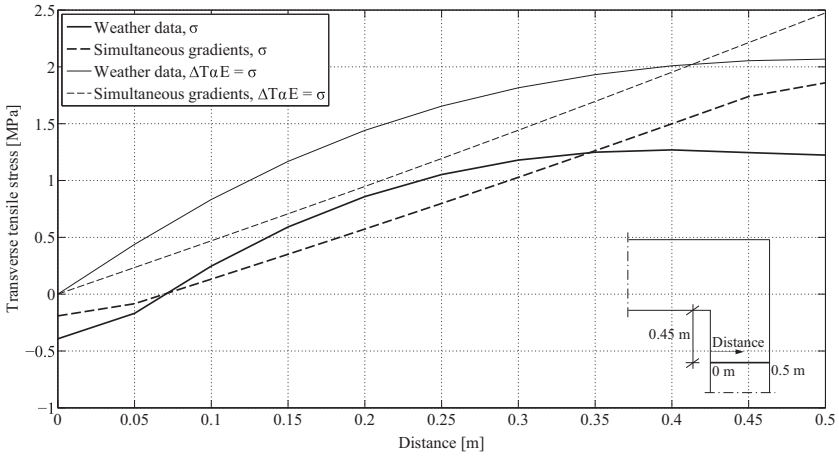

Fig. 13. Transverse tensile stresses over the abutment cross section.

4.4. Parametric study results

4.4.1. Fractional factorial design results

The main effects of the fractional factorial design, i.e. the influence of each factor on the maximum temperature difference, is shown in Fig. 14. In Fig. 15, the absolute values of the main effects are ordered after magnitude. It is shown that the bridge deck thickness had the largest influence on the temperature difference between the parts, followed in order of magnitude by asphalt conductivity, abutment thickness, absorptivity and asphalt thickness. The soil conductivity, which had been given a low value corresponding to no heat transfer at all between concrete and soil, was the sixth most influential parameter, with a main effect of almost 0.5 °C. Since soil is not included in the 3D models, and the results from the parametric study should be able to indicate stress values in a 3D-model, only the five most influential parameters are used in full factorial design. The rest are considered less significant, and are assigned the mean value of their former two values. The choice of not including these parameters in a more accurate way in the continuous work reduces the accuracy of the model. But since many other simplifications are made, such as assuming the same convection rate on all surfaces, it could be misguiding to include small factor effects and expect an accurate result.

4.4.2. Full factorial design results

In the full factorial design, the main effect of the asphalt thickness increased about 30% compared to the value in the fractional factorial design, while the other main effects increased with between 1% and 10%. The changes are explained by the influence of interaction effects in the main effects of the fractional factorial design. Some of the interaction effects were found to be large in the full factorial design, two were larger than the limit for significant effects of 0.5 °C, namely the interaction between bridge deck thickness and asphalt conductivity (1.3 °C) and the interaction between bridge deck thickness and asphalt layer thickness (0.6 °C). The absolute values of the main effects and interactions follow a lognormal distribution fairly well, which is shown in

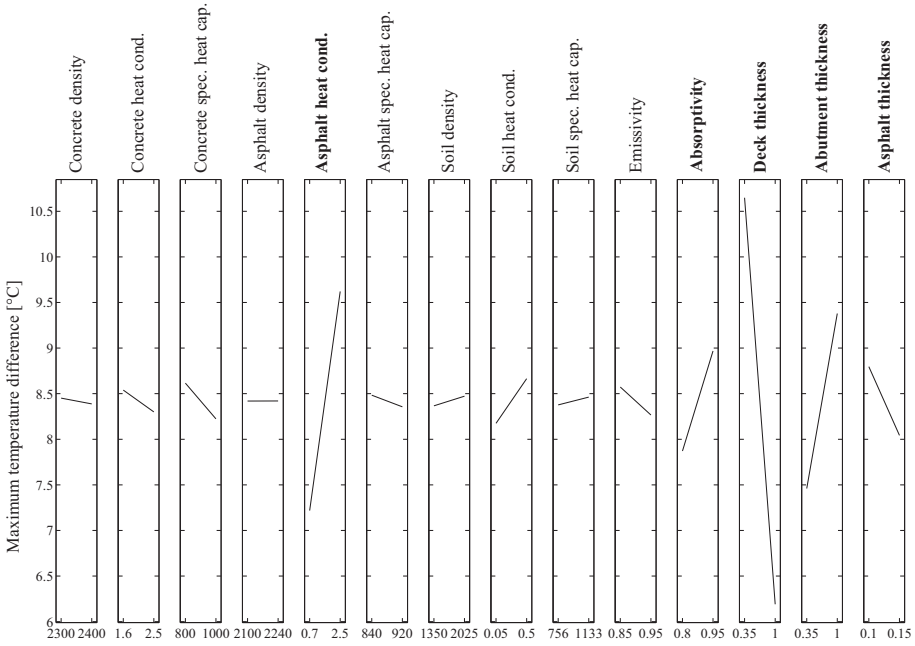

Fig. 14. Main effects obtained from the fractional factorial design, i.e. the influence of each factor on the maximum temperature difference.

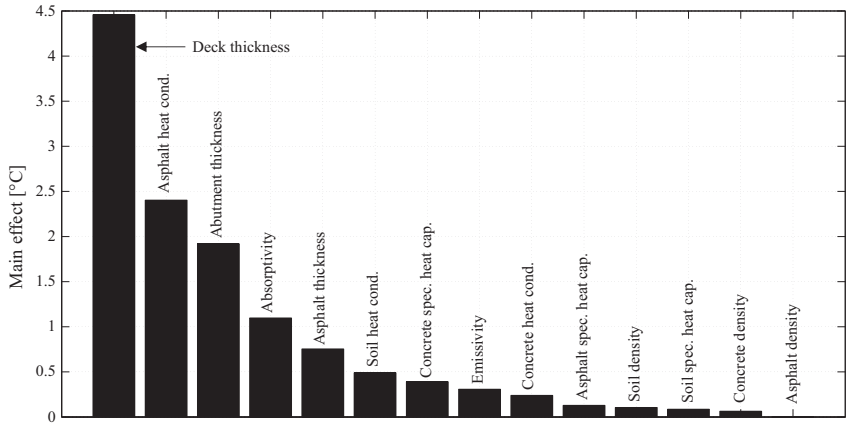

Fig. 15. Magnitude of main effects (absolute values) from the fractional factorial design.

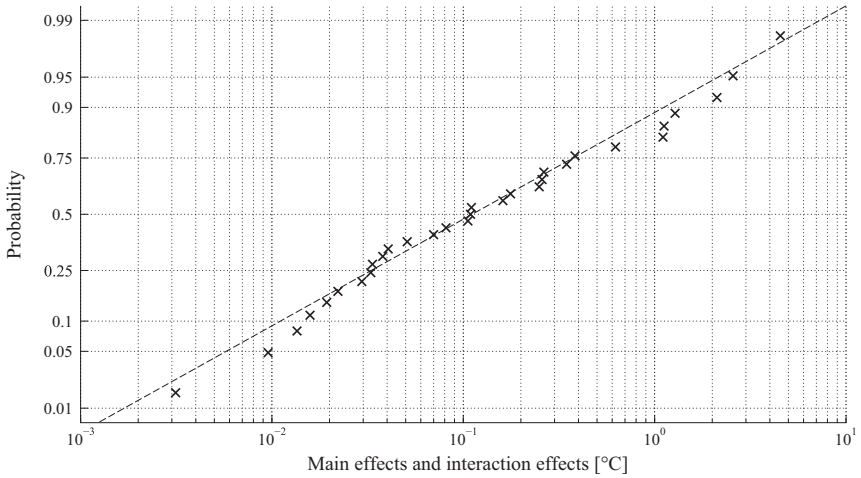

Fig. 16. Lognormal distribution of absolute values of main effects and interaction effects.

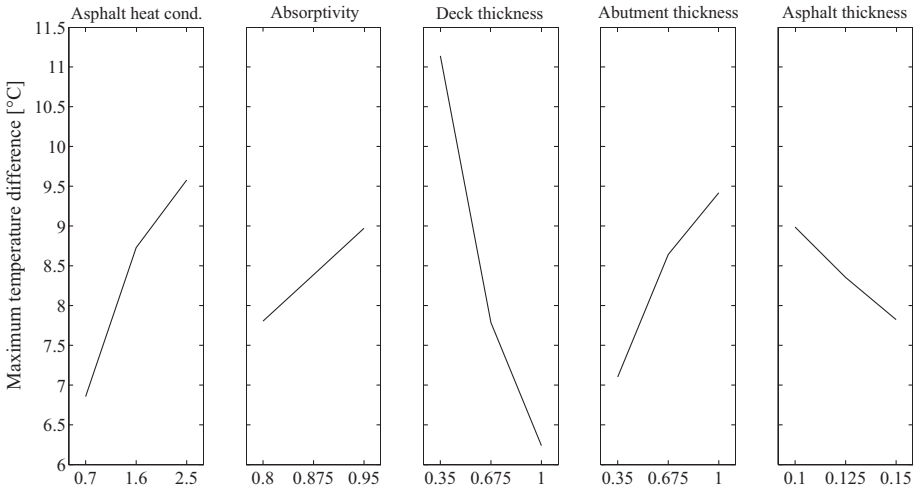

Fig. 17. Main effects from the 3^5 factorial design.

Fig. 16. This could imply that the main effects and interactions are not affected by any significant errors.

The mean values of the maximum temperature differences were 8.4 °C for both the fractional and the full factorial design, i.e. slightly larger than 8.1 °C which was the maximum temperature difference in the initial simulation. The largest temperature difference obtained in the full factorial design was 15.4 °C. This value was however obtained for a case when the bridge deck is thin and the abutment is thick, but portal frame bridges are generally constructed with similar thicknesses of bridge deck and

Table 5
Main effects in the different spans for each parameter. The quotient of the main effect in the lower span divided with the main effect in the higher span is also given.

Parameter	Main effect in lower span [°C]	Main effect in higher span [°C]	Quotient
Asphalt heat conductivity	1.87	0.850	2.2
Absorptivity	0.582	0.585	1.0
Deck thickness	−3.35	−1.55	2.2
Abutment thickness	1.54	0.775	2.0
Asphalt thickness	−0.633	−0.531	1.2

abutments. If only results for simulations where the thicknesses of bridge deck and abutment are equal are considered, the largest temperature difference becomes 13.2 °C. For this case, the bridge deck, abutment and asphalt layers were thin, while the absorptivity and asphalt conductivity were high. The value indicates that for an unfavorable combination of geometry and material parameters, a characteristic temperature difference of 15 °C should not be considered as an exaggerated value. Yet, the quasi-permanent value and the stress distribution is still likely to be unrealistic, but longer simulations are needed to conclude on updated load values.

The main effects of the 3^5 factorial design are shown in Fig. 17, where a nonlinear change in main effect is shown for all five factors except solar absorptivity. Table 5 shows the main effects and their relative magnitude for each factor. For asphalt heat conductivity, bridge deck thickness and abutment thickness, the main effect is about twice as big for the span with smaller values compared to the span with larger values, i.e. changing the parameter values have a larger effect on the maximum temperature difference when the parameter values are small.

5. Conclusions

This paper shows that uneven exposure to thermal loads causes the mean temperature to vary between the structural parts of a portal frame bridge. The bridge deck is generally warmer than the abutment during summer, while during winter the situation is the opposite. The change in temperature along the system line of the structure is most significant close to the frame corner, while gradients can be present in both parts simultaneously.

However, the median temperature difference in the initial simulation with two years of weather data was only 1.3 °C. This value corresponds to the quasi-permanent value of the time period, and indicates that it is unrealistic to assume a quasi-permanent value of 7.5 °C in portal frame bridges as suggested by Eurocode 1. More simulations with weather data from longer time periods and more locations are however needed to determine a new quasi-permanent load value.

For the worst realistic combination of parameter values in the parametric study, the maximum temperature difference between structural parts acquired in the simulations was 13.2 °C. To use 15 °C as a characteristic value could therefore be reasonable, or even an underestimation of the thermal load.

The parametric studies using factorial design show that the main factors influencing the maximum temperature difference between structural parts, for a given set of weather data, are in order of magnitude: (1) the bridge deck thickness; (2) asphalt conductivity; (3) abutment thickness; (4) solar absorptivity and (5) asphalt thickness. Among the factors considered less important are the soil parameters, which indicates that the 3D-models could be made without including the soil in the model.

The resulting transversal stresses obtained when using temperature distributions determined by thermal simulations are significantly different from the results obtained with the Eurocode 1 load cases describing temperature difference between structural parts, and gradients over bridge deck and abutment respectively. The difference concerns both the maximum stress values and the stress distribution within the bridge. Notably, a smoother temperature change caused by thermal simulations using weather data gives lower maximum tensile stresses in the model. However, assigning the Eurocode 1 temperature difference between structural parts and gradients on the two structural parts simultaneously gives temperature and stress distributions similar to the results obtained with weather data. This type of thermal distribution is therefore a possible answer to how a realistic thermal load can be added in a simple way, but more simulations are needed to evaluate its reasonableness.

In order to develop a new load case for temperature differences in portal frame bridges, more simulations using longer time series of weather data, and data from more locations, are needed. But it is likely that the quasi-permanent load effects can be reduced. Overestimating thermal loads will lead to the use of exaggerated reinforcement amounts. Therefore, determining a realistic thermal load is likely to reduce the reinforcement needed in portal frame bridges, which in turn makes the bridges cheaper to construct and also reduces the environmental impact of the structure. Another aspect that can be accounted for in design is the reduction of restraint stresses due to cracking. Nonlinear models can be used to estimate the width of cracks caused by restraint effects, which possibly could motivate an even further reduction of reinforcement use.

Acknowledgements

This work was supported by Trafikverket, the Swedish transport administration, and SBUF, the Swedish construction industry's organization for research and development.

References

[1] Kreith F. Principles of heat transfer. 3rd ed. New York: Intext Educational Publishers; 1973.
[2] Duffie J, Beckman W. Solar engineering of thermal processes. 3rd ed. Hoboken, New Jersey: John Wiley & Sons; 2006.
[3] Larsson O. Climate related thermal actions for reliable design of concrete structures (Ph.D. thesis). Lund, Sweden: Division of Structural Engineering, Lund University; 2012.
[4] Peiretti PH, Parrotta EJ, Oregui BA, Caldentey PA, Fernandez AF. Experimental study of thermal actions on a solid slab concrete deck bridge and comparison with Eurocode 1. J Bridge Eng 2014;19(10).
[5] Wang G, Ding Y, Wang X, Yan X, Zhang Y. Long-term temperature monitoring and statistical analysis on the flat steel-box girder of Sutong bridge. J Highway Transp Res Dev 2014;8(4).
[6] Yixiang F. Research on temperature effects of the pre-stressed concrete box girder bridge. Appl Mech Mater 2015;744–746:821–6.
[7] Rodriguez L, Barr P, Halling M. Temperature effects on a box-girder integral-abutment bridge. J Perform Constr Facil 2014;28(3):583–91.
[8] Zhou L, Xia Y, Brownjohn J, Koo KY. Temperature analysis of a long-span suspension bridge based on field monitoring and numerical simulation. J Bridge Eng 2016;21(1).
[9] Engström B. Restraint cracking of reinforced concrete structures. Gothenburg, Sweden: Chalmers University of Technology, Division of Structural Engineering; 2007.
[10] Jokela J. Behaviour and design of concrete structures under thermal gradients. Nordic Concr Res 1984;3:100–28.
[11] EN 1990. Eurocode - basis of structural design. Brussels: European Committee for Standardization; 2002.
[12] EN 1991-1-5. Eurocode 1: actions on structures – Part 1-5: general actions: thermal actions. Brussels: European Committee for Standardization; 2003.
[13] ENV 1991-2-5. Eurocode 1: basis of design and actions on structures – Part 2-5: actions on structures – thermal actions, 1996.
[14] Římal J, Šindler D. Comparison of temperature loadings of bridge girders. Acta Polytech 2008;48(5):22–8.
[15] Hillel D. Introduction to environmental soil physics. San Diego: Academic Press; 2004.
[16] Ljungkrantz C, Möller G, Petersons N. Betonghandbok - material. 2nd ed. Solna: Svensk byggtjänst; 1994.

[17] Dickinson EJ. Method for calculating the temperature gradients in asphaltic concrete pavement structures based on climatic data. Aust Road Res 1978;8(4):16–34.
[18] Bretz S, Akbari H, Rosenfeld A. Practical issues for using solar-reflective materials to mitigate urban heat islands. Atmos Environ 1997;32:95–101.
[19] Sundberg J. Termiska egenskaper i jord och berg. Linköping: Statens geotekniska institut; 1991.
[20] Scanscot Technology AB; https://scanscot.com/products/bridge-design/brigade-plus/ (2017-01-24).
[21] Dassault Systéms; http://www.3ds.com/products-services/simulia/solutions/architecture-construction/ (2017-01-24).
[22] Larsson O. Modelling of temperature profiles in a concrete slab under climatic exposure. Struct Concr 2009;10(4):193–201.
[23] Larsson O, Karoumi R. Modelling of climatic thermal actions in hollow concrete box-cross-sections. Struct Eng Int 2011;21(1):74–9.
[24] Swedish metrological and hydrological institute; Open data; available at: http://opendata-download-metobs.smhi.se/explore/# (2017-01-23).
[25] Nevander LE, Elmarsson B. Fukthandbok: praktik och teori. 3rd ed. Stockholm: Svensk Byggtjänst; 2006.
[26] Larsson O, Thelandersson S. Transverse thermal stresses in concrete box cross-sections due to climatic exposure. Struct Concr 2012;13(4):227–35.
[27] Box E, Hunter G, Hunter S. Statistics for experimenters: design innovation and discovery. 2nd ed. Hoboken, New Jersey: Wiley-Interscience, cop; 2005.
[28] Montgomery C. Design and analysis of experiments. 4th ed. New York: John Wiley & Sons; 1997.
[29] Chen V, Tsui K, Barton R, Meckesheimer M. A review on design, modeling and applications of computer experiments. IIE Trans 2006;38:273–91.
[30] Wiberg J, Karoumi R, Pacoste C. Statistical screening of individual and joint effect of several modelling factors on the dynamic finite element response of a railway bridge. Comput Struct 2012;106:91–104.
[31] Graciano C, Mendes J. Elastic buckling of longitudinally stiffened patch loaded plate girders using factorial design. J Constr Steel Res 2014;100:229–36.
[32] Moradi S, Alam S, Milani S. Cyclic response sensitivity of post-tensioned steel connections using sequential fractional factorial design. J Constr Steel Res 2015;112:155–66.
[33] Borges H, Martínez G, Graciano C. Impact response of expanded metal tubes: a numerical investigation. Thin Walled Struct 2016;105:71–80.
[34] Baroutaji A, Gilchrist MD, Smyth D, Olabi AG. Crush analysis and multi-objective optimization design for circular tube under quasi-static lateral loading. Thin Walled Struct 2015;86:121–31.
[35] Tran KL, Douthe C, Sab K, Dallot J, Davaine L. A preliminary design formula for the strength of stiffened curved panels by design of experiment method. 2014;79:129–37.

BILAGA D

Measurements and simulation of temperature in a portal frame bridge

Erik Gottsäter, Oskar Larsson Ivanov, Miklós Molnár

Lund University, Lund, Sweden

Mario Plos

Chalmers University of Technology, Gothenburg, Sweden

Contact: erik.gottsater@kstr.lth.se

Abstract

Since thermal loads can cause cracking, they are important to consider in bridge design. In order to evaluate and develop thermal load cases based on real simulations, models for simulating temperatures can be used. In this paper, a model for thermal simulation is used to simulate temperature in a portal frame bridge outside Lund, Sweden. The results are compared with temperature measurements in 13 locations in the same bridge, which were made during a 12-month period. The results show that although many important material parameters were unknown, the model could recreate both daily and seasonal temperature variations, although it tended to render temperatures about 1°C lower than the measurements, at least during summer. The model can be used in future work in determining thermal load values for the specific bridge type, assuming the inaccuracy of the model is considered by e.g. adding 1°C to calculated load values.

Keywords: Temperature, measurement, simulation, portal frame bridge, concrete.

Introduction

Cracks increase the risk of corrosion and may reduce the durability of structures. Since restraint loads may cause cracking, it is of importance to consider such loads in design. Therefore, many studies aiming to determine the thermal load magnitude caused by ambient climate in bridges have been performed. E.g. Peiretti et al. [1] measured temperature gradients over bridge cross sections, Fu [2] looked into the temperature difference between flange and web in a box section bridge, Barr et al. [3] measured the temperature in concrete girders and Rodriguez et al. [4] investigated temperature differences between box-girder and the bridge deck in a girder bridge.

Other studies have aimed at developing models for temperature simulations in bridges. In many studies, e.g. [5], [6] [7] and [8], calculated values for solar radiation was used in the models. Instead of using calculated values for radiation, measured radiation values were used by Larsson [9]. Also, measured values for air temperature and wind speed were used as input to the model. The model was validated for simulation of temperature in a concrete slab surrounded by air, and has later been used for temperature simulation in a box cross section [10] and for investigation of parameter

influence on temperature differences between structural parts in portal frame bridges [11].

In this paper, simulation results obtained using the model developed by Larsson [9] is compared with temperature measurements in a portal frame bridge. Temperature was measured in 13 locations in a concrete portal frame bridge during a 12-month period and simulations of the temperature in the same structure was made for the same time period. The aim is to determine whether the model can be used in the future to determine thermal load values for portal frame bridges. The need for a review of certain thermal load cases was stressed by Gottsäter et al. [12], who showed that the Eurocode load case describing different thermal loads in different structural parts [13] in combination with 3D design models using linear elastic material models are likely to overestimate thermal stresses in portal frame bridges. This is due to a combination of rigidly connected bridge deck and abutment in the frame corners and a simplistic description of the thermal load.

1 Temperature measurements

Temperature was measured in a portal frame bridge from the 6th of December 2016 to the 6th of December 2017. The bridge site is at 55°41'58" N, 13°8'12" E, i.e. close to Lund, Sweden. The surrounding landscape is dominated by flat fields and occasional copses. The bridge and parts of the surrounding landscape is shown in Figure 1. The geometry of the bridge cross section was obtained from the Bridge and Tunnel Management database (BaTMan) of the Swedish Transport Administration [14], and is illustrated in Figure 2.

Figure 1. Bridge seen from the east. Photo taken in September 2017.

Thermocouples were placed in the longitudinal mid-section of the bridge, in the points shown in Figure 3, by drilling holes in the concrete, placing the thermocouple wire and re-filling the holes with mortar. The used thermocouples were of type "K", which consist of one nickel-chrome wire and one nickel-aluminum wire. Information regarding the properties of the thermocouple wires can be found in e.g. [15] and [16]. The thermocouples were connected to data loggers of model Microedge Site-Log LPTM-1, which logged the measured temperatures. Measurements were performed in the southern abutment, due to the low amount of direct sunlight reaching it.

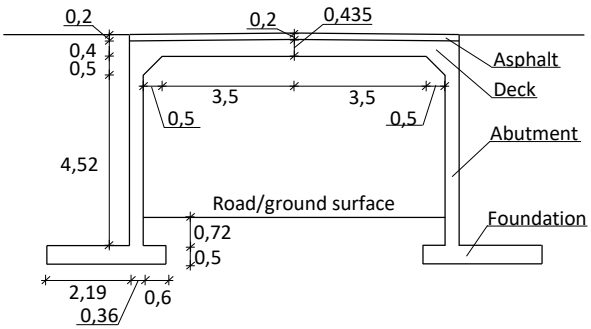

Figure 2. Geometry of the longitudinal bridge cross section, dimensions in m.

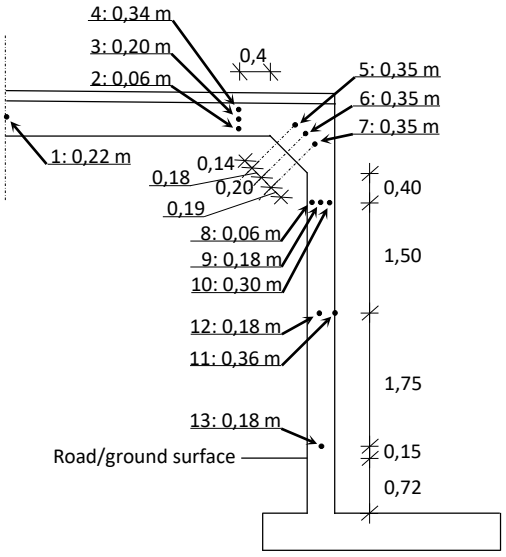

Figure 3. Thermocouple placement and numbering, with the depths of the thermocouples given as the distance from the closest concrete surface facing air underneath the bridge. Dimensions in m.

2 Thermal simulations

The model for thermal simulations is based on heat transfer by conduction, convection and radiation, and is described more extensively in Larsson [9].

2.1 Weather data

The weather data used in the model was air temperature, wind speed, short wave radiation and long wave radiation. The air temperature was measured at the bridge site using a thermocouple, while the wind speed data was obtained from the weather station "Malmö A" [17], operated by the Swedish metrological and hydrological institute (SMHI). The station is located in the outskirts of Malmö, about 15 km from the bridge site and is situated in a similar environment as the bridge. The radiation was measured at Lund University, Faculty of Engineering, about 5 km from the bridge site.

2.2 Simulation model

The thermal simulations were performed using a 2D finite element (FE) model of the longitudinal bridge cross section and adjacent soil and fill. The model is illustrated in Figure 4, and only includes the southern half of the cross section. Along the vertical edges of the model which are not facing air, heat transfer was prevented, corresponding to the case when temperature does not vary with horizontal position, but only with depth. To include a 4 m wide layer of soil and fill beside the abutment was motivated by previous convergence studies. The bottom of the model was 4 m below the road surface under the bridge, and was assigned a constant 9°C, corresponding to the annual mean temperature of the location. Doing so was motivated by Hillel [18], who illustrated soil temperature variation with depth over the year.

The FE-program DIANA version 10.1 [19] was used to run the simulations. Heat transfer elements were used, and were $0{,}05^2$ m^2 in the concrete and asphalt, and gradually increased to $0{,}25^2$ m^2 in the soil and fill away from the structure. The temperature measurements in the bridge started on the 6th of December 2016, but the simulation period started on the 1st of September 2016, using one-hour time-steps. This was done in order to eliminate the error caused by the rough estimate of the initial temperature used in the model. It is believed that the time period used for this purpose is more than sufficient, although the extensive soil and fill layers require considerable time for temperature adjustment. As the temperature measurements at the bridge site had not begun during this initial period, air temperature data from the SMHI weather station "Malmö A" [17] was used for this time period.

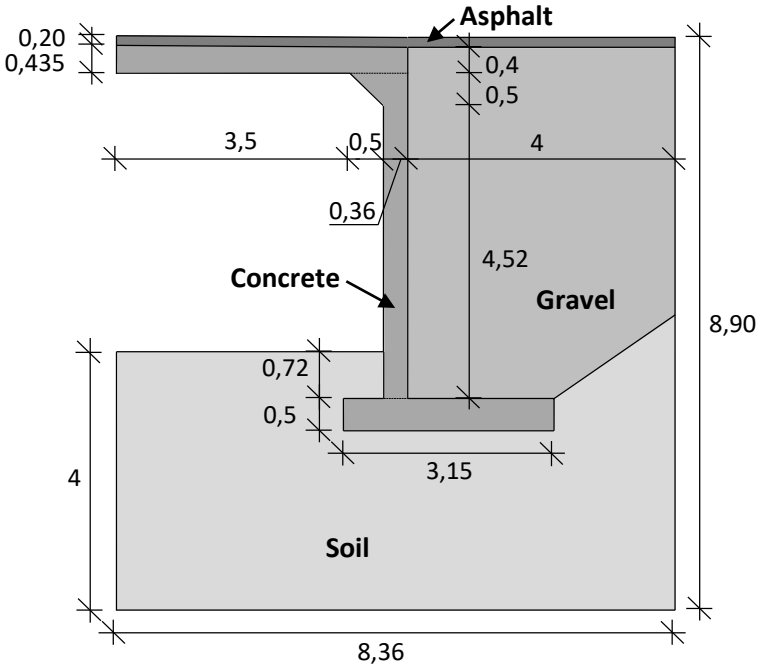

Figure 4. Illustration of the model used in simulations. Dimensions in m.

Parameters

Table 1 shows the values of density, heat conductivity and specific heat capacity for concrete, asphalt, soil and fill used in the study. The soil values correspond to a clay till, as this is the soil type at the location, according to the Geological Survey of Sweden [20]. For the other materials, the parameters used were chosen as mean values from spans with values used by other researchers. The spans with parameter values for concrete were taken from Ljungkrantz et al. [21], asphalt values were found in Larsson [22] and gravel values in Sundberg [23]. For the gravel, the span consisted of values corresponding to a dry friction soil with a porosity of 0,25 to 0,5.

Table 1. Parameters values used in the simulation.

Material	Parameter	Unit	Values used
Concrete	Density	kg/m3	2350
	Heat conductivity	W/(m·°C)	2,05
	Specific heat capacity	J/(kg·°C)	900
Asphalt	Density	kg/m3	2170
	Heat conductivity	W/(m·°C)	1,6
	Specific heat capacity	J/(kg·°C)	880
Soil	Density	kg/m3	2000
	Heat conductivity	W/(m·°C)	1,0
	Specific heat capacity	J/(kg·°C)	1600
Gravel	Density	kg/m3	1688
	Heat conductivity	W/(m·°C)	0,45
	Specific heat capacity	J/(kg·°C)	845
Other	Emissivity (asphalt)		0,90
	Absorptivity (asphalt)		0,80

Table 1 also shows the emissivity and absorptivity assigned to the asphalt layer. The emissivity value corresponds to the mean value of the span presented in Larsson [22], while the absorptivity was chosen as the lower value of the span given in Bretz et al. [24], as the asphalt surface looked weathered and relatively light-coloured.

Results

In Table 2 and 3, the min, mean and max temperatures are shown for selected thermocouples in January and July, respectively. The corresponding results obtained with the simulation model are also shown. When the measured and simulated temperatures are compared, it is seen that they agree quite well. One observation is that in July, the simulation gives lower temperatures than the measurements, as the mean temperatures as well as the extreme temperatures differ up to 1,1°C. The model can therefore be expected to give mean temperatures as well as extreme temperatures with an accuracy of about 1°C, when comparing temperature in specific points.

Table 2. Minimum, maximum and mean temperature during January for some of the measuring points in the bridge (see Figure 3).

Measurer	Min [°C]	Mean [°C]	Max [°C]
Air temperature	-11,0	0,8	6,9
Point 3 – measured	-5,7	1,1	6,2
Point 3 – simulated	-7,4	0,9	5,8
Point 6 – measured	-4,0	0,7	5,0
Point 6 – simulated	-3,7	1,2	5,1
Point 9 – measured	-1,5	1,5	5,6
Point 9 – simulated	-2,2	1,7	5,4
Point 12 – measured	-1,4	2,1	5,7
Point 12 – simulated	-2,2	1,9	5,6
Point 13 – measured	0,7	3,0	6,0
Point 13 – simulated	-0,3	2,8	6,0

In Figure 5, the air temperature as well as measured and simulated temperature are shown for two locations in the bride. The figure shows that the temperature variation is significantly different between the point in the bridge deck (point 4) and in the abutment (point 11), as the point in the bridge deck responds much faster to weather changes. It also shows that this difference is captured in the simulation, which shows similar temperature variations as the measurements do, although the simulated temperatures tend to be slightly lower than the measured during the illustrated period.

Table 3. Minimum, maximum and mean temperature during July for some of the measuring points in the bridge (see Figure 3).

Measurer	Min [°C]	Mean [°C]	Max [°C]
Air temperature	9.9	16.1	23.6
Point 3 – measured	16.2	20.3	23.7
Point 3 – simulated	15.9	19.3	22.5
Point 6 – measured	16.7	19.7	22.5
Point 6 – simulated	16.7	19.2	21.2
Point 9 – measured	15.6	17.9	19.3
Point 9 – simulated	14.5	16.8	18.7
Point 12 – measured	14.7	17.0	19.1
Point 12 – simulated	13.9	16.1	18.0
Point 13 – measured	13.7	15.4	17.0
Point 13 – simulated	13.3	15.2	16.9

3 Sources of error in measurements and simulation

There are many possible sources of error which may explain the differences in results between measurements and simulation. One of these is the weather data used in the simulation, as the radiation was measured 5 km from the bridge site and the wind speed 15 km, and could therefore have differed from the actual conditions. Also, as the thermocouples measure small voltages, any disturbance by e.g. moisture might have affected the measured result. Possibly, damage developed over time could lead to a constant overestimation of the actual temperature.

Also, as the material parameters shown in Table 1 were unknown at the bridge site, the simplification of using mean values of developed spans will affect the results. In order to obtain higher temperatures in the model, as needed according to Figure 5 and Table 3, other simulations were performed using other parameter values. It did however turn out to be difficult to adjust the parameters in such a way that the overall temperature increased equally, as e.g. increasing the solar absorptivity increased the temperature in the bridge deck much more than in the abutment. Attempts to account for the solar radiation reaching the abutment could not explain the deviation either, and since this rendered a significant complication of the model, it was not included in the final version of the simulation model.

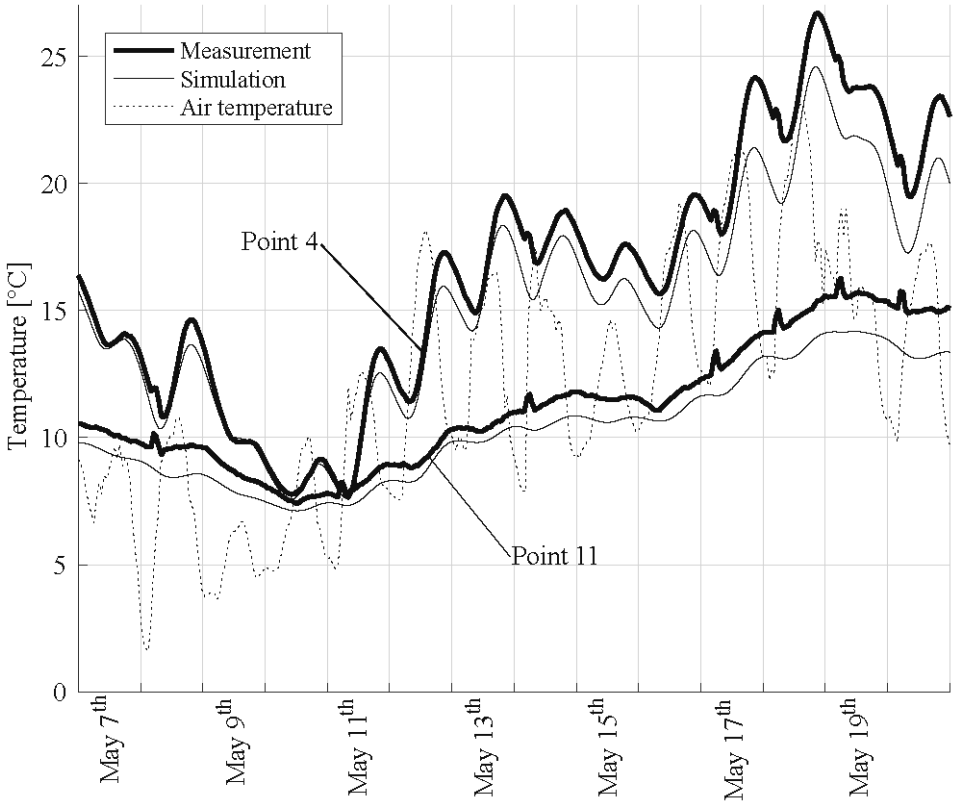

Figure 5. Temperature in point 4 (in the bridge deck, see Figure 3) and 11 (in the abutment, see Figure 3) according to measurement and simulation, as well as air temperature during 14 days in May 2017.

It should also be noted that the model was verified for a specific portal frame bridge in Lund, Sweden, and that the model error could depend on e.g. the climate of the bridge location. Therefore, before using the model for temperature estimation in locations with different climates, more validations might have to be performed.

4 Conclusions

In this study, a 2D FE-model for temperature simulation has been validated using temperature measurements in a portal frame bridge outside Lund, Sweden. Measurements were made during a 12-month period in 13 locations in a cross section of the bridge, both in bridge deck and in abutment.

The results show that the model can recreate both seasonal and daily variations, but often renders a result about 1°C colder than the measurements. If a sufficient safety margin is chosen, the model can be used in future determination of thermal load values for portal frame bridges. The magnitude of the safety margin would depend on the type of thermal load developed.

As the thermal loads given in the present Eurocode are quite general, developing load values for more specific purposes could lead to more effective use of reinforcement. Also, Gottsäter et al. [12] showed that the present Eurocode [13] in combination with 3D design models using linear elastic material models are likely to overestimate the need for reinforcement in portal frame bridges. Therefore, both financial and environmental benefits could be obtained by future work on the subject.

5 Acknowledgements

This research was sponsored by the Swedish Transport Administration, and SBUF, the Swedish construction industry´s organization for research and development.

6 References

[1] Peiretti CH, Parrotta EJ, Oregui BA, Caldentey PA, Fernandez AF. Experimental Study of Thermal Actions on a Solid Slab Concrete Deck Bridge and Comparison with Eurocode 1. *Journal of Bridge Engineering.* 2014; 19(10).

[2] Fu Y. Research on Temperature Effects iof the Pre-stressed Concrete Box Girder Bridge. *Applied Mechanics and Materials.* 2015; Vol. 744-746: 821-826.

[3] Barr PJ, Stanton J, Eberhard M. Effects of temperature variations on precast, prestressed concrete bridge girders. *Journal of Bridge Engineering.* 2005; 186.

[4] Rodriguez LE, Barr PJ, Halling MW. Temperature Effects on a Box-Girder Integral-Abutment Bridge. *Journal of Performance of Constructed Facilities.* 2014; 28(3): 583-591.

[5] Elbadry M, Ghali A. Temperature Variations in Concrete Bridges. *Journal of Structural Engineering.* 1983; 109(10): 2355-2374.

[6] Mirambell E, Aguado A. Temperature and Sterss Distributions in Concrete Box Girder Bridges. *Journal of Structural Engineering.* 1990; 116(9): 2388-2409.

[7] Westgate R, Koo KY, Brownjohn JMW. Effect of Solar Radiation on Suspension Bridge Performance. *Journal of Bridge Engineering.* 2015; 20(5).

[8] Zhu J, Meng Q. Effective and Fine Analysis for Temperature Effect of Bridges in Natural Environments. *Journal of Bridge Engineering.* 2017; 22(6).

[9] Larsson O. Modelling of Temperature Profiles in a Concrete Slab under Climatic Exposure. *Structural Concrete.* 2009; 10(4): 193-201.

[10] Larsson O, Karoumi R. Modelling of Climatic Thermal Actions in Hollow Concrete Box-Cross-Sections. *Structural Engineering International.* 2011; 21(1): 74-79.

[11] Gottsäter E, Larsson Ivanov O, Molnár M, Crocetti R, Nilenius F, Plos M. Simulation of thermal load distribution in portal frame bridges. *Engineering Structures.* 2017; 143: 219-231.

[12] Gottsäter E, Ivanov O, Crocetti R, Molnár M, Plos M. Comparison of Models for Design of Portal Frame Bridges with regard to Restraint Forces. *ASCE Structures Congress*

2017; Denver: American Society of Civil Engineers; 2017.

[13] EN 1991-1-5. *Eurocode 1: actions on structures – Part 1-5: general actions: thermal actions.* Brussels: European Committee for Standardization; 2003.

[14] Svedish transport administration (Trafikverket); BaTMan; available at https://batman.trafikverket.se/externportal (2018-02-08).

[15] American society for testing and materials; *Manual on the use of thermocouples in temperature measurement.* ASTM special technical publication; 470; 1970

[16] Eckert, Goldstein. *Measurements in Heat Transfer.* 2 ed. Hemisphere Publishing Corporation; 1976.

[17] Swedish Metrological and Hydrological Institute (SMHI); Open data; available at: http://opendata-download-metobs.smhi.se/explore/# (2018-02-08).

[18] Hillel D. *Introduction to environmental soil physics*. San Diego: Academic Press; 2004.

[19] DIANA; https://dianafea.com/content/DIANA (2018-02-08).

[20] Geological Survey of Sweden (SGU); https://www.sgu.se/en/products/maps/ (2018-02-08).

[21] Ljungkrantz C, Möller G, Petersons N. *Betonghandbok - material.* 2 ed: Solna: Svensk byggtjänst; 1994.

[22] Larsson O. *Climate related thermal actions for reliable design of concrete structures.* Division of Structural Engineering, Lund University; 2012.

[23] Sundberg J. *Termiska egenskaper i jord och berg.* Linköping: Statens geotekniska institut; 1991.

[24] Bretz, Akbari, Rosenfeld. Practical Issues for Using Solar-Reflective Materials to Mitigate Urban Heat Islands. *Atmospheric Environment.* 1997; 32 (1): 95-101.

BILAGA E:

Validation of model for temperature simulation using measurements in a portal frame bridge

Erik Gottsäter, Lund University*
Oskar Larsson Ivanov, Lund University
Miklós Molnár, Lund University
Mario Plos, Chalmers University of Technology

* corresponding author: erik.gottsater@kstr.lth.se

Key words: Validation, temperature, measurement, simulation, portal frame bridge, concrete

Abstract

In the design of bridges, thermal loads are important to take into account, since they can cause cracking if the structure or structural part is restrained from changing its size. Accurate thermal load values, based on the actual temperature distribution that may appear in a bridge, must therefore be used in bridge design. In this paper, the validation of a model for temperature simulation is presented by comparing simulated temperatures with temperature measured at 13 locations in a portal frame bridge during a period of 12 months. The simulation model uses measured air temperature, wind speed and long-and short wave radiation as input to calculate the temperature for every hour in the time period. The model is to be used in future work in the determination of temperature differences between deck and abutments in portal frame bridges. The results show that the model was capable of predicting the temperature distribution adequately, and that conservative values of the temperature difference between the structural parts can be obtained by adding no more than 1.5°C to the simulated temperature difference, depending on the application.

Introduction

It is important to take thermal loads into account in bridge design, since they can cause cracking of concrete in restrained structural parts. Cracks may in turn increase the risk of corrosion and thereby reduce the durability of the structure. Numerous previous studies aiming at determining the magnitude of thermal loads in bridges, caused by ambient climate, have been performed. These previous studies include e.g. Peiretti et al. (2014), who measured temperature gradients over bridge cross sections, Wang et al. (2014) and Fu (2015), who looked into the temperature difference between flange and web in a box section bridge, Barr et al. (2005), who measured the temperature in concrete girders and Rodriguez et al. (2014) and Zhou et al. (2016), who investigated temperature differences between box-girder and the bridge deck in a girder bridge.

Also, various studies aiming at developing computer models for temperature simulation have been performed. Elbadry and Ghali (1983) used an estimated sinusoidal temperature variation during the day, combined with solar radiation calculated from the angle of the sun towards the surface of the bridge. Mirambell and Aguado (1990) performed a comparison using a similar model, and took records of cloudiness into account when estimating radiation influx. Other studies simulating concrete bridge temperatures using calculated solar radiation include Xia et al. (2013), Westgate et al. (2015) and Zhu and Meng (2017). Instead of using calculated values for radiation, Larsson (2009) developed a model for simulating temperature in a concrete slab using measured radiation values. Measured values for air temperature and wind speed were also used as input to the model.

In the design of bridges, thermal loads are included through various load cases, describing different parts of the thermal load distribution in the bridge. One of the thermal load cases given in Eurocode EN 1991-1-5 (CEN 2003) assigns different uniform temperatures to different structural parts. This specific load case has been shown to predict large stresses in portal frame bridges if the transversal

direction of the bridge is included in design and a linear elastic material model is used (Gottsäter et al., 2017a). The stresses appear in the model since parts which have been assigned different temperatures are rigidly connected, causing a sudden temperature change over a connection which does not allow any relative movements. A sudden temperature change over the connection is however not realistic. Also, as the recommended load value for this specific load case (15°C, no specific limit state mentioned) is the same for all bridge types, the value could be exaggerated for portal frame bridges. This was indicated by Gottsäter et al. (2017b), who showed that a reasonable quasi-permanent load value for this specific load case is likely significantly lower than the present Eurocode value.

This article evaluates the use of the simulation model developed by Larsson (2009) for simulating temperature in portal frame bridges, by comparing the simulated temperature values with measurements. The measurements were made at 13 locations in a concrete portal frame bridge during a 12-month period, and simulations of the temperature in the structure were carried out for the same time period. The aim is to determine whether the simulation model is suitable for future use, i.e. for determining thermal load values for portal frame bridges. The model used in this study was developed by Larsson (2009) for thermal simulations of a concrete slab surrounded by air, and has later been verified for a hollow concrete box cross-section (Larsson and Karoumi, 2011). It was also used by Gottsäter et al. (2017b) for both comparison of simulated temperature with thermal load cases in Eurocode, and investigation of material and geometry parameter influence on thermal load magnitude.

Temperature measurements

From the 6th of December 2016 to the 6th of December 2017, temperature was measured in a portal frame bridge located about 1 km west of Lund, Sweden, its exact position being 55°41’58” N, 13°8’12” E. The bridge was constructed in 1989, the location is approximately 15 m above sea level and the surroundings are flat fields, except to the east where there is a copse with low trees, see Figure 1. The bridge deck is at the same level as the ambient ground level, and the road under the bridge is thereby lower than the ambient ground level. The geometry of the bridge section is shown in Figure 2. The information shown in the figure was obtained from the Bridge and Tunnel Management database (BaTMan) of the Swedish Transport Administration, (Trafikverket, 2017).

Figure 1. Bridge seen from the west. Photo taken in July 2017.

The locations for temperature measurement are shown in Figure 3. Holes were drilled in which thermocouples were inserted, and thereafter the holes were injected with mortar. Thermocouples of type “K” were used, which consist of one nickel-chrome wire and one nickel-aluminum wire. The properties and functionality of thermocouples is described more extensively in e.g. American society for testing and materials (1970) and Eckert and Goldstein (1976). The thermocouples were placed in the longitudinal mid-section of the bridge and connected to data loggers of model Microedge Site-Log

LPTM-1, using a sample period of one minute. Measurements were performed in the southern half of the bridge due to the low amount of direct sunshine reaching the southern abutment; this was preferable since sunshine was only included for the top surface of the bridge deck in the simulation model. To completely avoid sunshine reaching the abutments was however difficult at the latitude of the bridge, almost 56° north, since the positions of sunrise and sunset vary greatly over the year.

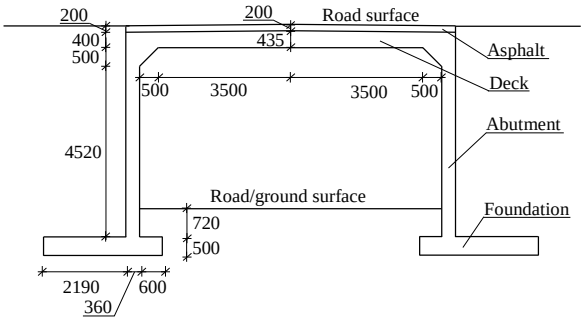

Figure 2. Geometry of the longitudinal bridge cross section. Dimensions in mm.

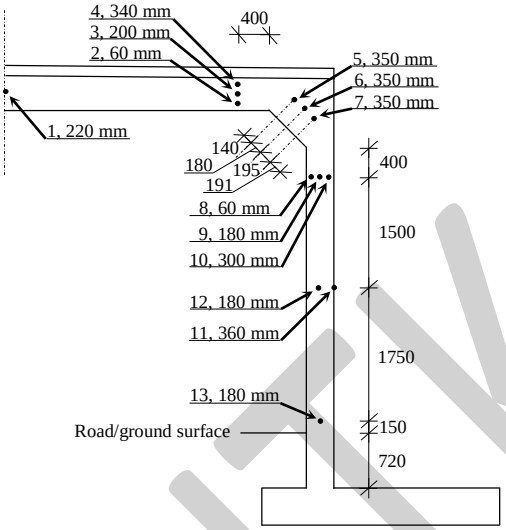

Figure 3. Thermocouple placement and numbering. The depths of the thermocouples are also given, and are measured from the closest concrete surface facing air underneath the bridge. Dimensions in mm.

Thermal simulations

The model for thermal simulations used in this study was developed by Larsson (2009). It describes heat transfer through conduction within the model, as well as heat flux to and from the model along surfaces facing air. The latter is described in Eq. (1) where q is the total heat flux in W/m^2, q_s is heat flux from solar radiation, q_c is heat flux due to convection and q_r is heat flux due to long wave radiation.

$$q = q_s + q_c + q_r \quad (1)$$

Thermal flux from solar radiation is calculated using Eq. (2) as the absorptivity of the material, a, multiplied by global radiation, G.

$$q_s = aG \quad (2)$$

Heat flux due to convection is dependent on the convection coefficient, h_c, surface temperature, T_s and air temperature, T_{air} as shown in Eq. (3).

$$q_c = h_c(T_s - T_{air}) \quad (3)$$

The convection coefficient h_c (in W/(m^2°C)) is in turn calculated from the wind speed according to expressions given by Nevander and Elmarsson (2006), shown in Eqs. (4) and (5).

$$h_c = 6 + 4v, \ v \leq 5 \text{ m/s} \quad (4)$$

$$h_c = 7.4v^{0.78}, \ v > 5 \text{ m/s} \quad (5)$$

Heat flux due to long wave radiation is determined by the Stefan Boltzman law shown in Eq (6), where σ is the Stefan-Boltzman constant of $5.67 \cdot 10^{-8}$ W/(m^2°C^4), ε is the emissivity of the surface material, T_s is the surface temperature and $T_{opposite}$ is the temperature of the opposite surface.

$$q_r = \sigma\varepsilon\left(T_s^4 - T_{opposite}^4\right) \quad (6)$$

Weather data

The weather data used as input in the simulation model included air temperature, short wave solar radiation, long wave radiation and wind speed. Air temperature was measured under the bridge with the same type of thermocouple as was used for the measurements within the structure. Wind speed data was obtained from the closest active measuring site of the Swedish Metrological and Hydrological Institute (SMHI). The station is named "Malmö A" (SMHI, 2017) and is situated in the eastern outskirts of Malmö. The location is 20 m above sea level and about 15 km south-southwest of the bridge site.

Radiation was measured at Lund University, Faculty of Engineering, approximately 5 km east-northeast of the bridge. Short wave radiation energy was measured with model BF3 of Delta-T Devices, and long wave radiation was measured with Huxeflux pyrgeometer model IR02. Both devices were dependent on connection to the electric grid, which was not available at the bridge site. This was the main reason for not measuring radiation and wind speed at the location of the bridge.

Simulation model

Thermal simulations were performed in a 2D finite element (FE) model of the longitudinal bridge cross section and adjacent soil, see Figure 4. The model only included the southern half of the bridge, where the temperature measurements were made. Along all vertical edges of the model not facing air, thermal flux was prevented, corresponding to a situation where temperature only varied with depth and was not affected by the horizontal position. Behind the abutment and below the road surface in the top of the model, the soil was replaced with gravel. This represents the fill that was placed after the construction of the bridge. The choice of including a 4 m wide layer of gravel and soil beside the abutment was motivated by previous simulations showing convergence of results for such levels of surrounding inclusion.

Along the bottom line of the model, 4 m below the surface of the road going under the bridge, a constant temperature of 9°C was assigned, which corresponds to the annual mean temperature of the location. Assigning this temperature at the depth of 4 m was motivated by Hillel (2004), who illustrated principal temperature variation with soil depth over a year. The measured solar radiation and long wave radiation acted on the top surface of the model. Along the surfaces beneath the bridge deck, neither solar nor long wave radiation was included. These surfaces were assumed to be shaded, and the absorbed long wave radiation was assumed to correspond to the emitted long wave radiation, causing the net radiation to be zero. This corresponds to the surfaces facing each other under the bridge deck having the same temperature and emissivity. Convection on the other hand occurred equally along all surfaces facing air.

Convection and long-wave radiation were modelled using boundary elements. Heat flux due to convection was calculated using Eq. (3), using the time-dependent convection coefficient and air temperature. The long wave radiation heat flux was calculated using Eq. (6), taking the time dependent long wave radiation value and the emissivity of the material into account. Solar radiation was on the other hand modelled as a boundary condition which added energy to the surface layer, taking the absorptivity of the surface into account according to Eq. (2).

The simulation was performed in the FE-program DIANA, version 10.1 (DIANA, 2018) using heat transfer elements. The size of the elements was 0.05^2 m^2 in the bridge structure and asphalt layer, and was gradually increased to 0.25^2 m^2 in the soil and gravel surrounding the structure. The calculation was made in one-hour steps, starting at 1st of September 2016, i.e. over three months before the measurement was initiated in the bridge. This was done in order to eliminate errors caused by the initial temperature distribution in the model, which was based on a rough estimate. The soil and gravel makes the model require a much longer time period for temperature adjustment compared to a model only including the bridge cross section. However, including a three-month period for elimination of the initial temperature error has in pre-studies been shown to be more than sufficient. As the temperature measurements were not started until the 6th of December, air temperature measured at the weather station "Malmö A", was used for the simulation during the initial period. Otherwise, the weather data used was obtained in the same way as during the measurement period.

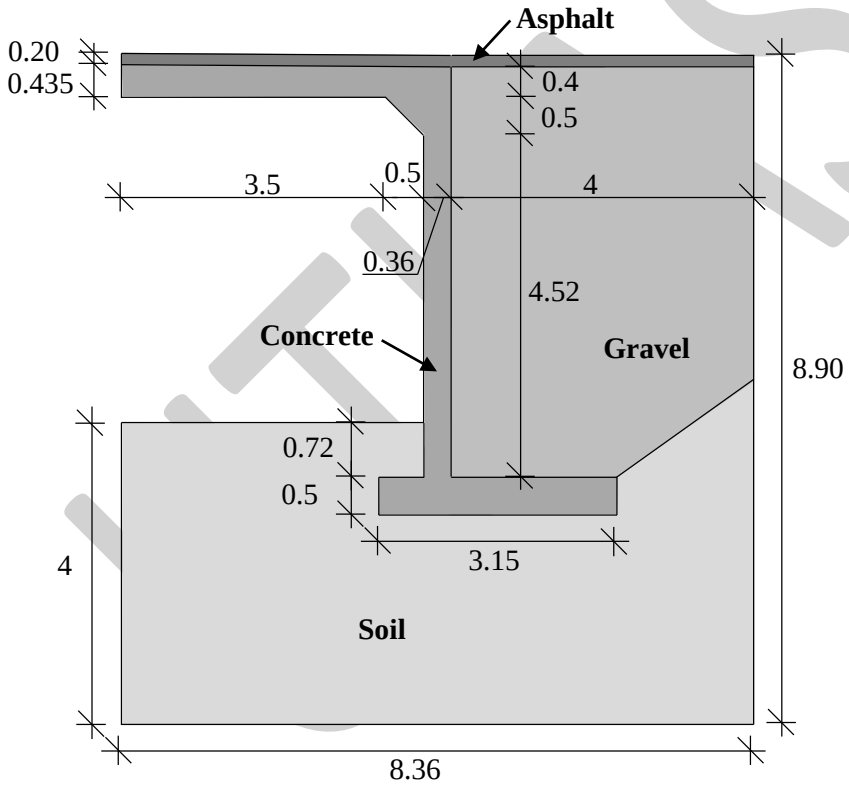

Figure 4. Illustration of the model used in simulations. Dimensions in m.

Parameters

Table 1 shows the values for density, specific heat capacity and thermal conductivity used in the model. The table also shows values for emissivity and absorptivity for the asphalt paving of the road carried by the bridge. As the actual material parameters at the bridge site were unknown, values used in previous work by other researchers were used in this study. For concrete and asphalt, the values used are mean values from spans corresponding to the maximum and minimum values given in each reference, respectively, except for the absorptivity, which was determined as the minimum value in the

given span as the road surface looked old and weathered. The maximum and minimum values are also given in Table 1, together with references to the publications where the values were found.

The soil and gravel parameters shown in Table 1 were on the other hand determined without the use of minimum and maximum values used in other studies, as the reference did not state such values. The soil parameters were instead determined directly for a soil consisting of clay till, with a clay content over 25%, as this is the soil type at the bridge location according to The Geological Survey of Sweden (SGU, 2017). The soil depth is 30-50 m, indicating that no bedrock should be included in the model, as it reaches less than 9 m below the ambient ground surface. The gravel parameters were determined in a similar way, and represent dry gravel with a porosity of 0.4. The gravel was never considered to be wet since it was judged to be well drained, was covered from above by the asphalt layer, and since capillary forces can be neglected in friction soils.

In Gottsäter et al. (2017b), the influence of the parameters shown in Table 1 on the temperature difference between bridge deck and abutment was investigated for a simulation model including a similar bridge cross section. The same maximum and minimum values for the parameters were used in that study, as well as a weather data from a similar climate (Stockholm, Sweden). It was found that the absorptivity and heat conductivity of the asphalt paving were the most influential parameters of the ones used in the present study. The possible variations in the material parameters of the concrete and the soil, in that case corresponding to a friction soil, turned out to have a relatively small impact on the result.

Table 1. Parameter values used in the simulations, and reasonable intervals to choose parameter values within, according to the references given.

Material	Parameter	Unit	Values used	Min value	Max value	Reference
Concrete	Density	kg/m^3	2350	2300	2400	(Ljungkrantz et al., 1994)
	Heat conductivity	W/(m·°C)	2.05	1.60	2.50	
	Specific heat capacity	J/(kg·°C)	900	800	1000	
Asphalt	Density	kg/m^3	2170	2100	2240	Larsson, (2012)
	Heat conductivity	W/(m·°C)	1.6	0.7	2.5	
	Specific heat capacity	J/(kg·°C)	880	840	920	
	Emissivity		0.90	0.85	0.95	
	Absorptivity		0.80	0.80	0.95	Bretz et al., (1997)
Soil	Density	kg/m^3	2000			Sundberg, (1991)
	Heat conductivity	W/(m·°C)	1.0			
	Specific heat capacity	J/(kg·°C)	1600			
Gravel	Density	kg/m^3	1688			Sundberg, (1991)
	Heat conductivity	W/(m·°C)	0.45			
	Specific heat capacity	J/(kg·°C)	845			

Results

Figure 5 shows the measured air temperature at the bridge site for the entire time period. As shown, there were a few short periods with cold weather during the winter, causing relatively large fluctuations in temperature. This was also seen during spring and somewhat during fall, but during summer the temperature variations were mostly due to daily variations. Such temperature shifts were on the other hand almost nonexistent during winter, when the influence of the solar radiation on the temperature is smaller.

Table 2 and 3 give the minimum, mean and maximum temperature for selected measurement points for January and July respectively, as well as the corresponding results from the thermal simulation.

The tables show that the temperature was less extreme in the abutment, with higher minimum and mean temperatures in winter, as well as lower temperatures in summer. Also, the results from the simulation agree well with the measured values, as the difference between measured and simulated values is less than 1°C for most cases. It can however be seen that the simulation tended to give a slightly lower temperature than the measurements, at least during summer.

As seen in Table 2 and 3, the simulation captured both the overall (mean) temperature in the structure and the extreme values fairly well. The simulation also gave a realistic temperature variation over the day, as can be seen in Figure 6. The figure shows the temperature variation during roughly the first half of May, a period during which the air temperature shifted significantly. Both measured and simulated temperatures in location 4 (top side of the bridge deck, see Figure 3) and location 11 (back side of the abutment, see Figure 3) are shown. Although the simulation model often gave a lower temperature than the measurement, the daily variations were similar, and the response to the colder air temperatures starting in the middle of the time period shown was similar in the measurements and simulations for each location, respectively. On the other hand, the two different locations reacted differently to weather changes, with location 4 showing larger temperature fluctuations than location 11. This shows that the model managed to capture the thermal changes both in the bridge deck and the abutment, as is also indicated by Table 2 and 3.

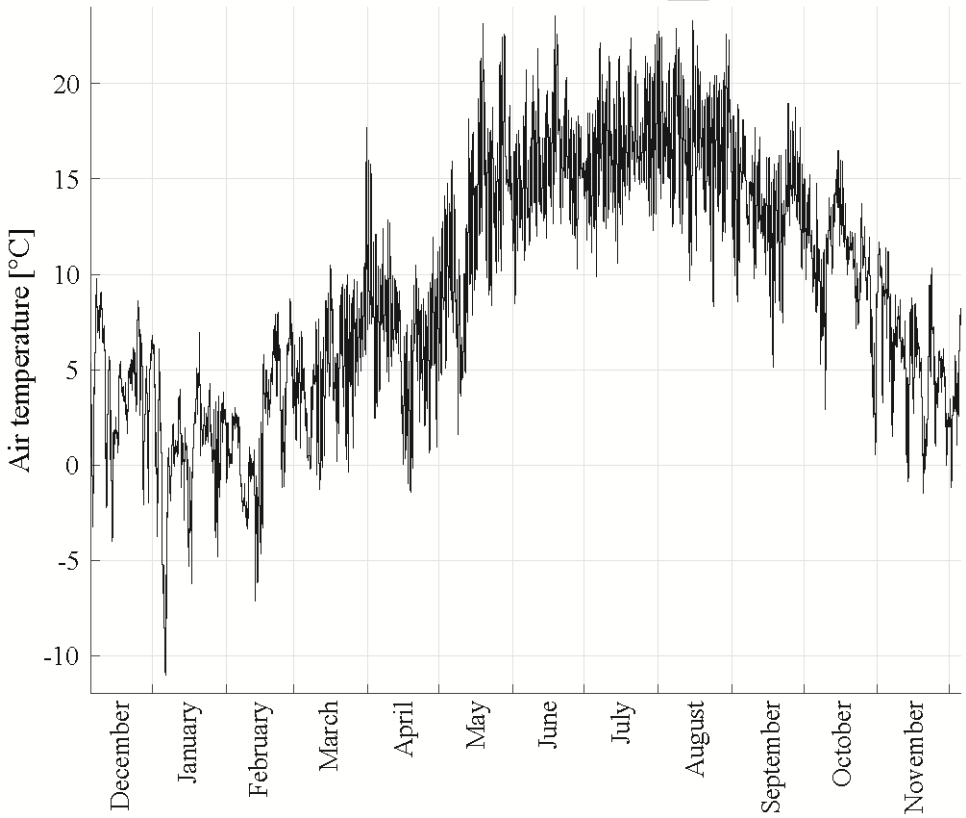

Figure 5. Air temperature during the measurement period, from 6th of December 2016 to 6th of December 2017.

Table 2. Minimum, maximum and mean temperature during January for some of the measurement locations in the bridge (see Figure 3).

Measurer	**Minimum [°C]**	**Mean [°C]**	**Maximum [°C]**
Air temperature	-11.0	0.8	6.9
Location 3 – measured	-5.7	1.1	6.2
Location 3 – simulated	-7.4	0.9	5.8

Location 6 – measured	-4.0	0.7	5.0
Location 6 – simulated	-3.7	1.2	5.1
Location 9 – measured	-1.5	1.5	5.6
Location 9 – simulated	-2.2	1.7	5.4
Location 12 – measured	-1.4	2.1	5.7
Location 12 – simulated	-2.2	1.9	5.6
Location 13 – measured	0.7	3.0	6.0
Location 13 – simulated	-0.3	2.8	6.0

Table 3. Minimum, maximum and mean temperature during July for some of the measurement locations in the bridge (see Figure 3).

Measurer	**Minimum [°C]**	**Mean [°C]**	**Maximum [°C]**
Air temperature	9.9	16.1	23.6
Location 3 – measured	16.2	20.3	23.7
Location 3 – simulated	15.8	19.2	22.5
Location 6 – measured	16.7	19.7	22.5
Location 6 – simulated	16.7	19.2	21.1
Location 9 – measured	15.6	17.9	19.3
Location 9 – simulated	14.4	16.8	18.7
Location 12 – measured	14.7	17.0	19.1
Location 12 – simulated	13.9	16.1	18.0
Location 13 – measured	13.7	15.4	17.0
Location 13 – simulated	13.3	15.2	16.9

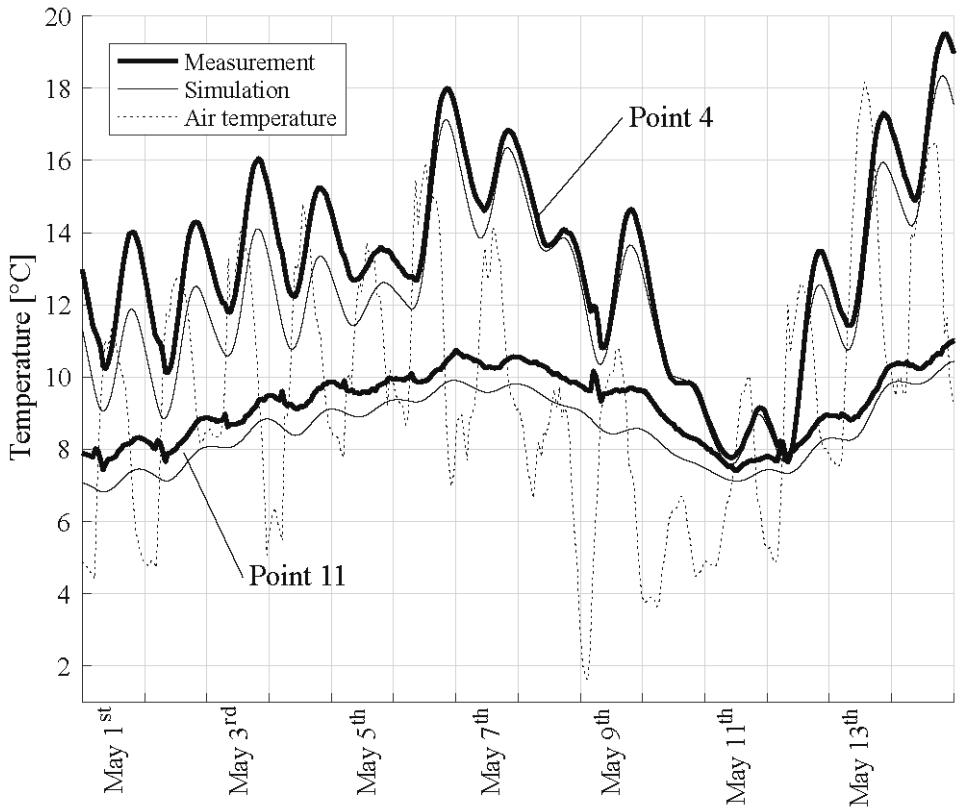

Figure 6. Temperature at location 4 (in the bridge deck) and 11 (on the back side of the abutment), see Figure 3, according to measurement and simulation, as well as air temperature during the first half of May 2017.

As the aim of the paper is to develop a simulation model that can be used to determine the temperature difference between structural parts in portal frame bridges, the accuracy and precision of the model in this aspect was also investigated. This was done by comparing the mean temperature in the locations in the bridge deck (locations 2-4, 1 was left out due to malfunction) with the mean temperature in the locationts in the abutment (8-9, 12 and 13. 11 was excluded since it is not located within the abutment, but at the edge), both using measured and simulated results. The locations in the frame corner (5-7) were left out since it was shown by Gottsäter et al. (2017b) that the transition from deck temperature to abutment temperature occurs in the corner area. To include the corner in a comparison between temperature in the deck and abutment could therefore lead to an underestimation of the temperature difference between the parts. The obtained values of the temperature difference do not correspond to the actual temperature difference between the structural parts as only a few locations are used. However, the difference in results obtained by using measured and simulated values can be used as an indication of the reliability of the simulation model, with respect to temperature differences between the studied structural parts.

Figure 7 shows the results of the comparison, as the absolute value of the temperature difference according to the measurements has been subtracted from the corresponding value obtained using the simulation for the entire period of time. Negative values thereby indicate that the temperature difference is underestimated by the simulation model, and the figure shows that such underestimations of more than 1.5°C are uncommon.

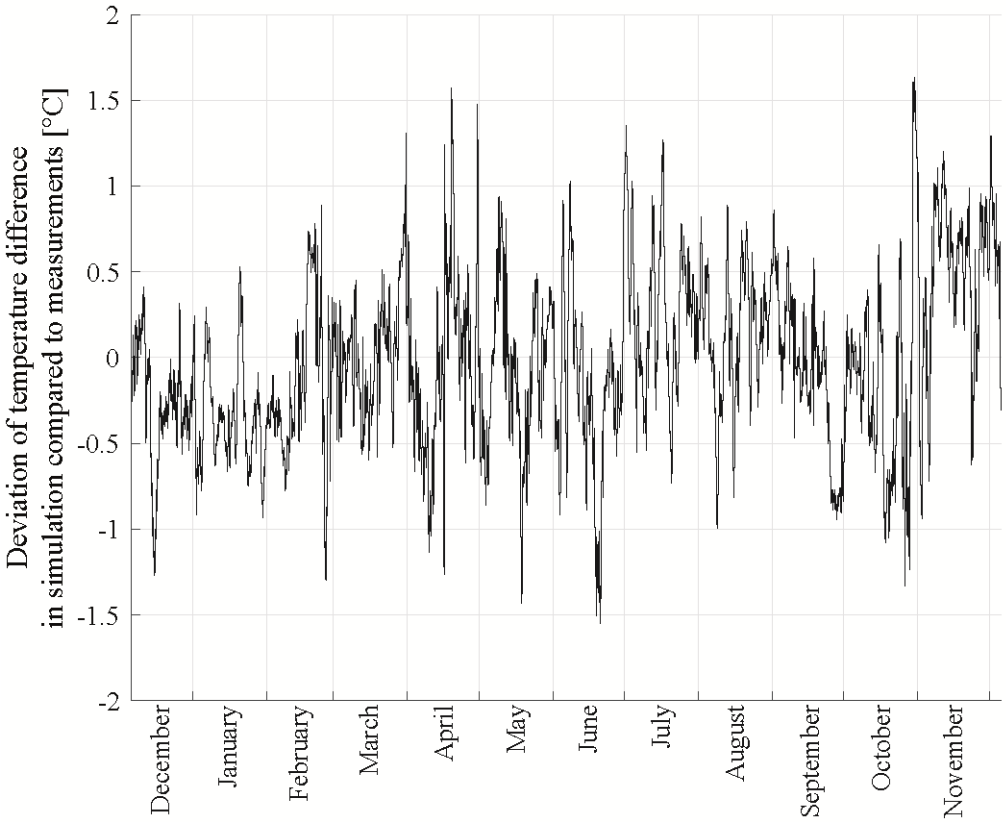

Figure 7. Deviation of temperature difference between deck and abutment in simulation, compared to the measurements. The temperature difference between the parts has in this case been calculated as mean temperature in measurement locations 2-4 minus mean temperature in locations 8-10, 12 and 13.

Discussion on uncertainties in measurements and simulation

The results show that the current simulation model predicted temperatures in the chosen portal frame bridge with an acceptable accuracy for both winter and summer conditions. Although the simulation model generally rendered slightly lower temperatures than the measurements (approximately 0-2°C), the difference was fairly similar in the entire bridge. Since the differences between temperatures within the structure is of interest, this should not hinder the use of the model.

As the mean values of the parameters were used in most cases, the model accuracy could possibly increase by adjusting these values. Attempts to increase the overall temperature in the model by increasing the solar absorptivity of the asphalt gave an increased temperature in the bridge deck, but had no significant impact on the temperature in the abutment. Also, since the road pavement on the bridge deck looked old and weathered, using a higher absorptivity value was considered unrealistic. Other attempts included adding solar radiation to the abutment at times when sunshine reached it. This did improve the agreement of the model in the lower part of the abutment, but as the higher parts were not as exposed to sunshine (due to shading by the bridge deck), it did not affect the temperature in the entire model, even when combined with the higher solar absorptivity value for the asphalt. Also, this adjustment in the model introduced more uncertainties and made the model more complex.

Other possible error sources relate to the weather data used in simulations. The radiation was measured 5 km from the bridge site and the wind speed 15 km away, and could therefore have differed from the actual conditions. However, since the difference between measured and simulated temperature was fairly constant over the time of comparison as exemplified in Figure 6, there must have been systematic differences between the used and actual weather conditions in order for this error to explain the difference in results. The climate preconditions are similar at the bridge site and the measurement sites, but the local surroundings such as the copse or the bridge itself could however affect the wind conditions. In the model, wind is added equally on all surfaces facing air, although the bridge structure itself is likely to influence the wind speed under the bridge deck, depending on the wind direction. Test simulations with a reduced wind speed under the bridge showed a better correlation during certain time periods, but a poorer correlation at other times. Attempts have also been made to adjust the wind speed depending on the wind direction, which did not render any significant general improvements either.

As the thermocouples measure small voltages, it is possible that e.g. moisture conditions in the structure could have affected the result. Other damage on the thermocouples could also have caused a small deviation of the measured temperature from the actual temperature over time. Some of the thermocouples did occasionally produce unrealistic temperatures, often as a sudden increase of temperature of about 10-50°C. These readings have been disregarded in the data analysis. Another uncertainty was the exact position of the thermocouples, which could have deviated slightly from the intended positions. During the installation, the thermocouple in measurement location no 1 was damaged and did not produce any results during the entire period.

It should also be noted that the model has been verified in Lund, Sweden and that other locations with different climates might be more sensitive to certain errors. Thus, the model needs to be verified in more locations before it can be used globally. However, currently the model is intended to be used to develop thermal loads for Swedish conditions, for which the study is expected to be adequate. One uncertainty could be the influence of colder winters in the north of Sweden, as e.g. heat conductivity changes when the materials freeze. This, as well as the energy required for melting and released by freezing, is not included in the model used in this study.

Estimation of temperature difference between structural parts

With the simulation model verified and considered reasonably suitable for the determination of temperature differences between bridge decks and abutments in portal frame bridges, this temperature difference was investigated with the results obtained from the performed simulation. Figure 8 shows

the difference in mean temperature between bridge deck and abutment according to the simulations, calculated as mean temperature of the nodes in the deck minus the mean temperature of the nodes in the abutment. As the transition from bridge temperature to abutment temperature occurs in the frame corner, as shown in (Gottsäter et al., 2017b), nodes less than 1 m from the system line frame corner were excluded from the comparison in order not to underestimate the temperature difference. Although the geometry and given weather data do not correspond to a worst case scenario to be considered in a design situation, the results shown in Figure 8 can be seen as yet another indication that the temperature difference to be considered in design for crack width limitation may be exaggerated in Eurocode (CEN 2003) for the specific bridge type. The maximum value of the temperature difference in the simulation was 7.9°C, compared to the Eurocode load value 15°C, which is not specified for a certain limit state, and could therefore be used to correspond a median (quasi permanent) value of the temperature difference.

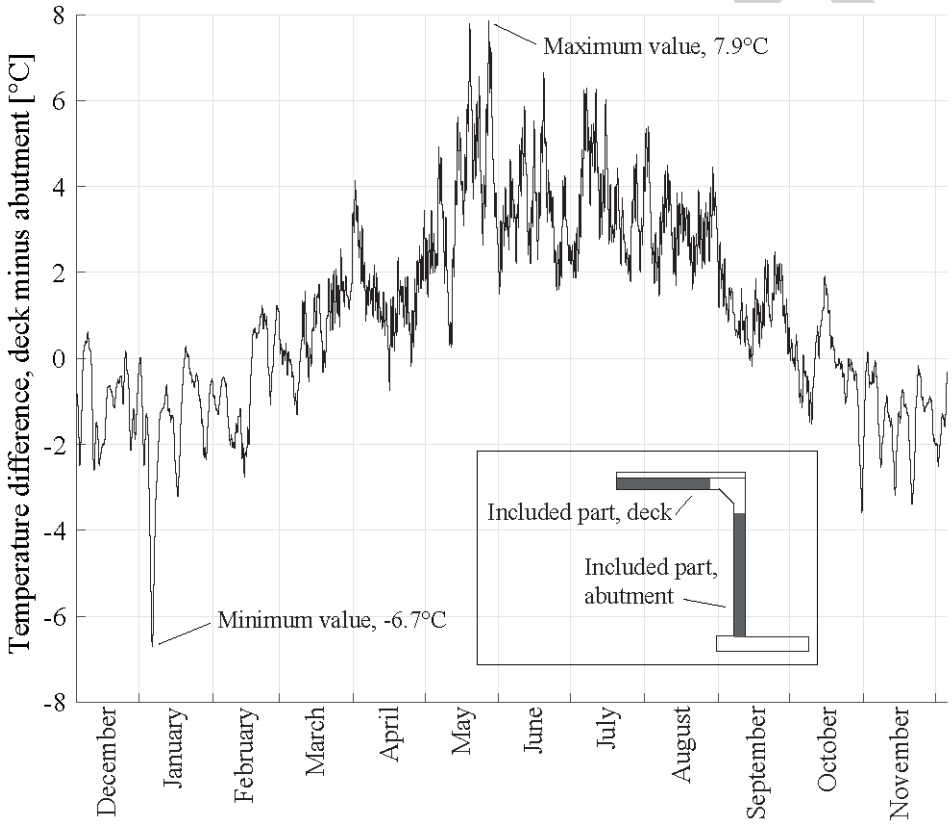

Figure 8. Temperature difference calculated as mean temperature in bridge deck minus mean temperature in the abutment. The frame corner has been excluded from the comparison, as shown in the illustration.

In Figure 9, the temperature distributions at the times for the largest negative (bridge deck colder than abutment) and positive (bridge deck warmer than abutment) differences are given. Figure 9 clearly shows that the temperature change from deck to abutment is gradual and occurs in the frame corner area, although gradients over the cross sections can be present simultaneously. Since previous work has shown that the way the temperature varies within the structural parts has a large impact on the resulting stresses (Gottsäter et al., 2017b), a thermal load case describing the difference in temperature between structural parts should also capture the variation of temperature within the model. It can also be noted in Figure 9 that there are substantial temperature changes in the lower part of the abutment,

just below the level of the road surface under the bridge. A more thorough investigation of this temperature difference is however outside the scope of this study.

When comparing the temperature difference according to the simulation shown in Figure 8 and the estimated deviation between temperature difference according to measurement and simulation shown in Figure 7, no clear correlation can be seen between large temperature differences and large deviations. In fact, at the time for the largest positive temperature difference at the end of May, Figure 7 shows the value 0.3°C, indicating a larger temperature difference in the simulation than in the measurements. When investigating the corresponding relation at the times for the 5 largest positive and negative temperature differences, only one coincides with a large positive deviation between measurement and simulation, and the mean difference between measured and simulated temperature difference between the parts for these 10 extreme value occasions becomes 0.13°C. The mean value for the entire period is -0.02°C. In order to avoid the risk of underestimating the temperature difference, we suggest that extreme values obtained in future simulations is increased by 1.5°C, as larger deviations were found to be almost nonexistent in this study. For mean and median values, a smaller increase is sufficient, as large deviations are unlikely to persist during longer periods of time.

Conclusions

In this study, a 2D FE-model for simulating temperature in a portal frame bridge has been evaluated by measurements in a bridge during a 12-month period. As the model is to be used for determining temperature differences between structural parts in portal frame bridges, the focus has been on evaluating the temperature difference between measurement locations in the bridge deck and in the abutment.

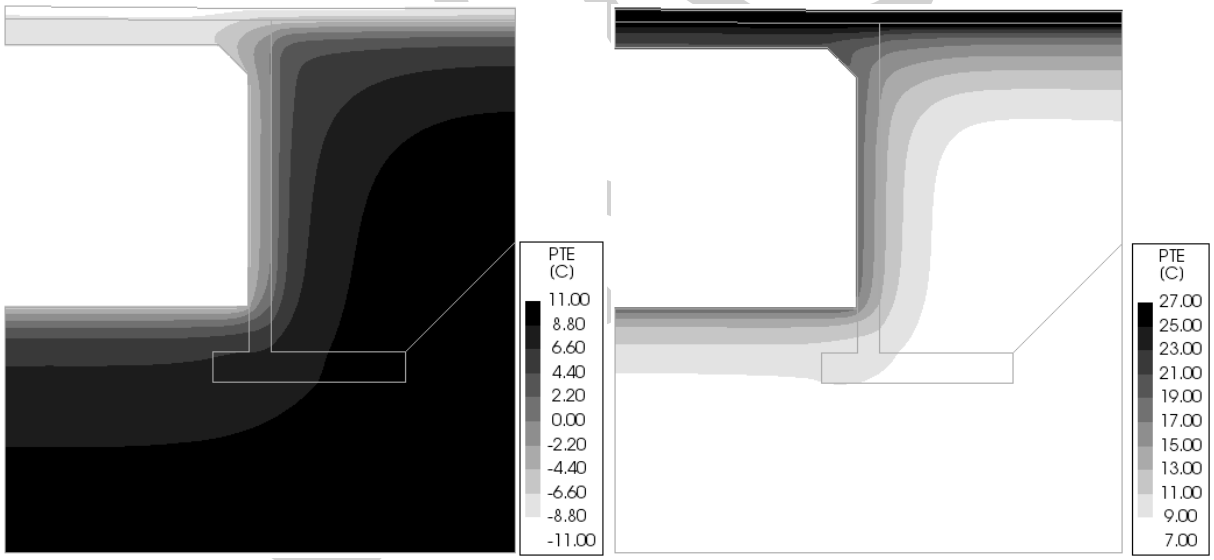

Figure 9. Temperature distribution in the simulation model at the time for the largest negative (left) and positive (right) temperature differences.

The results show that the model was capable of predicting the temperature distribution adequately, especially when the temperature distribution within the model is concerned. For the temperature difference between abutment and bridge deck, deviations of 1.5°C between measurement and simulation were rare, and also uncorrelated with the maximum temperature differences in the structure. Conservative values of the temperature difference can therefore be obtained by adding 1.5°C to the temperature difference obtained with the simulation model. This value can be reduced if mean values over time are of interest, as large deviations between model and reality are unlikely to be persistent over time.

Future work should aim to determine reasonable load values for load cases regarding temperature differences between bridge parts, using the simulation model validated in this paper. In order to obtain realistic thermal load values, this work needs to focus not only on the difference of the mean temperature in the structural parts, but also the temperature distribution within the parts. Improving the accuracy of the load case could in turn lead to a more effective use of reinforcement in the future, which would give both economic and environmental benefits.

Acknowledgements

This research was sponsored by the Swedish Transport Administration, and SBUF, the Swedish construction industry´s organization for research and development.

References

American society for testing and materials. (1970). “Manual on the use of thermocouples in temperature measurement”, Philadelphia.

Barr, P. J., Stanton, J. and Eberhard, M. 2005. "Effects of temperature variations on precast, prestressed concrete bridge girders." *J. Bridge Eng.*, 186.

Bretz, Akbari and Rosenfeld 1997. "Practical Issues for Using Solar-Reflective Materials to Mitigate Urban Heat Islands." *Atmospheric Environment*, Vol. 32, pp. 95-101.

CEN (European Committee for Standardization). (2003). “Actions on structures – Part 1-5: general actions: thermal actions” Eurocode 1, Brussels.

DIANA. https://dianafea.com/content/DIANA (2018-02-20).

Eckert and Goldstein 1976. *Measurements in Heat Transfer*, Hemisphere Publishing Corporation.

Elbadry, M. and Ghali, A. 1983. "Temperature Variations in Concrete Bridges." *J. Struct. Eng.*, 109, 2355-2374.

Fu, Y. 2015. "Research on Temperature Effects iof the Pre-stressed Concrete Box Girder Bridge." *Applied Mechanics and Materials*, Vol. 744-746, pp 821-826.

Gottsäter, E., Ivanov, O., Crocetti, R., Molnár, M. and Plos, M. 2017a. "Comparison of Models for Design of Portal Frame Bridges with regard to Restraint Forces." *ASCE Structures Congress 2017*, American Society of Civil Engineers, Denver.

Gottsäter, E., Larsson Ivanov, O., Molnár, M., Crocetti, R., Nilenius, F. and Plos, M. 2017b. "Simulation of thermal load distribution in portal frame bridges." *Engineering Structures*, 143, 219-231.

Hillel, D. 2004. *Introduction to environmental soil physics*, San Diego: Academic Press.

Larsson, O. 2009. "Modelling of Temperature Profiles in a Concrete Slab under Climatic Exposure." *Structural Concrete*, Vol. 10, pp. 193-201.

Larsson, O. 2012. *Climate related thermal actions for reliable design of concrete structures*, Division of Structural Engineering, Lund University.

Larsson, O. and Karoumi, R. 2011. "Modelling of Climatic Thermal Actions in Hollow Concrete Box-Cross-Sections." *Structural Engineering International*, Vol. 21, pp. 74-79.

Ljungkrantz, C., Möller, G. and Petersons, N. 1994. *Betonghandbok - material*, Solna : Svensk byggtjänst, 1994 ; (Stockholm : Svenskt tryck).

Mirambell, E. and Aguado, A. 1990. "Temperature and Sterss Distributions in Concrete Box Girder Bridges." *J. Struct. Eng.*, 116, 2388-2409.

Nevander, L. and Elmarsson, B. 2006. *Fukthandbok: praktik och teori*, Stockholm, Svensk Byggtjänst.

Peiretti, C. H., Parrotta, E. J., Oregui, B. A., Caldentey, P. A. and Fernandez, A. F. 2014. "Experimental Study of Thermal Actions on a Solid Slab Concrete Deck Bridge and Comparison with Eurocode 1." *Journal of Bridge Engineering*, 19, 04014041 (13 pp.).

Rodriguez, L. E., Barr, P. J. and Halling, M. W. 2014. "Temperature Effects on a Box-Girder Integral-Abutment Bridge." *Journal of Performance of Constructed Facilities*, 28, 583-591.

Sundberg, J. 1991. Termiska egenskaper i jord och berg. Linköping: Statens geotekniska institut.

Swedish Metrological and Hydrological Institute. “Open data” http://opendata-download-metobs.smhi.se/explore/# (2018-02-20).

The Geological Survey of Sweden. “Maps” https://www.sgu.se/en/products/maps/ (2018-02-20).

Trafikverket. “BaTMan” https://batman.trafikverket.se/externportal (2018-02-20).
Wang, G.-X., Ding, Y.-L., Wang, X.-J., Yan, X. and Zhang, Y.-F. 2014. "Long-Term Temperature Monitoring and Statistical Analysis on the Flat Steel-Box Girder of Sutong Bridge." *Journal of Highway and Transportation Research and Development (English Edition),* 8**,** 63-68.
Westgate, R., Koo, K. Y. and Brownjohn, J. M. W. 2015. "Effect of Solar Radiation on Suspension Bridge Performance." *J. Bridge Eng.,* 20.
Xia, Y., Chen, B., Zhou, X. Q. and Xu, Y. 2013. "Field monitoring and anumerical analysis of Tsing Ma Suspension Bridge temperature behavior." *Struct. Contr. Health Monit.,* 20**,** 560-575.
Zhou, L., Xia, Y., Brownjohn, J. M. W. and Koo, K. Y. 2016. "Temperature Analysis of a Long-Span Suspension Bridge Based on Field Monitoring and Numerical Simulation." *Journal of Bridge Engineering,* 21.
Zhu, J. and Meng, Q. 2017. "Effective and Fine Analysis for Temperature Effect of Bridges in Natural Environments." *Journal of Bridge Engineering,* 22.